FACULDADE DE CIÊNCIAS E TECNOLOGIA
UNIVERSIDADE NOVA DE LISBOA

Preparation of Affinity Membranes using Alternative Solvents

Telma Godinho Barroso

Monte da Caparica, 2008

Dissertação apresentada na Faculdade de Ciências e Tecnologia da Universidade Nova de Lisboa para obtenção do grau de Mestre em Mestrado Integrado em Engenharia Química e Bioquímica.

Coordenadores: Professora Doutora Ana Aguiar Ricardo e Professora Doutora Ana Cecília Roque

To my family, especially to my father!

To the memory of my grandfather that I will always remember!

To all people that I love and I bring in my heart!

Acknowledgments

This is the most important part of this work because without the right people by my side this work wouldn't make any sense. A great team led to a great work, this is my point of view. I cried, I laughed, I believed, I despaired, I made right, I failed but today, I am glad and at the same time confused because when I look to this work I think "I did it", but only because I am a lucky girl since I have the best people around me.

First I would like to thank to my supervisors Prof. Ana Aguiar Ricardo and Prof. Ana Cecília Roque.

To Prof. Ana Aguiar Ricardo I would like to say that it was a great pleasure to work with you because you knew how to be a good teacher and a good friend and therefore thank you for all the encouragement, help and advices.

To Prof. Ana Cecília Roque I would also like to thank you because you always believed in me and in my work, and for giving me the opportunity to work in your laboratory and the challenging me to deal with micro "things" because to a chemical engineer this is not easy.

To Prof. Manuel Nunes da Ponte for receiving me in his laboratory as well as to be the first person that made me enthusiastic about supercritical fluids in TLQV classes.

A special thanks to Márcio Temtem because he was a key point for the success of this work. He taught me to work "under pressure", to have more patience with bad results, to grow with good results and to believe that I had everything to do a great job. He was a wonderful teacher and the great friend that I bring in my heart, thank you!

To my great team in the lab 510: Teresa Casimiro (great women, great friend and great english teacher) Mara Silva (wonderful colleague), Eva Vão (I miss you…), Eunice Costa (new, nice and funny colleague), João Fernandes (big Jonny and big colleague), Ricardo Couto (be careful with the animals), Vasco Bonifácio (my best designer colleague) and my dear Gigi, the friend that always walked on my side and was my right hand, I just can say THANK YOU! You are the best and working with you was a pleasure!

To my other but also special team in the lab 621: Ana Pina (so many laughs, so many crazy days…the best was when we spend one day just to do buffer solution, do you remember?) Ana Cardoso (funny colleague) and Abid Hussein (the best organic chemistry teacher), thank you for all you patience with my "Telma's accidents" in the laboratory, for all the time that you spent with me and for all your encouragement and help! You are great and showed me that I can be one of you!

I would also to thank to Prof. João Sottomayor for letting me use the contact angles equipment, to Prof. Isabel Fonseca in pores size measurements, to Prof. Maria Helena Godinho in dynamic

mechanical analysis and to Mrs. Maria José Carapinha, Mrs. Joaquina Lopes, Mrs. Maria Palma Afonso, Mrs. Idalina Martins and Mrs. Conceição Luís for supporting me everytime I needed.

To my friends Susana Marques (the best friend…I will never forget each moment together), Ruben Freire (Tony of my life), Margarida Proença (nothing separate us…you are still the same special person for me), Filipe Ataíde (you are and always will be a special friend), and all the others that I didn't mention (you all know you are in my heart) thank you for your love, time, phonecalls, messages, parties, and smiles that always were a presence in my life.

To my family, especially to my father, the best man in the world that I love and that taught me to be the person that today I am, to my sister, the beautiful woman that I also love who is my pride, to Manuela Martins (for all encouragement) and to my beautiful cousins Ana Paula Batista, Liliana Nunes and Marta Nunes, a warm thanks because without you nothing of this would be possible!

To my dear Rui Sequeira…well, I think that I haven't got words for you…thanks for always believing in me, for knowing how to be the best friend and the best boyfriend and especially for always being my side!

Muito Obrigada a TODOS! ☺

Abstract

In this work it is reported the preparation of affinity membranes using green technologies. P(MMA-co-MAA) and cellulose were the polymers chosen. P(MMA-co-MAA) copolymers were synthesized with different monomers ratio (75-25%, 90-10% and 95-5%) in supercritical carbon dioxide in order to prepare membranes using CO_2-assisted phase inversion method. Cellulose membranes were also prepared from polymer-ionic liquid [BMIM][Cl] solutions by water induced phase inversion process. All membranes were analyzed in terms of morphology, hydrophilicity, transport properties and mechanical performance. P(MMA-co-MAA) and cellulose membranes were characterized by scanning electron microscopy (SEM). All membranes presented a cellular structure however significant changes of pore size are observed upon the increase of polymer percentage in the casting solution. As expected, the mercury porosimetry data confirmed higher porosities for membranes prepared from more diluted polymer solutions and higher water fluxes were obtained for membranes with higher porosity. The viscoelastic properties of the membranes prepared in this work were studied by dynamical mechanical analysis (DMA). These measurements showed that all membranes have an elastic behavior and that the ones prepared from more concentrated polymer-solvent solutions are more stiff, with exception to P(MMA-co-MAA) membranes prepared from casting solutions with 40% of polymer. By increasing the MAA ratio in the copolymer synthesis it was observed an increase of the elastic behavior of P(MMA-co-MAA) membranes. The cellulose membranes dried by evaporation also showed an elastic behavior.

A synthetic ligand, proven to mimic the interaction between Protein A and human IgG (hIgG) was synthesized, characterized and immobilized in cellulose membranes. The ligands purity, between 80-90%, was confirmed by ^{1}H- and ^{13}C-NMR spectra.

The membranes were activated with epoxy groups (150 μmol epoxy groups / g memb) and the biomimetic ligand was immobilized following two different routes. The maximum capacity of ligand immobilization was 93 μmol lig / g memb.

In preliminary tests using the affinity activated cellulose membrane, it was possible to bind 5 mg hIgG / g memb and to recover 3 mg hIgG / g memb.

Resumo

Neste trabalho é descrita a preparação de membranas de afinidade utilizando tecnologias limpas. P(MMA-co-MAA) e celulose foram os polímeros seleccionados. Sintetizaram-se copolímeros de P(MMA-co-MAA) usando soluções reaccionais com diferentes percentagens de monómeros (75-25%, 90-10% e 95-5%), em dióxido de carbono supercrítico. Estes copolímeros foram estudados na preparação de membranas pelo método de inversão de fases induzida por CO_2. A preparação das membranas de celulose foi feita a partir de soluções de polímero em líquido iónico, [BMIM][Cl], mas induzindo a inversão de fases com a adição de água. Todas as membranas foram analisadas em termos de morfologia, hidrofobicidade, propriedades de transporte e desempenho mecânico. A caracterização morfológica foi feita por análise de SEM. Todas as membranas apresentam uma estrutura celular, sendo no entanto visíveis as significativas alterações no tamanho de poro com o aumento da percentagem de polímero na solução. Como se esperava, os resultados de medidas com o porosímetro de intrusão de mercúrio confirmaram elevadas porosidades para as membranas preparadas a partir de soluções de polímero mais diluídas e foram obtidos fluxos de água mais elevados para as membranas com maior porosidade. As propriedades visco elásticas das membranas preparadas neste trabalho foram estudadas através de análises mecânicas dinâmicas (DMA). Essas análises mostraram que todas as membranas possuem um comportamento elástico e que as que são preparadas a partir de soluções de polímero-solvente mais concentradas são mais rígidas, com a excepção das membranas de P(MMA-co-MAA) preparadas com 40% em polímero. Com o aumento da percentagem mássica de MAA utilizada na síntese do copolimero, observou-se um aumento do comportamento elástico nas membranas de P(MMA-co-MAA). As membranas de celulose secas por evaporação também mostraram um comportamento elástico.

Um ligando sintético desenvolvido para mimetizar a interacção entre Proteína A e IgG humana (hIgG), foi sintetizado, caracterizado e imobilizado nas membranas de celulose. A pureza dos ligandos entre 80-90%, foi confirmada por análise de ^{1}H- e ^{13}C-NMR. As membranas foram activadas com grupos epóxido (150 µmol / g memb) e o ligando biomimético foi imobilizado seguindo dois processos diferentes. A máxima capacidade de imobilização de ligando foi 93 µmol / g memb. Em testes preliminares usando a membrana de celulose de afinidade activada foi possível ligar 5 mg hIgG / g memb e recuperar 3 mg hIgG / g memb.

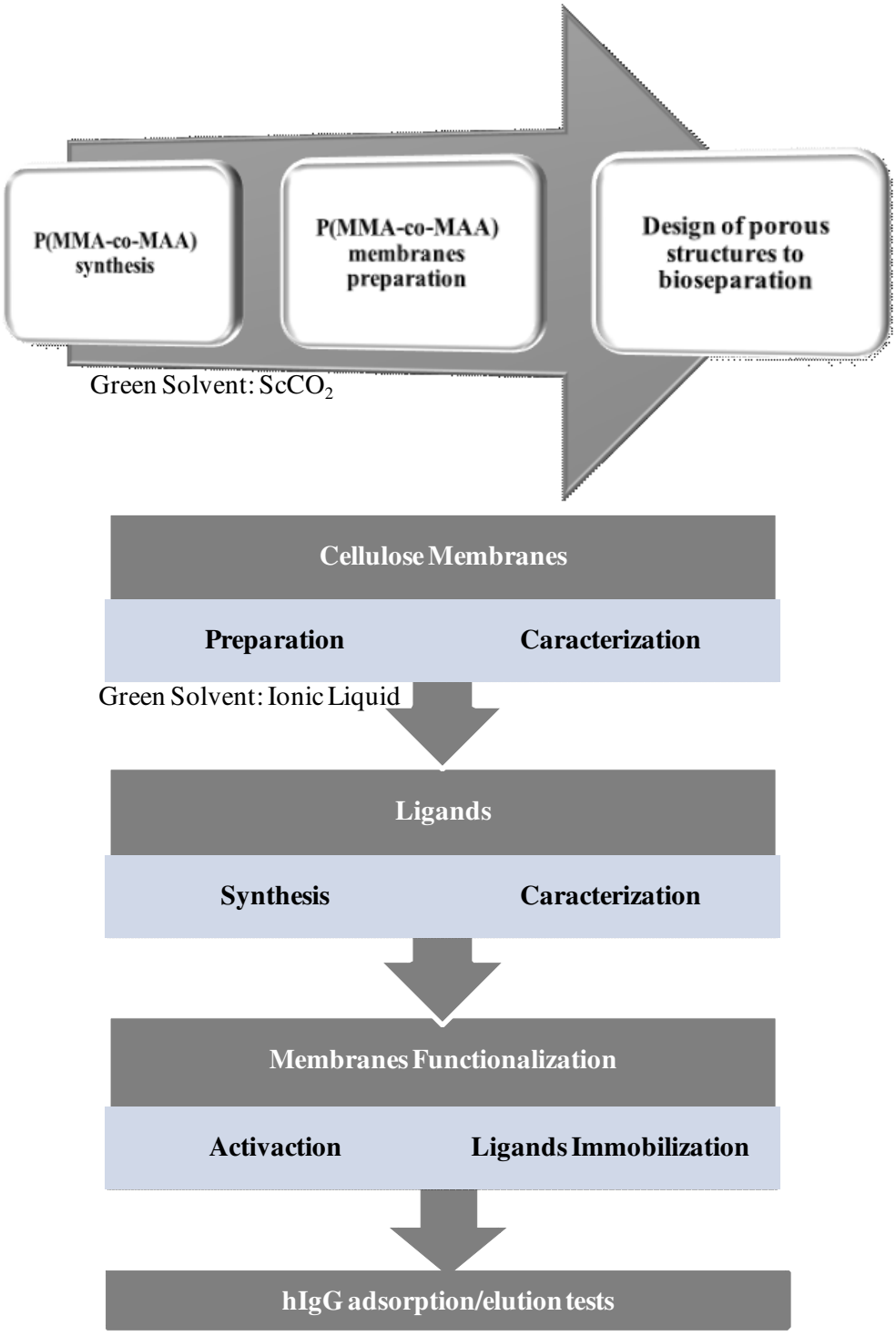

Scheme 1 – Schematic work plan

Contents

Index of Figures

Chapter 1

Chapter 2

Appendix Section

Index of Tables

Chapter 1

Chapter 2

Chapter 3

1. Introduction

Nowadays a chromatographic membrane or an affinity membrane is an integrative concept in downstream processing of proteins and antibodies [1].

The main feature of chromatographic separations based on membranes is the absence of pore diffusion, which is the main transport resistance in conventional column chromatography using porous particles. This is achieved by attaching the active ligands to the inner surface of the pores, where mass transport takes place mainly by convective flow, thus reducing the transport limitations from pore to film diffusion [2].

One the other hand, stricter health, safety and environmental regulation are pushing researchers to find cleaner technologies and alternative solvents, in particular for bio-applications.

The development of affinity membranes using green methodologies such as supercritical fluids and ionic liquids is the main challenge of this work.

1.1 Supercritical fluids

In 1822, the baron Charles Gagniard de la Tour, in his famous cannon experiments, measured for the first time the critical point of a substance. The experiments consisted in listening to discontinuities in the sound of a rolling revolving rock ball in a sealed cannon filled with a fluid, when increasing temperature [3]. At a given temperature he stopped to hear the sound of the ball, which corresponded to the critical point of the fluid in question. Above this temperature the densities of the liquid and the gas phases become equal, the interface disappears, resulting in a single phase, the supercritical phase [3].

A pure component enters the supercritical status when both temperature and pressure are above its critical pressure and temperature values. In this region, the SCF exists in an intermediate phase between liquid and gas phases. The macroscopic appearance of the SCF is a homogeneous and opalescent system without phase separation (single phase) since, at this point, the density of the gas and liquid is the same [4].

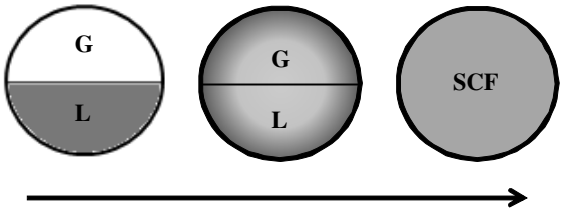

Figure 1.1 - Schematic representation of the change from liquid–gas equilibrium to a supercritical fluid (adapted from [4])

Supercritical fluids present a particular combination of liquid and gas properties [5, 6], which are the density and the solubilization power of liquids and with transport properties and compressibility of gases [5, 7, 8]. The SCF is dense but highly compressible, particularly near the supercritical region. Thus, any change of pressure alters its density and consequently the solvent power. Like a liquid, the SCF shows a density value appreciable for the solvation power, while the viscosity and diffusivity similar to a gas facilitate the mass transfer [3].

Table 1.1 shows the density, viscosity and compressibility values to gases, supercritical fluids and liquids [6].

Table 1.1 - Comparison of physical properties of gases, SCF`s and liquids (adapted from [6])

Properties	Gas	SCF	Liquid
Density (g mL^{-1})	10^{-3}	0.3	1
Viscosity (Pa.s)	10^{-5}	10^{-4}	10^{-3}
Diffusity (cm^2s^{-1})	0.1	10^{-3}	5×10^{-6}

These properties can be adjusted with changes in pressure and temperature. Several precipitation methods using these fluids take advantage of the possibility to tune their properties, or suddenly change these properties during the process with a change in pressure and temperature, which led to different supersaturation conditions [8].

CO_2 is the most used solvent in critical conditions, because it has a relatively moderate critical point (31.1 ºC and 7.38 MPa), is inert, an environmentally friendly alternative to conventional solvents and readily available in high purity [3, 9, 10]. Figure 1.2 shows the pressure-temperature phase diagram for CO_2. For a pure substance the critical point marks the end of the vapour-liquid coexistence curve.

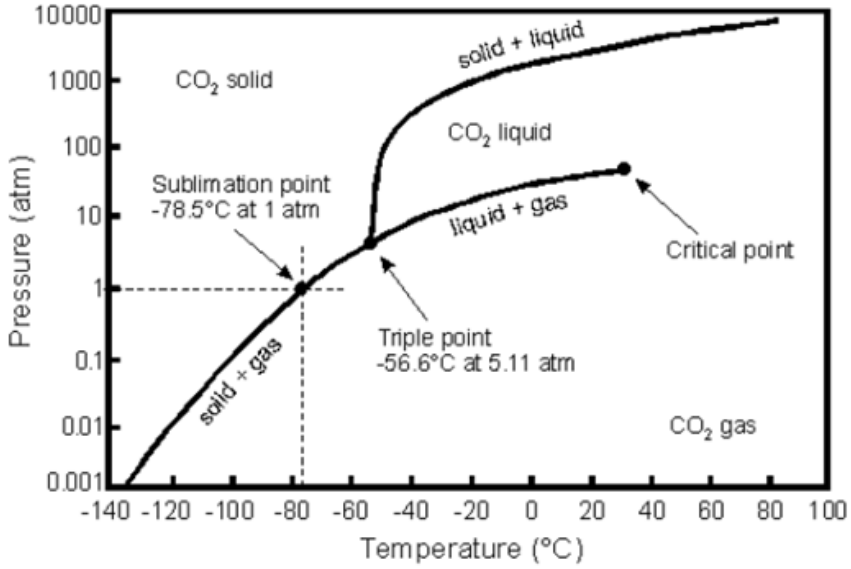

Figure 1.2 - Phases diagram of CO_2

All gases can form SCF above specific sets of critical conditions (*p*, *T*), but it should be kept in mind that, for many cases, the transition to the supercritical state occurs at high temperatures not compatible with pharmaceutical compounds (e.g., SC water, see Table 1.2).

Table 1.2 - Supercritical properties of other substances (adapted from [3])

Fluid	T_c (ºC)	P_c/bar
Ethane	32.2	48.8
Ethylene	9.3	50.4
Propane	96.7	42.5
Propylene	91.9	46.2
Water	374.2	220.5

1.1.1 Applications and advantages of using supercritical fluids

Typical organic solvents are volatile, flammable and may pose a risk to human health and to environment. Alternative approaches are being developed, and the use of supercritical fluids increased in different areas [9]. The increasing interest of both industry and research in exploring the green advantages of these fluids, prompted the development of new techniques and cleaner processes [11]. These fluids have already a diverse number of application areas, such as: extraction of oils [12]; polymerizations of acrylates and esters [3, 13]; impregnation and encapsulation of

pharmaceutical compounds [14]; paintings and coverings [15]; drawing particles (rapid expansion of supercritical solutions (RESS), supercritical anti-solvent (SAS), particle generation from supercritical solutions or suspensions (PGSS), microencapsulation) [16]; polymers processing [15]; and chemical reactions [16].

Supercritical fluids are potential and viable alternatives in diverse processes due to their high versatility, the flexibility in offering alternative processing approaches, the possibility to avoid or minimize the use of organic solvents, and the ability to reach peculiar processing conditions (e.g., changes in pressure and in the rate of solvent evaporation) which would otherwise be difficult to obtain with traditional processes. All these parameters provide additional dimensions for process control and manipulation of the solid-state properties [17]. Furthermore, the original concept of supercritical fluid as a "green" alternative has become very important as the regulatory requirements for the use and residual contents of volatile organic compounds in the drug product become more and more restrictive[18].

1.1.2 Polymerization reactions in $scCO_2$

Environmental and human safety concerns have become determining factors in chemical engineering and process development. Many conventional polymer production routes involve an excessive use of organic solvents both as reaction medium and purification steps [19].

Approximately 20 million tons of VOCs are emitted to the atmosphere each year as a result of industrial activities. Based on these facts, it is highly desirable from an environmental safety and economical point of view, to develop alternative routes to reduce the use of organic solvents in polymer processes. The supercritical fluids are a sustainable alternative [20].

In the last decades, there has been an intensive research on the area of polymerization reaction using supercritical fluids, an area where these fluids can really have a vast applicability [21].

The solubility of monomers in supercritical systems depends on the temperature, pressure and concentration, but also of their nature [22].

Carbone dioxide is a good solvent for the majority of non polar substances and for some polar substances with low molecular weight [23, 24], however, it is a bad solvent for the majority of polymers with high molecular weight in average conditions (<100ºC, <350 bar). The only polymers that show good solubility in CO_2 under mild conditions are amorphous fluoropolymers and some siloxanes [25, 26].

As a polymerization medium, CO_2 offers advantages over conventional solvents. The $scCO_2$ can be used to extract unreacted monomer, initiator, catalyst and some stabilizers from the polymer product, leading to highly pure materials. $ScCO_2$ is also able to plasticize glassy polymers, which

results in a reduction of the polymer's glass transition temperature, Tg, which plays an important role in the formation of foams and in the incorporation of additives [5].

Depending on the nature of the reactant species it is possible to establish a classification of polymerization types in chain: free-radical polymerization, cationic polymerization, anionic polymerization and polymerization catalyzed by metals [23].

Only the free-radical polymerization will be described because is the one used in this work. The free-radical polymerizations can be homogenous or heterogeneous. In the homogenous polymerizations all components, including monomer, initiator, and polymer, are soluble throughout the duration of the reaction; a heterogeneous polymerization contains at least one insoluble component at some point during the reaction [23].

There are four types of heterogeneous polymerization: precipitation, suspension, dispersion and emulsion.

In a precipitation polymerization, an initial homogenous mixture of monomer, initiator and solvent becomes heterogeneous during the reaction as insoluble polymer chains aggregate to form a separate polymeric phase [4, 23].

In a suspension polymerization the polymer, monomer and initiator are insoluble in the continuous phase. The resulting polymer is also insoluble in the continuous phase acting as a dispersant and heat-dissipation agent during the reaction.

A dispersion polymerization begins as a homogeneous mixture because the solubility of monomer and initiator in the continuous phase. Once the growing oligomeric radicals reach a critical molecular weight, the chains are no longer soluble in the reaction medium and phase separation occurs. At this point the active surface stabilizing molecule adsorbs to or becomes chemically attached to the polymer colloid and prevents coagulation or agglomeration of the particles. The resulting typical spherical polymers particles ranging in size from 100nm to 10µm critical CO_2 [4, 23].

In an emulsion polymerization the initial reational mixture is heterogeneous due to the low solubility of monomer in the continuous phase [23]. Usually emulsion polymerizations employ oil-soluble monomers such as acrylates, or styrenics dispersed in an aqueous medium containing a water-soluble initiator, while "inverse" emulsion polymerizations employ water-soluble monomers dispersed in an organic medium. In this type of polymerization, normally spherical particles result with diameters inferior to 1µm [23].

The use of supercritical CO_2 in polymerizations introduces new properties in the synthesized polymers such as the control of polymer morphology and in average molecular weights. Being CO_2 a gas at room temperature, the polymers can be isolated from reaction media by simple depressurization, resulting a dry polymer product [23].

1.1.3 Porous structures formation using $scCO_2$

Another area where supercritical fluids have an increasingly important role is in the preparation of porous structures [27, 28]. Porous structures can be obtained by foaming, crystallization of swollen cross-linked polymers (CSX), non reactive gelation of SCF solutions using organogelators, particle formation and anti-solvent-induced phase separation [27, 28].

In the foaming process a polymer is saturated with supercritical CO_2, followed by rapid depressurization at constant temperature. This method takes into account the depression of glass transition (Tg) of many polymers in $scCO_2$, which can be kept in liquid state at relatively low temperatures [27].

In the CSX method the crosslinked polymer is heated above the crystal melting temperature followed by the addition of the supercritical fluid in order to transform the polymer into a swollen gel. The temperature decreases and a rigid structure is formed. At the end the supercritical fluid is vented and a crystalline structure is formed [27].

Materials produced by non-reactive gelation of SCF solutions using organogelators, are fragile. They are gels that upon removal of the CO_2 phase, produce free-standing foams with average diameters of 1 μm. Density reductions of 97% relative to the parent compound can be obtained [27].

Porous particles formation or SCF precipitation methods are very useful in pharmaceutical formulations. These different methods can be classified according to the role of SCF in the process. It can be act as a solvent, as in the Rapid Expansion of Supercritical Solutions (RESS) process, as anti-solvent, as in the Supercritical Anti Solvent (SAS) process, as a solute, as in the Precipitation from Gas Saturated Solution (PGSS) process or as in the Supercritical Assisted Atomization process (SAA) [8, 27, 28]. In case of the anti-solvent-induced phase separation, the $scCO_2$ works as anti-solvent for the preparation of porous materials. This technique is very common in the preparation of membranes [29]. The $scCO_2$ removes the organic solvent which is usually used to dissolve the polymer in the membrane preparation.

The membranes preparation by evaporation methods sometimes have some problems such as in hydraulic permeability and resistance due to their irregular pore size and pore size distribution [30].

Nowadays, the majority of the porous membranes extensively used in membrane processes are prepared from homogeneous polymer solutions by the wet phase inversion method [31]. In this method the solution consisting of polymer and solvent is immersed in a non-solvent coagulation bath causing the solution to be phase-separated. This type of experimental process involves hard and expensive membrane treatments to remove the organic solvents and can pose serious problems if considered for biomedical applications.

Recently, a new technique was developed which uses supercritical CO_2 to induce the phase separation of the polymer solution [32], avoiding the disadvantages of the previous processes.
Supercritical carbon dioxide has been applied to induce the phase separation of the polymer solution and produce membranes of nylon [32], polystyrene [9], cellulose acetate [33], polysulfone [31], and more recently of poly(methyl methacrylate) [34].
In comparison with wet phase inversion method, this technique presents many advantages: $scCO_2$ allows the production of a dry polymeric membrane, the dry membrane can be obtained without additional post-treatment because there are no traces of organic solvents, introduces additional parameters (pressure, temperature, depressurization) to control membrane morphology, improves mass transfer (much lower viscosities than organic liquids, and easily adjusted by tuning pressure and temperature) [9], and CO_2 is non-toxic, non-flammable and cheap [33].

1.2 Ionic liquids

Ionic liquids (ILs) are a new group of organic salts that exist as liquids at relatively low temperatures (<100ºC) [35]. These liquids offer interesting properties such as: they are good solvents for a wide range of inorganic, organic and polymeric materials, have a great chemical and thermal stability beginning to decompose around 400 °C, non-inflammable, easy to prepare and principally present a low vapor pressures [36, 37].
In contrast to organic solvents, these liquids are considered "green solvents", because usually they possess lower toxicity and flammability than organic solvents and electrolyte salts [38]. The increase of governmental regulations prompts the necessity to draw greener and cleaner processes, thus diminishing the environmental impact, pollutions and residues. Thus, the ionic liquids appear as an alternative to conventional organic solvents in chemistry, biochemistry and separation processes [39].
The ILs are typically comprised of combinations of organic cations, such as imidazolium, pyridinium, pyrrolidinium, ammonium, sulfonium and phosphonium derivatives, and bulky and soft anions: $[BF_4]$, $[PF_6]$, $[CF_3SO_3]$, and $[(CF_3SO_2)_2N]$ [40].
These possible combinations determine the physical and chemical properties of the ILs [35]. Nowadays a vast group of possible combinations are available, contributing to the versatile use of these liquids.

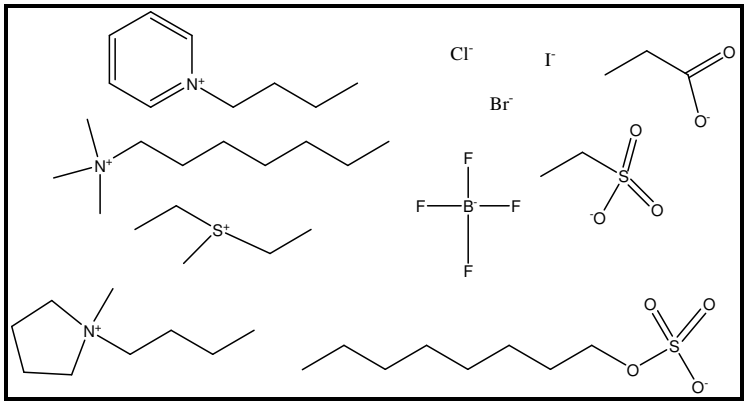

Figure 1.3 - Types of cations and anions present in ionic liquids

The investigation related to the use of ionic liquids (ILs) as alternative solvents has steadily increased over the past 10 years [39]. This increase is explained by the attractive ILs properties. Melting point, density, viscosity, solubility in water and transport properties are important parameters in ionic liquids performance [40]. The melting point of ILs represents the lower limit of the liquid gap and together with thermal stability defines the interval of temperatures within which it is possible to use the ILs as solvents [41].

Table 1.3 – Densities and viscosities of typical ionic liquids (adapted from [42])

Ionic Liquid	Density at 20 ºC (g cm^{-3})	Dynamic viscosity at 20 ºC (cP)
[BMIM][PF_6]	1.37	330
[BMIM] [BF_4]	1.24	154
[BMIM] [Tf_2N]	1.43	52
[BMIM] [Tf_2O]	1.29	90
[BMIM] [Cl]	1.08[a]	716[a]

[a] at 25ºC

In general, ionic liquids have densities >1, and thus exist as the lower phase in most biphasic systems [42]. Usually, ionic liquids are denser than water. The molar mass of the anion significantly affects the overall density of ILs [43]. They are also generally quite viscous compared with conventional organic solvents, which means that phase separation from organic solvents is often more rapid than with two solvents of similar viscosity [42]. The viscosity of ILs is usually higher than water, similar to those of oils, and decreases with increasing temperature [43].

The hydrophilic and hydrophobic behavior of ILs is an important parameter because it is related with solvation properties and consequently with their capacity to dissolve reactants. Furthermore, the water content of ILs can affect the rates and selectivity of reactions. The solubility of these ILs in water depends on the nature of the anion, temperature and the length of the alkyl chain on the imidazolium cation [41].

These characteristics resume the interesting character of the ILs as green solvents.

1.2.1 Applications and advantages of ionic liquids

Ionic liquids have applications in diverse areas such as in catalysis [36, 44, 45], separation [35], biochemistry [46, 47], organic synthesis [45], polymerizations [48], electrochemistry [49], among many others.

Ionic liquids can be used to dissolve some polymers and macromolecules, overpassing the typical difficulties found in the dissolution of these molecules using organic solvents [48].

By choosing the correct ionic liquid, it is possible to obtain a higher efficiency and a reduced amount of possible waste produced. Another great advantage of these fluids is the possibility of being recovered [39]. Literature shows [50] that it is possible to distillate ionic liquids. This characteristic can severely restrict the attainability of high purity levels for ionic liquids when they contain poorly volatile components, in recycling schemes, as well as, excluding their use in gas-phase processes. Nevertheless it was demonstrated that some selected families of commonly ionic liquids can be distilled at 200–300 ºC and low pressure, with concomitant recovery of significant amounts of pure substance [50].

It must be emphasized that reactions in ionic liquids are not difficult to perform and usually require no special apparatus or methodologies being easier to carry out than in conventional organic solvents [51].

Hence, it is possible to design a “green” solvent with the desired properties according with a specific target application.

1.3 Supercritical fluids and ionic liquids

The most recently goal of green chemistry is to create a cleaner and more sustainable chemistry and it has received more and more attention in recent years. The ideal situation for a safe and green chemical process is using no solvent; however most of the chemical processes depend on solvents [52]. Supercritical fluids and ionic liquids are considerable green solvents due their properties described previously.

In order to develop green synthesis and processes, the great challenge is to combine the advantages properties of $scCO_2$ and of ionic liquids.

Preliminary works have shown that $scCO_2$ extraction is a viable method for solute recovery from an IL. Early studies [52] of IL–CO_2 phase behavior showed that systems present very unusual biphasic systems. No measurable amount of ionic liquid could be found in the CO_2-rich phase, although a

large amount of CO_2 can be dissolved in the IL-rich phase, reducing the viscosity of IL. This point is a key phenomenon which makes extraction of solutes from IL with CO_2 attractive [52].

Researchers found that nonvolatile organic compounds can be extracted from ILs using $scCO_2$, which is widely used to extract large organic compounds with minimal pollution [49].

The use of $scCO_2$ to separate ILs from their organic solvents, the addition of CO_2 to separate hydrophobic and hydrophilic imidazolium-based ILs from aqueous solutions has all been important applications of IL–$scCO_2$ systems [52]. The recent applications of room temperature IL–$scCO_2$ systems are in metal catalyzed organic reactions and enzyme-catalyzed transformations [52]. The solubility or stability of organometallic or enzymatic catalysts in ILs and their negligible solubility in $scCO_2$ is the basic advantage of IL–$scCO_2$ systems [49].

Volatile and nonpolar $scCO_2$ has become a good partner of nonvolatile and polar IL and this new system with its unique properties have been utilized to extract organic compounds from ILs using $scCO_2$.

The primary disadvantage of these biphasic systems is the cost of the equipment for producing and handling $scCO_2$. Another disadvantage is the very limited amount of information available on the toxicity and other physiological effects of ILs. For biocatalytic IL systems the enzymes are currently limited to lipases [49].

However, this alternative route which promotes the combination of $scCO_2$ and ILs as solvents becomes an important route in further development of sustainable chemistry.

1.4 References

1. Ghosh, R., *Protein separation using membrane chromatography: opportunities and challenges.* Journal of Chromatography: opportunities and challenges, 2002. **952**: p. 13-27.
2. Thommes, J.a.K., M.R., *Membrane Chromatography-An Integrative Concept in the Downstream Processing of Proteins.* Biotechnol. Prog., 1995. **11**: p. 357-367.
3. Kemmere, M., Meyer, T., *Supercritical Carbon Dioxide: in Polymer Reaction Engineering*, ed. Wiley. 2005.
4. Cooper, I.A., *Polymer synthesis and processing using supercritical carbon dioxide.* J.Mater.Chem, 2000. **10**: p. 207-234.
5. Casimiro, T., *Chemical synthesis and phase behaviour in supercritical carbon dioxide*, in *Chemistry*. 2003, Universidade Nova de Lisboa - Faculdade de Ciências e Tecnologia: Almada, Portugal.
6. Jessop, P., Leitner, W., *Chemical Synthesis using supercritical fluids*, ed. Wiley-VCH. 1999, New York.
7. Charles, A.E., Barbara, L. K., Pablo, G. D., *Supercritical fluids as solvents for chemical and materials processing.* Nature, 1996. **383**: p. 313-318.
8. Martin, A., Cocero, M.J., *Micronization processes with supercritical fluids: Fundamentalsand mechanisms.* Advanced Drug Delivery Reviews 2008. **60**: p. 339-350.
9. Temtem, M., Casimiro, T., Aguiar A.R., *Solvent power and despressurization rate effects in the formation of polysulfone membrane with CO2-assisted phase inversion method.* Journal of Membrane Science, 2006. **282**: p. 244-252.
10. Tai, H., Popov, V.K., Shakesheff, K.M., and Howdle, S.W., *Putting the fizz into chemistry: applications of supercritical carbon dioxide in tissue engineering, drug delivery and synthesis of novel block copolymers.* Biochemical Society, 2007. **35**: p. 516-521.
11. Ginty, J.P., Shakesheff, M.K., Howdle, M.S., *Drug delivery goes supercritical.* Elsevier, 2005. **8**(8): p. 42-48.
12. Davarnejad, R., Kassim, M.K., Zaina, l. A., *Supercritical fluid extraction of b-carotene from crude palm oil using CO2 Journal of Food Engineering.* Journal of Food Engineering, 2008. **89**: p. 472-278.
13. Desimone, J.M., *Cationic Polymerization of Vinyl and Cyclic Ethers in Supercritical and Liquid Carbon Dioxide.* Macromolecules, 1994. **265**: p. 356.
14. Duarte, C.M., et al., *Supercritical fluid impregnation of a biocompatible polymer for ophthalmic drug delivery* Journal of Supercritical Fluids, 2007. **42**: p. 373-377.

15. Perrut, M., *Supercritical Fluid Applications: Industrial Developement and Econimic Issues*, in *UNION CARBIDE Patents*. 1993.

16. Jung, J., and Perrut, M., *Particle design using supercritical fluids: Literature and patent survey.* Journal of Supercritical Fluids, 2001. **20**: p. 179-219.

17. Pasquali, I., Bettini, B.,Giordano, F., *Supercritical fluid technologies: An innovative approach for manipulating the solid-state of pharmaceuticals.* Advanced Drug Delivery Reviews, 2008. **60**(3): p. 399-410.

18. Temtem, M., Casimiro, T., Mano, J.F., Aguiar, A.R., *Green synthesis of a temperature sensitive hydrogel.* Green Chem., 2007. **9**: p. 75-79.

19. Cowie, J.M.G., *Polymers: Chemistry and Physics of Modern Materials,*, ed. I.T.C. Limited. 1973, London.

20. Woods, H.M., et al., *Materials processing in supercritical carbon dioxide: surfactants, polymers and biomaterials.* J.Mater. Chem, 2004. **14**: p. 1663-1678.

21. Giles, R.M., Hay, N. J., Howdle, M.S., *The copolymerization of methyl and ethyl methacrylate in supercritical carbon dioxide.* Macromol. Rapid Commun, 2000. **21**: p. 1019-1023.

22. Kunita, M.H., *Enxertia de metacrilato de glicidila em filmes poliméricos por processo com fluidos supercríticos*, in *Chemistry departement*. 2005, Maringá University: Maringá, Brasil.

23. Kendall, J.L., Canelas, D., Young, J. DeSimone, J., *Polymerizations in supercritical Carbon Dioxide.* Chem. Rev., 1999. **99**: p. 543-563.

24. Hyatt, J.A., *Liquid and supercritical carbon dioxide as organic solvents.* J. Org. Chem, 1984. **49**: p. 5097-5101.

25. McHugh, M.A., Krukonis, V., *Supercritical Fluid Extraction: Principles and Practice*. B.-H. Stoneham, ed. 2. 1993.

26. Hoefling, T.A., *Effect of structure on the cloud-point curves of silicone-based amphiphiles in supercritical carbon dioxide.* Journal of Supercritical Fluids, 1993. **6**: p. 165.

27. Cooper, I.A., *Porous materials and supercritical fluids.* Advanced Materials, 2003. **15**: p. 1049-1059.

28. Quirk, R.A., France, R. M., Shakesheff, K. M., Howdle, S.M., *Supercritical fluid technologies and tissue engineering scaffolds.* Current Opinion in Solid State & Materials Science, 2004. **8**: p. 313-321.

29. Temtem, M., Casimiro, T., Mano, J.F., Aguiar, A.R., *Preparation of membranes with polysulfone/polycaprolactone blends using a high pressure cell specially designed for a CO_2-assisted phase inversion* Jounal of Supercritical Fluids, 2007. **43**: p. 542-548.

30. Tung, L.K., Chuang, C.J., *Effect of pore morphology on fluid flow and particle deposition on a track-etched polycarbonate membrane.* Desalination, 2002. **146**: p. 129.

31. Reverchon, E., Cardea, S., *Formation of polysulfone membranes by supercritical CO_2* Journal of Supercritical Fluids, 2005. **35**: p. 140.

32. Kho, Y.W., Kalika, D. S., Knutson, B.L., *Precipitation of Nylon 6 membranes using compressed carbon dioxide.* Polymer, 2001. **42**: p. 6119-6127.

33. Reverchon, E., Cardea, S., *Formation of cellulose acetate membranes using a supercritical fluid assisted process.* Journal of Membrane Science, 2004. **240**: p. 187-195.

34. Reverchon, E., and Cardea, S., *Production of loaded PMMA structeres using the supercritical CO_2 phase inversion process.* Journal of Membrane Science, 2006. **273**: p. 97.

35. Brennecke, J.F., Maginn, E. J., *Ionic Liquids: Innovative Fluids for Chemical Processing.* AIChE Journal, 2001. **47**(11): p. 2384-2389.

36. Seddon, K.R., *Ionic Liquids for Clean Technology.* J. Chem. T ech. Biotechnol, 1997. **68**: p. 351-356.

37. Zhu, S., *Dissolution of cellulose with ionic liquids and its application: a mini-review.* Green Chem., 2006. **8**: p. 325-327.

38. Hagiwara, R., Ito, R., *Room temperature ionic liquids of alkylimidazolium cations and fluoroanions.* Journal of Fluorine Chemistry, 2000. **105**: p. 221-227.

39. Turner, M.B., et al., *Production of Bioactive Cellulose Films Reconstituted from Ionic Liquids* Biomacromolecules, 2004. **5**(4): p. 1379 -1384.

40. Tokuda, H., et al., *Physicochemical Properties and Structures of Room Temperature Ionic Liquids. 1. Variation of Anionic Species.* J. Phys. Chem. B, 2004. **108**: p. 16593-16600.

41. Chiappe, C., Pieraccini, D., *Ionic liquids: solvent properties and organic reactivity.* J. Phys. Org. Chem., 2005. **18**: p. 275–297.

42. Gordon, C.M., *New developments in catalysis using ionic liquids.* Applied Catalysis A:, 2001. **222**: p. 101–117.

43. Huddleston, J.G., et al., *Characterization and comparison of hydrophilic and hydrophobic room temperature ionic liquids incorporating the imidazolium cation.* Green Chem., 2001. **3**: p. 156–164.

44. Zhao, D., Wu, M., Kou, Y., Enze, M., *Ionic liquids: applications in catalysis.* Catalysis Today, 2002. **74**: p. 157-189.

45. Zhao, H., Malhotra, S. V., *Applications of Ionic Liquids in Organic Synthesis.* Aldrichimica ACTA, 2002. **35**: p. 72-83.

46. Kragl, U., Eckstein, M., Kaftzik, N., *Enzyme catalysis in ionic liquids.* Chemical Biotechnology, 2002. **13**: p. 565-571.

47. Rantwijk, F., Madeira, R., Sheldon, R. A., *Biocatalytic transformations in ionic liquids.* TRENDS in biotechonology, 2003. **21**: p. 131-138.

48. Kubisa, P., *Application of ionic liquids as solvents for polymerization processes.* Progress in Polymer Science, 2004. **29**: p. 3-12.

49. Dzyuba, S.V., Bartsch, R. A., *Recent Advances in Applications of Room-Temperature Ionic Liquid/Supercritical CO2 Systems.* Angew Chem, 2003. **42**(2): p. 148-150.

50. Earle, M.J., et. al., *The distillation and volatility of ionic liquids.* Nature, 2006. **439**(16): p. 831-834.

51. Earle, M.J., Seddon, K. R., *Ionic liquids. Green solvents for the future.* Pure Appl. Chem., 2000. **72**: p. 1391–1398.

52. Keskin, S., et al., *A review of ionic liquids towards supercritical fluid applications.* Jounal of Supercritical Fluids, 2007. **43**: p. 150–180.

2. Synthesis of P(MMA-co-MAA) and Membranes Preparation

2.1. Introduction

In the last decades there was a rapid increase in the study of supercritical carbon dioxide as a potential candidate to replace conventional solvents [1]. There has been an extensive research on $scCO_2$ as a reaction medium for the polymerization of acrylates, especially methyl methacrylate (MMA) [1-4]. PMMA is a versatile transparent thermoplastic that is used in a wide range of fields and applications such as in lenses of exterior lights of automobiles, in electronics, in food containers and in artificial marble [5].

Poly(methylmethacrylate-co-methacrylic acid) is a copolymer synthesized by the reaction of two monomers, MMA (methyl metacrylate) and MAA (metacrylic acid). Polymers possessing high glass transition temperature provide attractive interest in polymer science due the strong economic incentives arising from their special applications for example in optical materials [6, 7]. The PMMA has to be modified to raise its glass transition temperature by blending it with other polymers containing rigid or bulky structure, however, immiscibility problems with phase separation often occur [6].

In this study, MMA and MAA are copolymerized in $scCO_2$ in order to produce a rigid structure, with attractive properties: thermal stability, mechanical strength [8] and desirable functional groups for the design of specific separation devices. An important aspect that allows P(MMA-co-MAA) synthesis by precipitation polymerization in scCO2 is the high solubility of both monomers in this green solvent [1, 9-11].

PMAA is a pH-sensitive polymer [12] with applications in different areas. These polymers are nominated with different names such as stimuli-responsive polymers, smart polymers (SP), intelligent polymers or environmental-sensitive polymers [12].

MMA and MAA polymerization reactions have been extensively studied. In1996, Desimone and co-workers studied the dispersion polymerization of MMA utilizing poly(1,1,-dihydroperfluorooctyl acrylate) as a steric stabilizer in $scCO_2$. The reactions were carried out in the presence of helium as non solvent [13]. They concluded that the particle size distribution of PMMA was influenced by the helium amount, being this parameter very useful to manipulate the size of PMMA particles.

Later on, a series of graft copolymers, poly (methylmethacrylate-*co* hydroxyethylmethacrylate)-*g*-poly(perfluoropropylene oxide), were synthesized to be used as stabilizers in the dispersion polymerization of methyl methacrylate in supercritical medium [14] in order to find the best stabilization conditions.

In 2000, Muth et al [11] studied the modification of polymeric substrates with some monomers such as methyl methacrylate (MMA) and methacrylic acid (MAA), under supercritical conditions. The polymers were impregnated with the monomers and a radical initiator, followed by a polymerization inside the swollen substrates to generate a polymer within a polymer. The process parameters were controlled by the radical initiator and by the solubility of the monomers in $scCO_2$.

Later, Park et al., studied the emulsion stability of PMMA particles formed by dispersion polymerization of methyl methacrylate in $scCO_2$ [15]. The amount of surfactants showed to be an important factor in polymer synthesis as well as the amount of initiator in terms of molecular weight and yield.

In the same year, Huang and Chang prepared a series of miscible PMMA/PMAA blends and PMMA-co-PMAA copolymers with different compositions. It was observed that with few variations in the ratio of monomers the differences between copolymers were relevant [6]. This copolymer showed also to have a diffraction efficiency behavior as photopolymer [7]. The optical transparence of the photopolymers enhanced by the increase of acid content in the polymer make these polymers potential candidates to be used as recording medium devices for high-density optical data storage.

The commercial success of a supercritical-polymer process lies not just only in the process design but also in understanding other relevant aspects to the process such as polymer–CO_2 interaction, solubility, and viscosity reduction [3, 16]. This kind of process brings large advantages to the polymers when compared with polymerizations studied using organic solvents [17, 18].

The interest of PMMA, PMAA and P(MMA-co-MAA) was extended to the preparation of membranes [12, 19]. Some studies in order to prepare PMAA or PMMA membranes with other polymers were performed to develop new devices with pH-responsive character. The different PMAA contents in membranes composition led to differences in morphologies, fluxes, and permeabilities.

Being PMAA a “smart” polymer, PMAA membranes were also studied in order to develop engineered devices for bioseparation in areas such as biotechnology and medicine [20].

In 2005, Shumei Wang et al, studied the morphology of polymeric membranes, including PMMA membranes, applying chemical methods by phase inversion process [21]. The membrane pores resulted from the CO_2 release of the reaction between acetic acid, which is the solvent in casting solution, and sodium carbonate that worked as anti-solvent [21].

Another application of PMMA membranes is in the area of gas separation [22, 23]. Several studies were performed in order to understand gas transport properties in PMMA membranes because it was demonstrated that PMMA membranes are permeable and selective for gas separation applications [22].

Silvestri and co workers prepared P(MMA-co-AA) membranes by the phase inversion method, using water, in order to imprint affinity molecules/nanospheres to specific targets to separation processes [24]. P(MMA-co-AA) membranes modified for the introduction of the nanoparticles on the surface or inside the membrane body showed a great improve in the selectivity to certain molecules. This approach proved to be an interesting alternative to membrane preparation where the recognition sites are obtained during the phase inversion technique.

Recently, butadiene MMA and MAA emulsion copolymerizations were performed in batch mode under pressure, allowing to design characteristic films with useful applications in products such as gloves and condoms [25]. It was concluded that the chemistry and physical properties of these films depends on the MAA content.

In this work, in order to use P(MMA-co-MAA) to prepare "green" specific separation devices, the membranes preparation of this copolymer were performed using $scCO_2$.

Recently, a new technique was reported in which supercritical CO_2 is used to induce the phase separation of the polymer solution [26].

In 2006 Reverchon et al produced PMMA structures in $scCO_2$ using the phase inversion method [27]. PMMA structures were prepared and loaded with an antibiotic, amoxicillin, using two different techniques: dissolving the drug in the same organic solvent used to solubilize the polymer or suspending the drug in the organic solution formed by polymer and solvent. The results confirmed the feasibility of the loading process and the advantages with respect to traditional methods; it was possible to obtain an efficient encapsulation of the drug and the tuning of the drug release rate by modifying the process parameters [27].

Many polymeric membranes were prepared using this methodology in order to study the effect of pressure [28], temperature [28], concentration [28, 29], solvent [30-32], depressurization times [27, 31] porosity [29, 31], morphology [28, 30], hydrophilicity, transport properties and mechanical performance [29, 33]. The $scCO_2$-process brings two important advantages: the control of membranes average pore size and the ability to extract any vestiges of organic solvents used in the membrane preparation.

In this study P(MMA-co-MAA) was synthesized using three different monomer ratios in supercritical medium, followed by the preparation of membranes through $scCO_2$-process, in order to study these porous structures in the bioseparation.

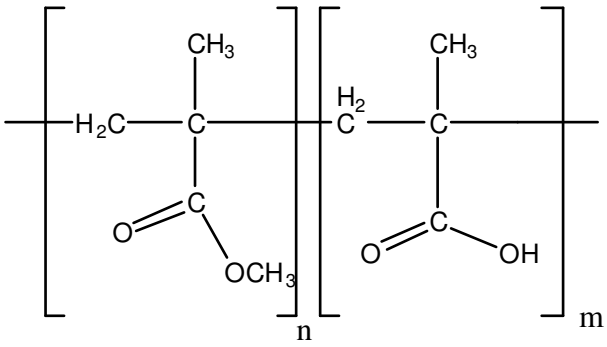

Figure 2.1 - P(MMA-co-MAA) structure

2.2. Experimental

2.2.1. Materials

Methyl methacrylate (MMA, 99 % purity), metacrylic acid (MAA, 99% purity), 2,2'-azobis(isobutyronitrile) (AIBN, 98% purity), N,N-dimethylformamide (purity ≥95%) and acetone-d_6 were purchased from Sigma-Aldrich. Acetone (p.a.) was purchased from Pronalab. Carbon dioxide (CO_2) was supplied by Air Liquide with 99.995% purity. All the reagents have been used with no further purification.

2.2.2. Synthesis of P(MMA-co-MAA)

2.2.2.1. Polymerization in scCO_2

The synthesis of the P(MMA-co-MAA) copolymers were performed in a high pressure apparatus schematically shown in Figure 2.2. The reactions were performed in a 33 mL stainless steel high-pressure cell equipped with two aligned sapphire windows in both tops stamped with Teflon o-rings. The cell is immersed in a thermostatted water bath with ± 0.01ºC of stability. Temperature control was done with a RTD with a precision ±0.001 K probe contacting the cell, connected to a Hart Scientific PID controller. The internal agitation is assured by magnetic stirring. The pressure is controlled with a manometer (SETRA, model Datum 2000) with a precision of ±0.01Mpa.

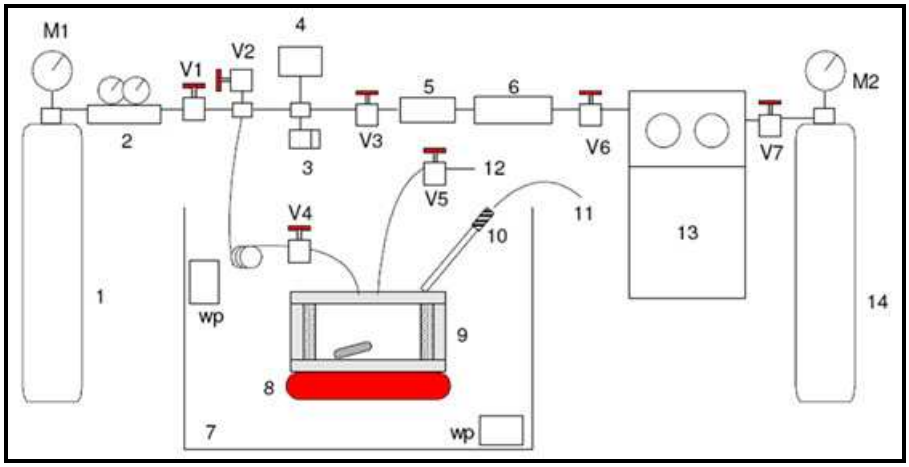

Figure 2.2 - Schematic representation of the apparatus used in the polymerization reactions. 1- nitrogen cylinder; 2- gas regulator; 3- rupture disc; 4- high-pressure manometer; 5- check-valve; 6- line filter; 7- water bath; 8- immersible stirrer; 9- high-pressure cell; 10- platinum resistance RTD probe; 11- temperature controller ; 12- vent; 13- pneumatic CO_2 compressor; 14- CO_2 cylinder; M1,M2- bourbon manometer; wp- water recirculation pump; V1 to V7- HIP valves.

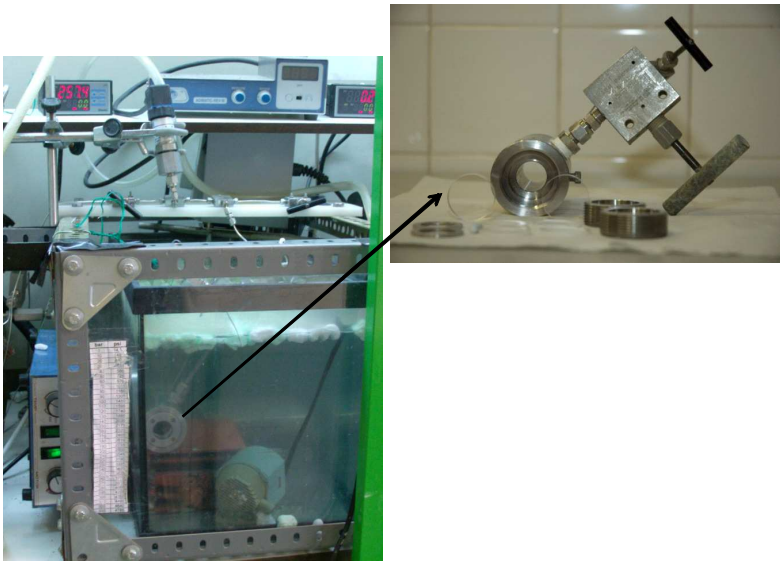

Figure 2.3 - Real apparatus of polymer synthesis

In a typical polymerization the cell is charged with MMA and MAA monomers, in composition ratios varying from 75-95% w/w of MMA and 5-25% w/w of MAA, and initiator (2% w/w of AIBN with respect to total mass of monomers). The cell is sealed and nitrogen is added to purge the cell. The nitrogen is slowly released and liquid carbon dioxide is loaded into the cell using a high-pressure compressor (NMA GmbH). The cell is immersed in the water bath at 65ºC and loaded with CO_2 up to 20 MPa.

The reaction was allowed to proceed for 24 hours under stirring. It could be seen through the sapphire windows that all polymerizations started as a completely homogeneous phase, with all reactants completely dissolved in scCO_2.

At the end of the reaction the resulting polymeric material was slowly washed with fresh high-pressure CO_2 for one hour in order to remove unreacted monomer.

2.2.2.2. Characterization of synthesized copolymers

Particle morphology observations were based on scanning electron microscopy (SEM) data. SEM micrographs were obtained on a Hitachi S-2400 equipment. All samples were mounted on aluminum stubs using carbon cement (D-400, Neubaeur Chemikalien) and were gold coated.

Average molecular weights of the polymer samples were determined by GPC using HPLC grade DMF as eluent. The solutions were analyzed in a KNAUER system with evaporative

light scatter detector from Polymer laboratories (temperature of evaporator: 175ºC, temperature of nebulizator: 85ºC and rate flow was 1.5mL min^{-1}). A series of two Polypore columns were used. Sample analyses were conducted at a flow rate of 1mL min^{-1}, at 85ºC.

^{1}H-NMR spectra were recorded on a Bruker ARX 400MHz spectrometer. Approximately 10 mg of sample were dissolved in 500 µL of deuterated acetone.

FT-IR measurements were performed using Winfirst Lite equipment (16 scans and 1cm^{-1} resolution). A small amount of each sample was mixed with dried KBr (1:5 mass ratio) and thin pellets were prepared.

Thermal analysis was carried out on a differential scanning calorimetry (DSC) instrument from Setaram (Model DSC 131) with a scan rate of 10 ºC min^{-1} and a temperature range of 25-250ºC. Approximately 10 mg of sample were used. The glass transition temperature is taken as the midpoint of the heat capacity transition between the upper and lower points of deviation from the extrapolated glass and liquid lines.

2.2.3. Membranes preparation

2.2.3.1. Membranes prepared by phase inversion method in $scCO_2$

Membranes production was undertaken in a high-pressure apparatus schematically presented in Figure 2.4. Membranes were prepared in a 200 mL stainless steel cylindrical high-pressure cell with an internal mechanism to homogenously disperse CO_2 in the top of the casting solution. Around the cell, two sapphire windows, sealed with a teflon o-ring, supports the membrane formation. The stainless steel cover of the cell contains openings for the inlet valve of CO_2 admission and pressure transducer. The cell is immersed in a visual thermostatted water bath, heated by means of a PID controller (Hart Scientific, Model 2200) that maintained the temperature within ±0.01 ◦C. The pressure is monitored with a pressure transducer (Setra Systems Inc., Model 204) with a precision of ±100 Pa. In a typical procedure, the casting solution is loaded into a teflon cap (with a diameter of 68 mm) which is placed inside of high-pressure vessel which is then immersed in the thermostated water bath. Approximately 400 mg of solution was spread over the sapphire window (with a diameter of 2.4 cm) in order to produce membranes with thickness ranging from 1 to 1.5 mm. The casting solutions were prepared by solubilizing the P(MMA-co-MAA) polymers in acetone with the following composition: 20, 30 and 40% w/w. CO_2 is added until the desired pressure, with an exact flow, using a Gilson 305 piston pump. After reaching the normal operational pressure, the supercritical solution passes through a back pressure regulator (Jasco 880-81) which separates

the CO_2 from the solvent. All the experiments were realized at 20±0.7 MPa with a CO_2 flow of 10.0 g min^{-1} during 2 h. At the end, the system is depressurized during 10 min and a thin homogeneous membrane is obtained.

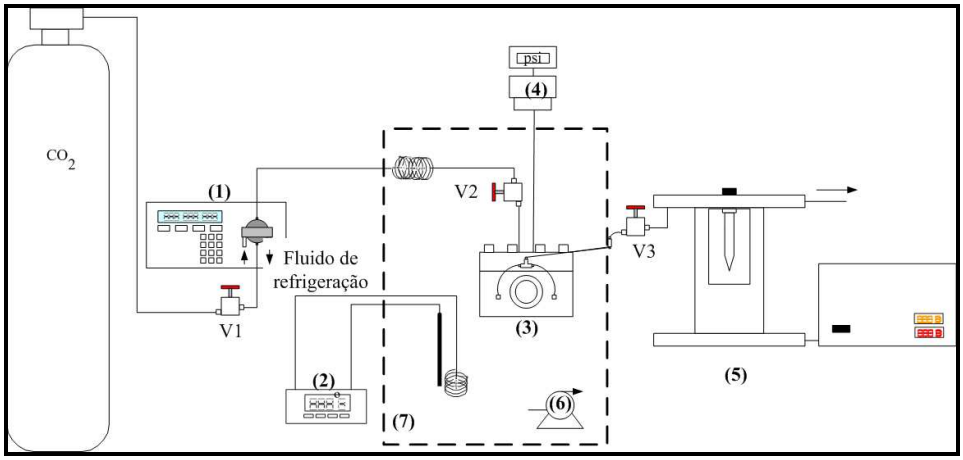

Figure 2.4 - Layout of the high-pressure apparatus for the membrane formation: (1) Gilson 305 piston pump; (2) temperature controller; (3) high-pressure cell; (4) pressure transducer; (5) back pressure regulator.

Figure 2.5 – Real apparatus of membranes preparation

2.2.3.2. Characterization of membranes

Membranes morphology studies were based on SEM data. SEM micrographs were obtained on a Hitachi S-2400 equipment. All samples were mounted on aluminum stubs using carbon cement (D-400, Neubaeur Chemikalien) and were gold coated.

The permeability to pure water was determined by measuring the water flux trough the membranes using a 10 mL filtration unit (Amicon Corp., Model 8010) with an effective area

of 4.1cm^2. All the experiments were carried out varying the applied hydrostatic pressure from 0-2.4 bar. At least three clean water flux measurements were performed for each membrane.

The permeability of the membranes was obtained by the slope of linear relation between flux and pressure, and it is given by Darcy Law:

$$F = Lp \times \Delta P$$

Figure 2.6 - Darcy's Law: F: Flux (L m^{-2}h^{-1}); Lp: Permeability (L m-2h-1bar-1); ΔP: Drop of pressure (bar)

Membrane hidrophobicity was evaluated through the measurement of the contact angles of water droplets Goniometer MODEL CAM 100.

The size porous distribution was determinated in a Micromeritics Auto Pore IV mercury porosimeter using sample weights between 0.080-0.122g in order to obtain a good distribution. These analyses were performed in two steps, first applying low pressure at 345 KPa and in the second applying high pressure at 223 MPa. The results were treated using SigmaPlot program.

The tensile properties of the membranes were determined with tensile testing equipment (*MINIMAT firm-ware* v.3.1) at room temperature. The samples were cut into strips with 2x15 mm^2. The length between the clamps was set at 5 mm and the speed of testing set at 0.1 mm min^{-1}. A full scale load of 20 N and maximum extension of 90 mm were used.

The elastic modulus was calculated from the slope of the linear portion of the stress-strain curve. Samples were tested in dry state at 25 ºC.

Load extension graphs were obtained during testing and converted to stress strain curves applying equations:

$$\text{Stress}=\sigma=F/A$$
$$\text{Strain}=\varepsilon=\Delta l/L$$

Figure 2.7 - Equation of stress and strain: F: Applied force; A: Cross sectional area; Δl: Change in length; L: Length between clamps

2.3. Results and Discussion

2.3.1. P(MMA-co-MAA) copolymers

2.3.1.1. Influence of polymers composition

The polymerization reaction of P(MMA-co-MAA) follow the scheme presented in Figure 2.8:

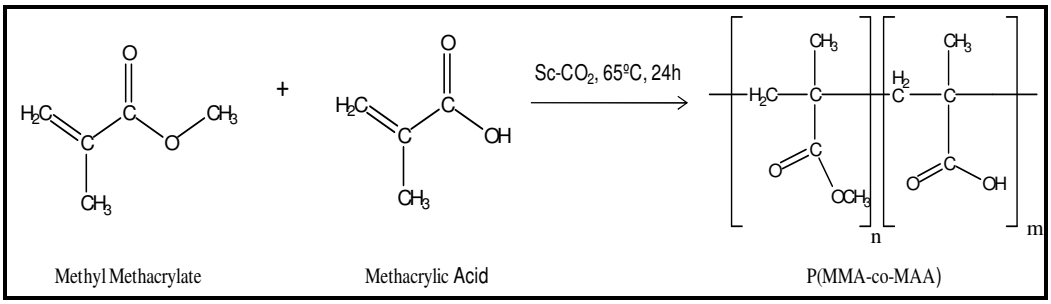

Figure 2.8 - Reaction synthesis of P(MMA-co-MAA)

Table 2.1 presents the characteristics of the polymer samples produced and the reaction yields obtained as a function of different initial compositions of monomers. The reactions were carried out at 20 MPa and 65ºC for 24h. High yields were obtained for all the tested compositions and the polymer morphology was similar in all experiments.

Table 2.1 - Effect of monomers concentration in polymerization of P(MMA-co-MAA) in $scCO_2$

Experiment	Copolymer	%MMA	%MAA	Yield	Polymer Morphology	Product
1	CO75_25	75	25	97	Aggregated	Powder
2	CO90_10	90	10	96	Aggregated	Powder
3	CO95_5	95	5	97	Aggregated	Powder

Figure 2.9 show the SEM images of the synthesized P(MMA-co-MAA) copolymers corresponding to the experiments 2 and 3. As it can be seen the materials have an irregular structure with very small particle agglomerates in a net. Similar structure was already obtained for other polymers synthesized by precipitation polymerization in $scCO_2$ [34].

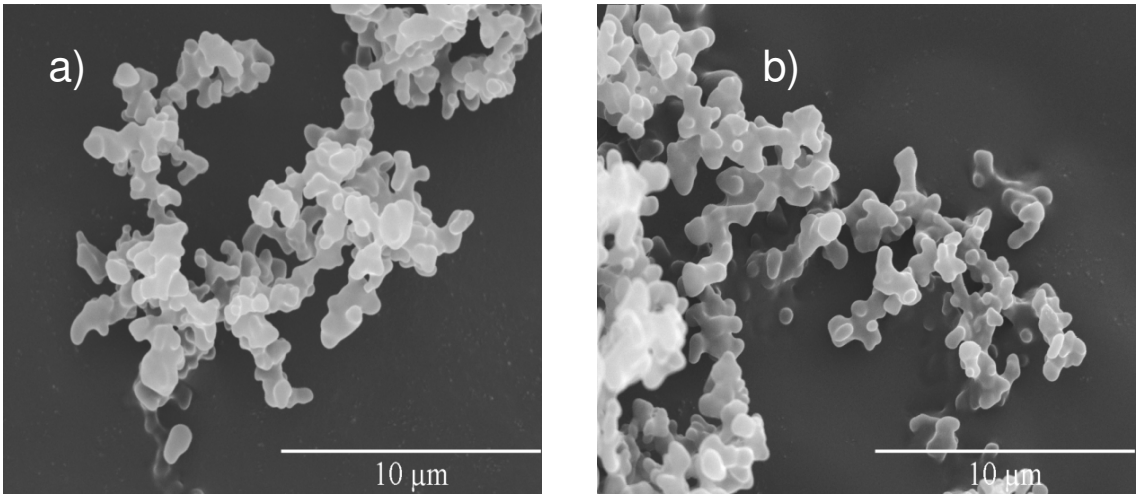

Figure 2.9 - SEM results of P(MMA-co-MAA): a) co90_10 1.5K b) co95_051.5K

Surfactants are a critical component in polymerizations due to the inherent insolubility of most polymers in CO_2 [35]. The stabilizers have been successfully employed in the heterogeneous polymerizations of CO_2-insoluble polymers, controlling the final properties and morphology of the synthesized polymer. In this case as the monomers are highly soluble in $scCO_2$ the polymerization could be performed to a certain extent without any surfactants and optimizing the morphology was not one of the objectives of the work.

The molecular weights and polydispersivity of synthesized copolymers are presented in Table 2.2.

Table 2.2- Molecular weights and polydispersion of P(MMA-co-MAA) copolymers

Polymer	M_n	M_w	M_w/M_n
co75_25	1906687	2307249	1.21
co90_10	187066	323127	1.72
co95_5	199532	257618	1.29

By increasing MAA amount a significant increase in the molecular weight could be observed in P(MMA-co-MAA) copolymers. A possible explanation for this effect can be the fact of MAA works as a surfactant or cross-linker increasing the solubility of copolymer and its molecular weight [36].

Polydispersion (M_w/M_n) results are closer to one, excepted in experiment 2, meaning that there are no large differences between molecular weights in mass and in moles. The polymeric materials produced in this work present polydispersion values (1.21-1.72) lower than the results reported in literature for P(MMA-co-MAA) polymers synthesized in conventional organic solvents (2.39-2.78) [6] and also lower than values reported for MMA copolymerizations with other monomers performed in supercritical medium (1.95-3.23) [37]. The obtained results confirm that in this work, particularly for experiment 1, high molecular weights were obtained surprisingly higher than the ones obtained also with conventional organic solvents [6].

2.3.1.2. ^{1}H-NMR and FT-IR analysis

^{1}H-NMR spectroscopy was performed for better understanding of the phase behavior and morphology of copolymers. Figure 2.10, Figure 2.11 and Figure 2.12 show the ^{1}H-NMR spectra of the produced polymers:

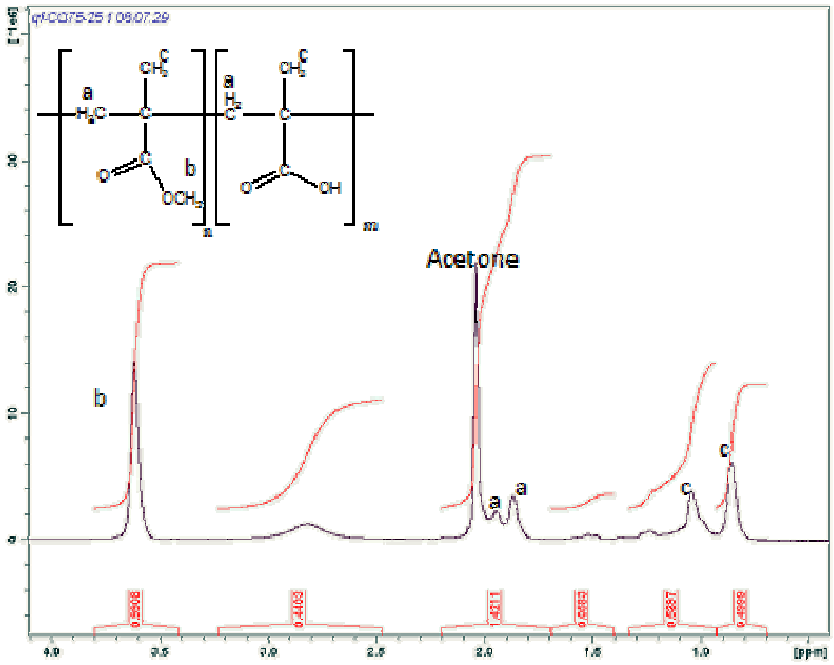

Figure 2.10 - ^{1}H-NMR spectrum of CO75_25

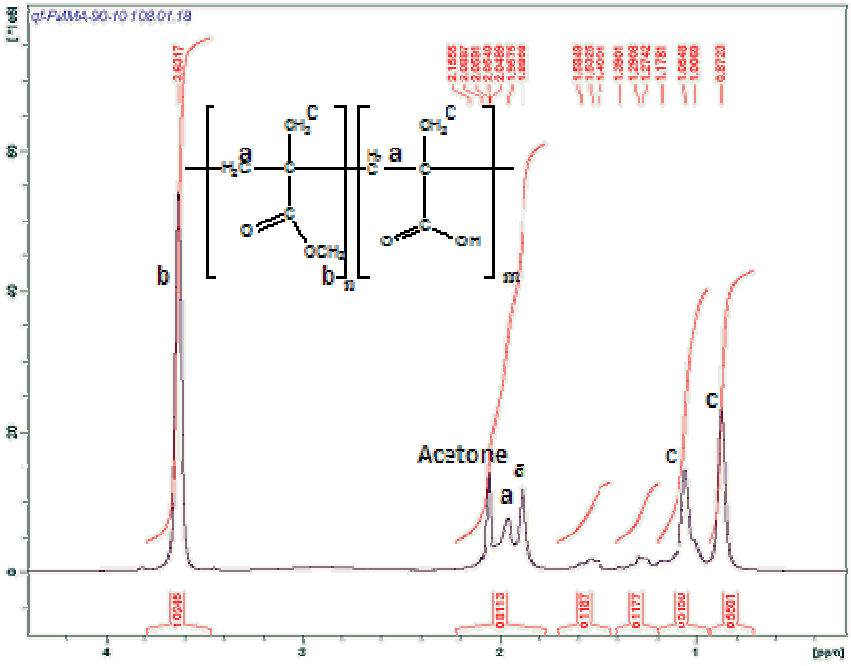

Figure 2.11 - ^{1}H-NMR spectrum of CO90_10

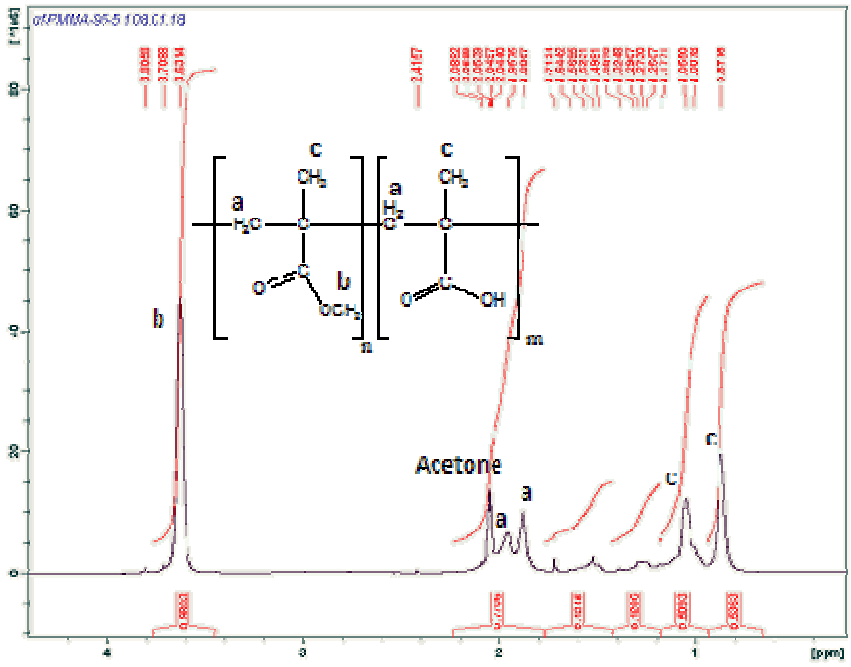

Figure 2.12 - ^{1}H-NMR spectrum of CO95_5

Comparing all ^{1}H-NMR spectra it is possible to observe that while decreasing the MAA proportion, they become more similar to the PMMA spectrum [38].Spectra show the expected peaks confirming that the desired copolymers were synthesized [38]. Figures also show the peak assessment.

The resonance band at δ~3.6 ppm is attributed to the methyl protons of the ester group, and bands at δ~1.5 to 2.0 and 0.8 to 1.2 ppm belong to the resonance absorptions of methylene and the pendant methyl protons, respectively [39].

Comparing the ratio between areas of CH_3 groups of MMA and MAA and the OCH_3 group of MMA it is possible to observe that these areas increase when the amount of MMA also increases, meaning that when the ratio between initial amounts of monomers change, the polymers conversion is different as it was pretended.

Figure 2.13 shows the FT-IR spectra of the copolymers. Results show the principal chemical groups of P(MMA-co-MAA) polymers.

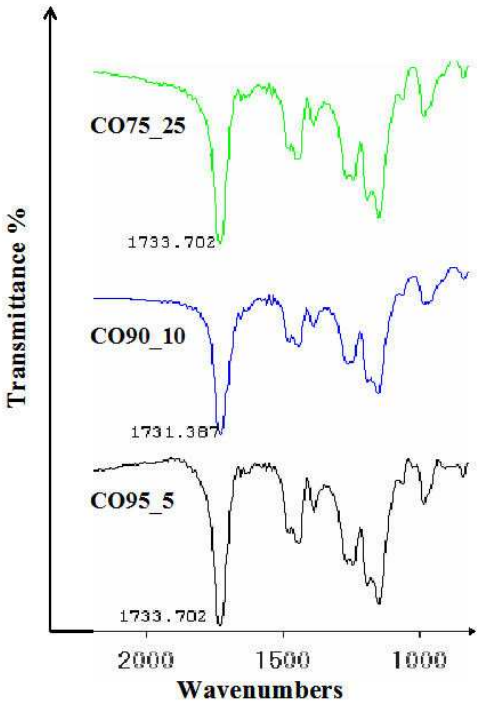

Figure 2.13 - FT-IR spectra of P(MMA-co-MAA)

Chemical structures of PMMA and PMAA are very similar. Usually the MAA unit may exist as the free state, self-associated dimmer, or inter-association with PMMA [6].

In the literature it is reported that the carbonyl stretching bands of MAA unit appear at 1742 and 1699 cm^{-1} for associated dimmer and free state, respectively [6]. In case of MMA unit, the carbonyl stretching bands appear at 1730 cm^{-1} [6]. However, MMA and MAA associations in blends and copolymers, the carbonyl stretching bands appear between 1675 and 1770 cm^{-1} according to the monomer ratio [6].

In the FT-IR spectra presented in Figure 2.13 it is possible to observe a characteristic peak of P(MMA-co-MAA) copolymers between 1731-1734 cm^{-1}. This peak can result of two overlapped peaks because the carbonyl of carboxylic acid and ester appears at 1710-1760 cm^{-1} and 1740-1750 cm^{-1}, respectively.

^{1}H-NMR and FT-IR analysis are complementary and confirm the synthesis of the P(MMA-co-MAA) copolymer.

2.3.1.3. Differential scanning calorimetry (DSC)

Thermal analysis is one of the most convenient methods to determine the miscibility in polymer blends [6]. The DSC results are in agreement with the results presented in literature [6].

Table 2.1 shows the different glass temperatures of the produced copolymers.

Table 2.3 – Glass temperatures of the copolymers samples

Polymer	Glass Temperature (ºC)
CO75_25	170.0
CO90_10	132.1
CO95_5	132.3

Higher glass temperatures were obtained for different experiments. The glass temperature increases by increasing the ratio of MAA in the copolymer. This was expected since the glass temperature of PMAA is approximately 200ºC while for PMMA is 120ºC [6, 40, 41]. The glass temperatures of copolymers are between these values however they are closer to the one of PMMA, because in all polymer synthesis the content of MMA is higher than MAA content.

Therefore, the DSC data obtained is consistent with the synthesis of the different P(MMA-co-MAA) copolymers.

By tuning the monomer ratio in the copolymer it is possible to create polymers with different and significant glass temperatures.

Nevertheless, the results obtained from all characterization techniques proved the success of P(MMA-co-MAA) synthesis.

2.3.2. P(MMA-co-MAA) membranes

2.3.2.1. Influence of the casting solution and porosity

In this study, the process parameters that were able to influence membrane formation - temperature (40ºC), pressure (20MPa) and depressurization rate (10 min) – were fixed. All the experiments were performed using a CO_2 flow of 10 mL min^{-1} for 2h.

Table 2.4 presents a summary of the casting solutions composition prepared as well as the membrane porosities obtained.

Observing the results it is possible to notice a clear dependence of the porosity, characteristic length and pore size with the polymer content in the casting solution. By increasing the polymer concentration in the casting solution a decrease in porosity characteristic length and pore size is observed.

The porosity also decreases in CO95_5 membranes when compared with CO90_10 membranes meaning that the porosity is not only affected by the concentration but also by the copolymer composition.

Table 2.4 - Effect of P(MMA-co-MAA) content in casting solution and in membranes porosity

Experiment	Polymer	%Polymer[a] (w/w_{total})	Membrane	Porosity (%)	Characteristic length (µm)	Pore Size (µm)
1	CO90_10	20	20CO90_10	65	24.1783	21
2	CO90_10	30	30CO90_10	56	1.8047	1
3	CO90_10	40	40CO90_10	55	0.8923	0.05 and 12
4	CO95_5	20	20CO95_5	58	64.4786	18
5	CO95_5	30	30CO95_5	56	1.8533	2
6	CO95_5	40	40CO95_5	45	0.9210	0.04 and 0.9

[a] % polymer (w/w_{total}) in casting solution

SEM micrographs show the different porous membranes that can be obtained just by changing the polymer concentration in the casting solutions.

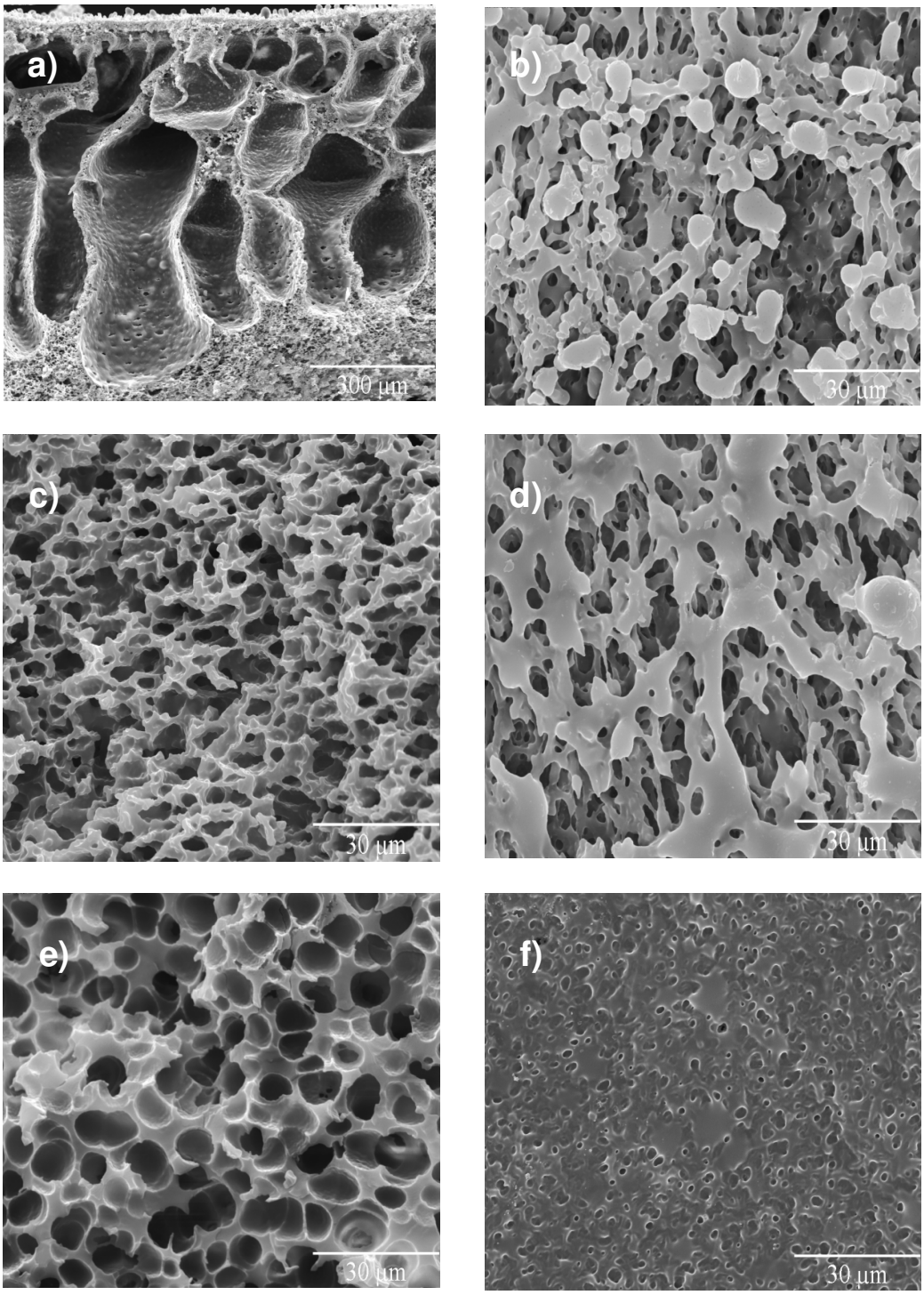

Figure 2.14 - CO90_10 Membranes: a) 20% (w/w) cross-section; b) 20% (w/w) surface; c) 30% (w/w) cross-section; d) 30% (w/w) surface; e) 40% (w/w) cross-section; f) 40% (w/w) surface.

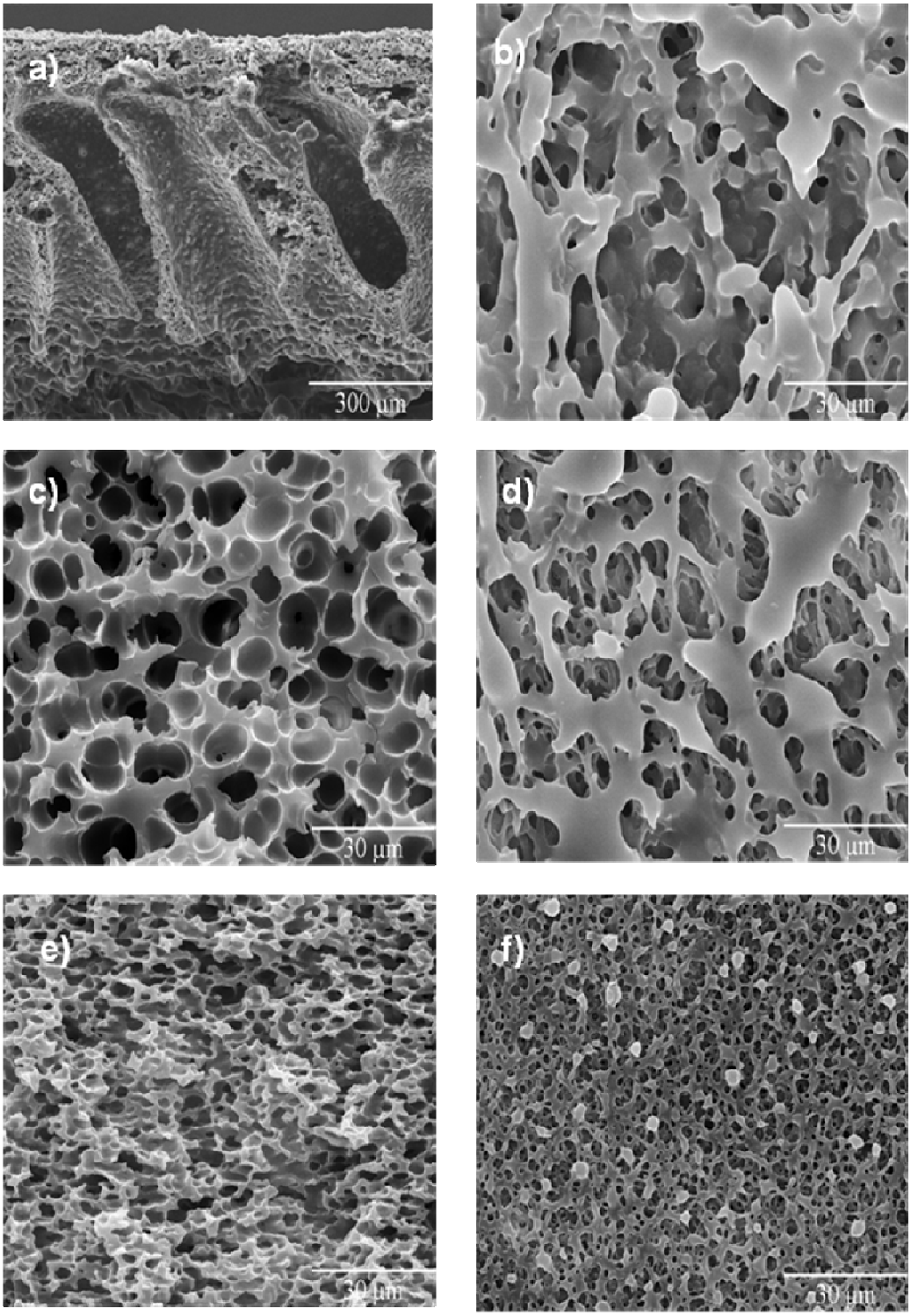

Figure 2.15 - CO95_5 Membranes: a) 20% (w/w) cross-section; b) 20% (w/w) surface; c) 30% (w/w) cross-section; d) 30% (w/w) surface; e) 40% (w/w) cross-section; f) 40% (w/w) surface.

To a better interpretation of the SEM results it is important to understand the possible routes that are available to produce different porous structures changing the polymer content in casting solution. The ternary diagram represented in Figure 2.16 shows these possible routes.

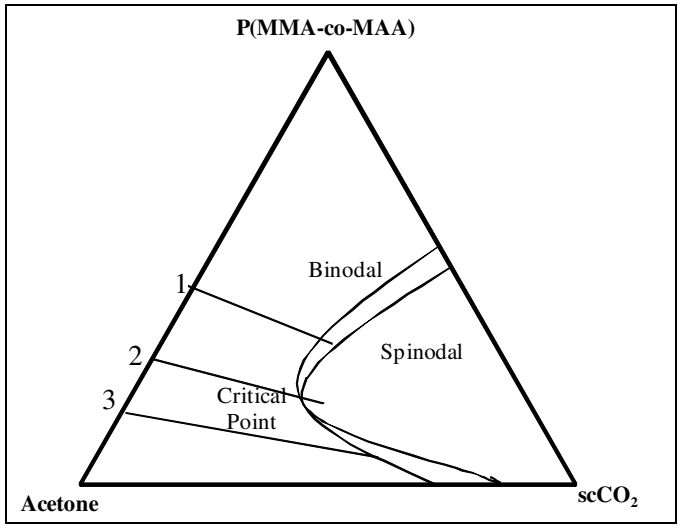

Figure 2.16 - Ternary phase diagram of a generic polymer(e.g. P(MMA-co-MAA)/solvent (e.g. acetone)/non-solvent (e.g. $scCO_2$) system with various composition paths indicated by numbers (adapted from [42])

As it was previously described, in this work all the parameters were fixed except the polymer concentration in casting solution.

The different paths indicated in the diagram show the three different kinds of mass transport that can occur during the polymer membranes formation. These are: path 1- the nucleation and growth of droplets of the polymer lean phase with further solidification of the polymer rich phase which forms the membrane cellular structure (dense structure); path 2- spinodal phase separation with subsequent solidification of the polymer rich phase which forms a bicontinous (spinodal) membrane structure and path 3- the nucleation and growth of droplets of the polymer rich phase is followed by solidification of the polymer rich phase which leads to the beads like particles [42, 43].

Observing the SEM micrographs presented in Figure 2.14 and Figure 2.15 it is possible to note a strong dependence of membranes morphology with the polymer concentration used in the casting solution. The same conclusion can be attempted for the results of porosity. Membranes produced from solutions with higher polymer content exhibit smaller pores than membranes prepared from more diluted solutions. This trend is in agreement with literature [42].

Figure 2.17 and Figure 2.18 show the pores size distribution of P(MMA-co-MAA) membranes.

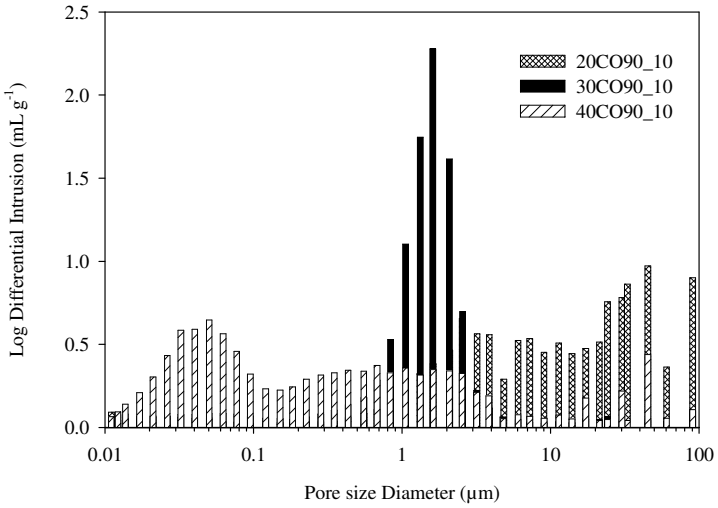

Figure 2.17 – Pore size distribution in CO90-10 Membranes

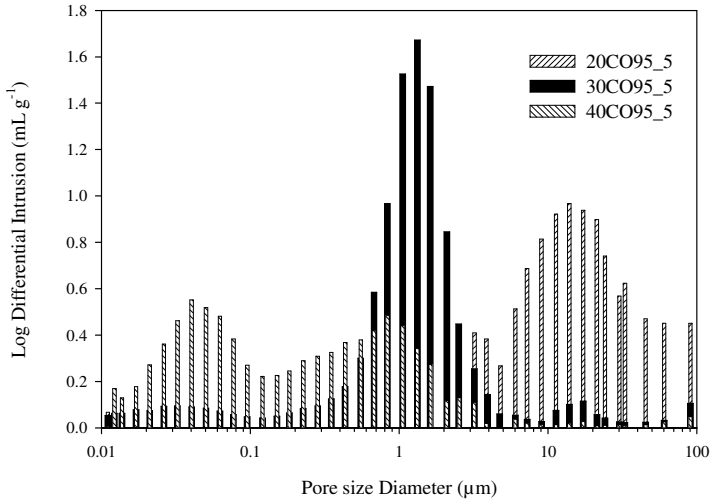

Figure 2.18 – Pore size distribution in CO95-5 Membranes

Data of mercury intrusion porosimetry show, in both cases, the presence of three distinct pore size distributions. 40CO90_10 and 40CO95_5 membranes have a broad porous distribution. This fact can have one explanation: when the casting solution is loaded into the casting disk some acetone evaporates because the casting solutions are saturated, resulting in the first pores formation (large pores). The second pores formation occurred by $scCO_2$ action (small pores due to the high polymer content present in the casting solution). Hence, these membranes contain two predominant mean pore sizes, in case of 40CO90_10 membrane one is 0.05 µm and the other is 12 µm and in case of 40CO95_5 membrane the mean pore sizes are 0.04 µm and 0.9 µm.

The mean pore size diameters of CO90_10 membranes with 20% (w/w) and 30% (w/w) of polymer are 21 µm and 1 µm, respectively, while CO95_5 membranes with 20% (w/w) and 30% (w/w) of polymer are 18 µm and 2 µm, respectively.

By varying the polymer content on the casting solution as well as changing the monomers ratio in polymers composition, it is possible to design different porous structures with different mean pore sizes.

Different pores sizes of PMMA or P(MMA-co-MAA) films can be found in the literature [44, 45], depending on the preparation method and parameters involved.

2.3.2.2. Water permeability and contact angles

The pure water flux which is defined as the volumetric flow rate divided by the membrane area and the pressure difference was determined for all the membranes varying the applied hydrostatic pressure from 0 to 3 bar.

Table 2.5 resumes the permeabilities and the contact angles of the different P(MMA-co-MAA) membranes.

Looking to the results it is possible to observe a relation between permeabilities and contact angles. It must be noted that contact angles measurements are dependent on the hydrophilicity, on the roughness and porosity of the surface membrane [33].

Table 2.5 – Effect of P(MMA-co-MAA) concentration in permeability and contact angles

Membrane	Permeability (L $m^{-2}h^{-1}$ bar^{-1})	Contact angle (º)
20CO90_10	89	104
30CO90_10	4	92
40CO90_10	-	85
20CO95_5	**	84
30CO95_5	18	98
40CO95_5	-	75

** Impossible measurement of permeability because water permeated without pressure being applied

Permeability data presented in Table 2.5 indicate that membranes permeability decrease for membranes prepared from more concentrated polymer-solvent solutions. Consequently, the contact angles decrease when permeability also decreases.

Figure 2.19 and Figure 2.20 show the profile of membranes water flux.

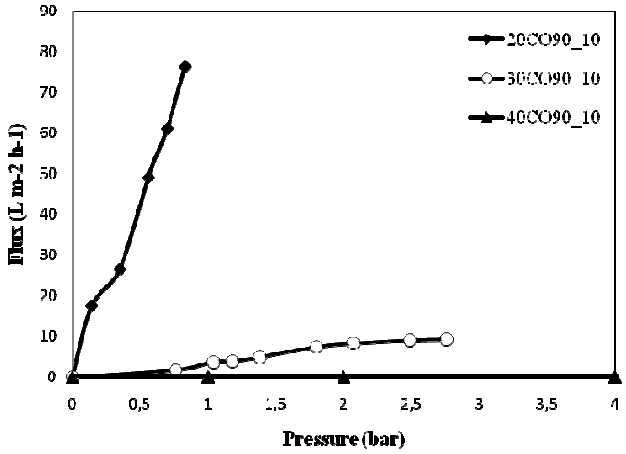

Figure 2.19 - Permeability of the CO90_10 membranes

Membranes prepared from more concentrated casting solutions show lower permeability values and this is explained by the pore sizes on the membranes surface, Figure 2.14 and Figure 2.15 When the pores are large the permeability is high as it occurs for the 20CO90_10 membrane, that has pores like channels, Figure 2.14. The opposite is also true. By increasing the polymer concentration in membranes preparation pores become smaller, the characteristic length decrease and consequently the permeability also decreases to such low values that cannot be experimentally measured as it was the case of the 40CO90_10 membrane.

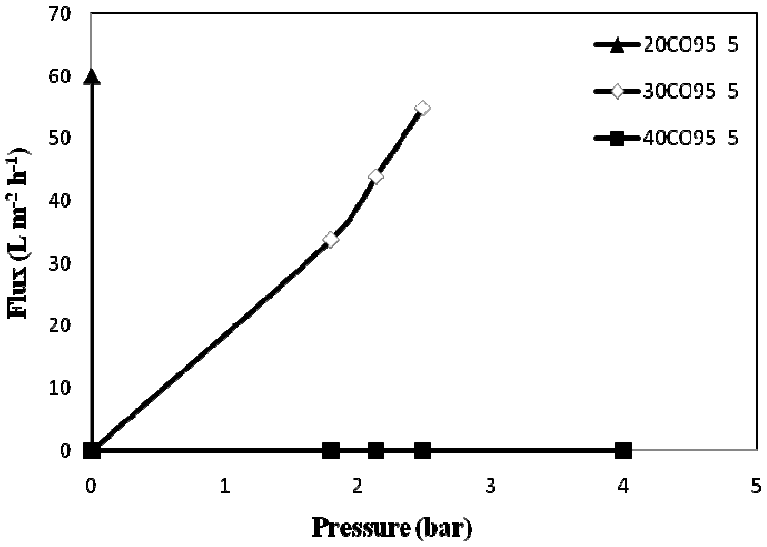

Figure 2.20 - Permeability of the CO95_5 membranes

A difference of 5% in the MAA ratio in the copolymer used for membranes preparation was enough to significantly change their water fluxes. The same tendency according to the concentrated casting solutions is observe. For the 20CO95_5 membrane it is not necessary to apply pressure to pass water through it. This behavior is explained by the large pores that this

membrane presents (Figure 2.15). Contrary, the 40CO95_5 membrane has the behavior previously mentioned to 40CO90_10 membrane: the pores on the membrane surface are small and the water does not pass through it, consequently, the permeability could not be determined. Only the 30CO95_5 membrane exhibit permeability control.

A recent study [46] showed that the irregular nature of PMMA pore surface can cause significant localized energy barriers inside the pore, thereby reducing the water flux. This effect can justify the behavior change between CO95_5 and CO90_10 membranes. Consequently, the decrease of MAA in this kind of membranes also can explain the reduction of permeability due to less OH groups on the membrane surface.

The measurement of contact angles is important to understand the chemical groups that are at the surface of the membranes and consequently their hydrophilicity. An increase of MAA concentration increases the carboxylic groups present in the membranes. It was expected that membranes with more carboxylic groups would have more interactions between water and hydroxyl groups leading to lower contact angles. However 20CO95_5 and 30CO95_5 membranes do not follow this behavior. A possible explanation can be the broad pores and the high permeability of this membrane. The experimental contact angle data are in accordance with the trend described in the literature for P(MMA-co-MAA) structures [47]. In general, the contact angles of CO90_10 should be lower than the ones of CO95_5 membranes, but this behavior is not clear due to the proximity of polymers composition.

In order to check if the anti-solvent used to induce the phase inversion has any influence in the groups presented on membrane surface, it was prepared one membrane of 30% (w/w) of CO90_10 by conventional phase inversion using water as anti-solvent. The contact angle measured with water was 46º. This means that the water affinity was higher for the membrane prepared with water than the membrane prepared with $scCO_2$. Water is polar while CO_2 is a non polar solvent, so this parameter is very important in the conception of the membrane which chemical groups are predominant on the membrane surface. However with $scCO_2$, it is possible to obtain “dried” surfaces without any contaminants and a high efficiency in morphology control.

2.3.2.3. Mechanical properties measurements

DMA was used to characterize the viscoelastic properties of the membranes developed in this work. Tensile tests provide an indication of the strength and elasticity of the membranes which are important for their different applications. Figure 2.21 and Figure 2.22 represent the

relation between the force (stress) applied to the membranes and their elongation capacity (strain). Usually higher porosities lead to higher tearing stress [29], however this trend can be influenced by other parameters such as pore sizes or pore size distribution [29]. 20CO90_10 and 30CO90_10 membranes show the expected behavior, 30CO90_10 membrane was the membrane that supported more stress (10 MPa), while the 20CO90_10 membrane supported much less (5 MPa), but both exhibited the same elongation (8%) at failure, (please refer to Figure 2.21.). However, the maximum tensile strength of 40CO90_10 was 8.5 MPa, achieved at an ultimate strain of 10%. As it was described in 2.3.2.1, 40CO90_10 has a very broad pore diameter range with resulting two different mean pore sizes, and these morphological characteristics assume an important role in their mechanical behavior.

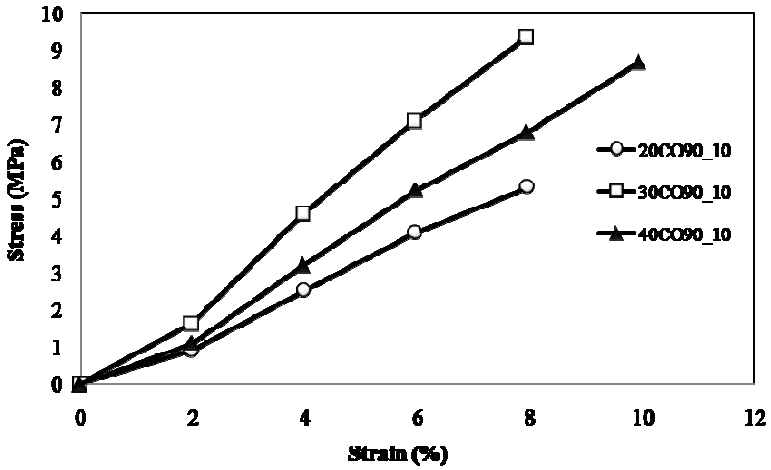

Figure 2.21 – Effect of P(MMA-co-MAA) concentration in the mechanical properties of CO90_10 membranes

The stress/strain plot of CO95_5 membranes is presented in Figure 2.22. The ultimate elongations increased from 6 % to 16% with increasing concentration of the casting solutions. The stress at brake followed a different trend: 20CO95_5 and 40CO95_5 had similar values (3.5 MPa and 4.5 MPa, respectively,) but 30CO95_5 exhibited much higher value (7.5 MPa).

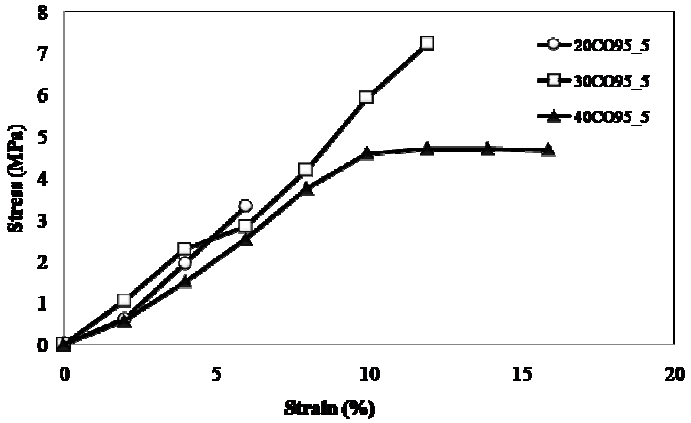

Figure 2.22 - Effect of P(MMA-co-MAA) concentration in the mechanical properties of CO95_5 membranes

CO90_10 and CO95-5 membranes present different mechanical behavior, however in both cases it is possible to observe a relevant dependence of their stress at brake and their achieved elongation with the polymer concentration used in the casting solutions. Looking to the results for the 40CO95_5 membrane it is possible to observe that two behavior types are present: elastic (0-10%) and plastic (10-16%). This can be explained by the fact that the polymer used in the membrane preparation has low MAA content (5%) and the polymer concentration in the membrane is the highest, therefore, this is the case where the amount of MMA is maximum. Both facts explain the trend for the CO95_5 membranes with the evident loss of elastic behavior.

PMAA structures have a strong mechanical elastic behavior [48] and it justifies the main differences between the CO90_10 and CO95_5 membranes.

Membrane rigidity is translated by Young modulus, which is the slope of stress-strain. A brief resume of Young modulus of all prepared membranes is presented in Table 2.6.

Table 2.6 - Young modulus of P(MMA-co-MAA) membranes

Membrane	Young Modulus (MPa)
20CO90_10	69
30CO90_10	121
40CO90_10	89
20CO95_5	50
30CO95_5	60
40CO95_5	40

The results in Table 2.6 suggest that Young modulus tends to decrease when MMA content increases in the polymer. The same trend is observed when polymer concentration increases in casting solution.

PMMA has excellent high mechanical strength [8], however it is clearly that MAA content improve the mechanical properties of MMA. Young modulus data show that CO90_10 membranes are more rigid than CO95_5 membranes. In research found in literature it is evident the effort to improve mechanical properties of PMMA structures [41, 49] being PMAA used to improve the material properties [6].

2.4. Conclusion

This work reports the P(MMA-co-MAA) synthesis using supercritical carbon dioxide and the production of P(MMA-co-MAA) membranes using a CO_2-assisted phase inversion method.
$ScCO_2$ showed to be a versatile solvent to produce different porous structures with different chemical and physical properties and without traces of organic solvents.
P(MMA-co-MAA) was synthesized with success. Using ^{1}H-NMR and FTIR it was possible to identify the characteristic chemical groups of this copolymer as well as to analyze the changes introduced in the polymer properties by adding MAA. When the amount of MAA increased in the polymer content, the physical properties such as average molecular weight and glass transition temperature also increased. Consequently, the membranes prepared with these copolymers also showed improvement on mechanical properties and a better morphology control with the increase of MAA content. The presence of OH groups introduced by MAA on membrane surfaces was confirmed by contact angles measurements with a polar solvent, water. The membranes permeability also confirmed the dependence of water fluxes with the polymer content used in the casting solutions what is related with their morphological characteristics (mean pore sizes, porosity).
P(MMA-co-MAA) polymers and membranes characterization shows that these membranes have the desired requirements and properties to be considered as potential matrices in separation devices.

2.5. References

1. Giles, M.R., Hay, J. N., Howdle, S.M., *The copolymerisation of methyl and ethyl methacrylate in supercritical carbon dioxide.* Macromol. Rapid Commun, 2000. **21**(15): p. 1019-1023.
2. Silvares, A., et al., *Optimization of the photochemically initiated polymerization of methyl methacrylate.* Chemical Engineering and Processing, 2006. **45**: p. 1001-1010.
3. Nalawade, S., Picchion, F., Jannsen, L., *Supercritical carbon dioxide as a green solvent for processing polymer melts: Processing aspects and applications.* Progress in Polymer Science, 2006. **31**: p. 19-43.
4. Arita, T., et al., *High-pressure atom transfer radical polymerization of methyl methacrylate for well-defined ultrahigh molecular-weight polymers.* Polymer, 2008. **49**: p. 2426-2429.
5. Kang, B.S., Kim, S.G., Kim, Joo-Sik., *Thermal degradation of poly(methyl methacrylate) polymers: Kinetics and recovery of monomers using a fluidized bed reactor.* Journal of Analytical and Applied Pyrolises, 2008. **81**: p. 7-13.
6. Chih-Feng., H., *Comparison of hydrogen bonding interaction between PMMA/PMAA blends and PMMA-co-PMAA copolymers.* Polymer, 2003. **44**: p. 2965-2974.
7. Kim, W.S., et., al., *Diffraction efficiency behavior of photopolymer based on P(MMA-co-MAA) copolymer matrix.* Optical Materials, 2007. **29**: p. 1736-1740.
8. Wang, M., Hshie, A. J., Rutledge, G. C., *Electrospinning of poly(MMA-co-MAA) copolymers and their layered silicate nanocomposites for improved thermal properties* Polymer, 2005. **46**(10): p. 3407-3418.
9. Lora, M., McHugh, M. A., *Phase behavior and modeling of the poly methyl methacrylate.–CO –methyl methacrylate system.* Fluid Phase Equilibria, 1999. **157**: p. 285-297.
10. Christian, P., et., al., *Free Radical Polymerization of Methyl Methacrylate in Supercritical Carbon Dioxide Using a Pseudo-Graft Stabilizer: Effect of Monomer, Initiator, and Stabilizer Concentrations.* Macromolecules, 2000. **33**: p. 9222-9227.
11. Muth, O., Hirth, Th., Vogel, H., *Polymer modification by supercritical impregnation.* Journal of Supercritical Fluids, 2000. **17**: p. 65-72.
12. Dai, S., Ravi, P., Tam, K. C., *pH-Responsive polymers: synthesis, properties and applications.* Soft Matter, 2007. **4**: p. 435-449.

13. Hsiao, Y.-L., Desimone, M.J., *Dispersion Polymerization of Methyl Methacrylate in Supercritical Carbon Dioxide: Influence of Helium Concentration on Particle Size and Particle Size Distribution.* John Wiley & Sons, 1996. **97**: p. 2009-2013.
14. Lepilleur, C., Beckman, E. J., *Dispersion Polymerization of Methyl Methacrylate in Supercritical CO_2.* Macromolecules, 1997. **30**: p. 745-756.
15. Park, J.Y., Shim, J.J., *Emulsion stability of PMMA particles formed by dispersion polymerization of methyl methacrylate in supercritical carbon dioxide.* Journal of Supercritical Fluids, 2003. **27**: p. 297-307.
16. Davies, O.R., et al., *Applications of supercritical CO_2 in the fabrication of polymer systems for drug delivery and tissue engineering.* Advanced Drug Delivery Reviews, 2006. **60**: p. 373-387.
17. Yagci, Y., Yildiz, U., *Redox polymerization of methyl methacrylate with allyl alcohol 1,2-butoxylate-block-ethoxylate initiated by Ce(IV)/HNO3 redox system.* European Polymer Journal, 2005. **41**: p. 177-184.
18. Lung, C.Y.K., Darvell, B.W., *Methyl methacrylate monomer–polymer equilibrium in solid polymer.* Dental Materials, 2007. **23**: p. 88-94.
19. Hester, J.F., Olugebefola, S. C., Mayes, A. M., *Preparation of pH-responsive polymer membranes by self-organization.* Journal of Membrane Science, 2002. **208**: p. 375-388.
20. Kumar, A., Srivastava, A., Galaev, I.Y., Mattiasson, Bo., *Smart polymers: Physical forms and bioengineering applications.* Progress in Polymer Science, 2007. **32**: p. 1205-1237.
21. Wang, S., et al., *Experimental study of the control of pore sizes of porous membranes applying chemicals methods.* Desalination, 2005. **177**: p. 7-13.
22. Hu, C.-C., et al., *Effect of physical aging on the gas transport properties.* Journal of Membrane Science, 2007. **303**: p. 29-36.
23. Hu, C.-C., et al., *Zeolite-filled PMMA composite membranes: influence of coupling agent addition on gas separation properties.* Desalination, 2006. **193**: p. 14-24.
24. Silvestri, D., et al., *Molecularly imprinted membranes for an improved recognition of biomolecules in aqueous medium.* Journal of Membrane Science, 2006. **282**: p. 284-295.
25. Aungsupravate, O., et al., *Water vapour transmission in butadiene–MMA–methacrylic acid latex films.* European Polymer Journal, 2008. **44**: p. 342-356.

26. Kho, Y.W., Kalika, D. S., Knutson, B.L., *Precipitation of Nylon 6 membranes using compressed carbon dioxide.* Polymer, 2001. **42**: p. 6119-6127.
27. Reverchon, E., Cardea, S., Rappo, E. S., *Production of loaded PMMA structeres using the supercritical CO2 phase inversion process.* Journal of Membrane Science, 2006. **273**: p. 97.
28. Reverchon, E., Cardea, S., *Formation of polysulfone membranes by supercritical CO2.* Journal of Supercritical Fluids, 2005. **35**: p. 140-146.
29. Kim, M.-S., Lee, Sang-Joon., *Characteristics of porous polycarbonate membrane with polyethylene glycol in supercritical CO2 and effect of its porosity on tearing stress.* Journal of Supercritical Fluids, 2004. **31**: p. 217-225.
30. Xu, Q., et., al., *Effect of different experimental conditions on biodegradable polylactide membranes prepared with supercritical CO2 as nonsolvent.* J.Appl. Polym Sci, 2005. **98**: p. 831.
31. Temtem, M., Casimiro, T., Aguiar-Ricardo, A., *Solvent power and depressurization rate effects in the formation of polysulfone membranes with CO2-assited phase inversion method.* Journal of Membrane Science, 2006. **283**: p. 244-252.
32. Matsuyama, H., et., al., *Effect of organic solvents on membrane formation by phase separation with supercritical CO2.* Journal of Membrane Science, 2002. **204**: p. 81.
33. Temtem, M., Casimiro, T., Mano, J. F., Aguiar-Ricardo, A., *Preparation of membranes with polysulfone/polycaprolactone blends using a high pressure cell specially designed for a CO2-assisted phase inversion.* Journal of Supercritical Fluids, 2008. **43**(3): p. 542-548.
34. Casimiro, T., et al., *Synthesis of highly cross-linked poly(diethylene glycol dimethacrylate) microparticles in supercritical carbon dioxide.* European Polymer Journal, 2005. **41**: p. 1947-1953.
35. Kendall, J.L., et., al., *Polymerizations in supercritical Carbon Dioxide.* Chem. Rev., 1999. **99**: p. 543-563.
36. Temtem, M., Casimiro, T., Mano, J. F., Aguiar-Ricardo, A., *Green synthesis of a temperature sensitive hydrogel.* Green Chemistry, 2007. **9**: p. 75-79.
37. Shin, J., et al., *Dispersion Polymerization of Methyl Methacrylate using Poly(HDFDMA-co-MMA) as a Surfactant in Supercritical Carbon Dioxide.* Ind. Eng. Chem. Res., 2008. **47**: p. 5680–5685.

38. Xiao-Ping, C., Kun-Yuan, Q., *The in situ atom transfer radical polymerization of MMA using the TD-FeCl3-PPh3 initiating system.* New J. Chem., 2000. **20**: p. 865-869.

39. Yang, B.H., et., al., *Synthesis and characterization of poly(methyl methacrylate-co-polyhedral oligomeric silsesquioxane) hybrid nanocomposites.* Chinese Chemical Letters, 2007. **18**: p. 960-962.

40. Chang, Z., Liu, G., Zhang, Z., *Effects of electric fields in polymerization on enthalpy of PMAA anhydridization.* Thermochimica Acta, 2004. **411**: p. 95-100.

41. Carrizales, C., et al., *Thermal and mechanical properties of electrospun PMMA, PVC, Nylon 6, and Nylon 6,6.* Polym. Adv. Technol., 2008. **19**: p. 124-130.

42. Reverchon, E., Cardea, S., *Formation of cellulose acetate membranes using a supercritical fluid assisted process.* Journal of Membrane Science, 2004. **240**: p. 187-195.

43. Reverchon, E., Cardea, S., Rapuano, C., *Formation of Poly-Vinyl-Alcohol Structures by Supercritical CO2.* Journal of Applied Polymer Science, 2007. **104**: p. 3151–3160.

44. Yanase, I., Ishikawa, Y., Matsuura, S., Kobayashi, H., *Effects of PMMA on porous structure of pollucite.* Journal of the European Ceramic Society, 2006. **26**: p. 474-479.

45. Lin, D.-J., Chang, C-H., Lee, C-H., Cheng, L-P., *Preparation and characterization of microporous PVDF/PMMA composite membranes by phase inversion in water/DMSO solutions.* European Polymer Journal, 2006. **42**: p. 2407-2418.

46. Suk, M.E., Raghunathan, A. V., Aluru, N. R., *Fast reverse osmosis using boron nitride and carbon nanotubes.* Applied Phisics Letters, 2008. **92**: p. 133120 (1-3).

47. Zuyderhoff, E.M., et al., *An AFM, XPS and wettability study of the surface heterogeneity of PS/PMMA-r-PMAA demixed thin films.* Journal of Colloid and Interface Science, 2008. **319**: p. 63-71.

48. Turner, J.S., Cheng, Y.L., *Heterogeneous polyelectrolyte gels as stimuli-responsive membranes.* Journal of Membrane Science, 1998. **148**: p. 207-222.

49. Zeng, J., et al., *Processing and properties of poly(methyl methacrylate)/carbon nano fiber composites.* Composites: Part B, 2004. **35**: p. 173-178.

3 Green Affinity Membranes

3.1 Introduction

3.1.1 Antibodies and Related Molecules

Antibodies or immunoglobulins are important components of the animal immune system present in the serum and tissue fluid. Structurally, antibodies are glycoproteins with a Y-shaped building block comprised of two identical light chains (L) (~25 kDa) and two identical heavy chains (H) (~50 kDa), associated by disulphide covalent forces and by non-covalent interactions [1]. Antibodies bind to target molecules with high affinity and specificity. Although naturally produced by the immune system, the necessity for antibodies with unique specificity at a large scale has encouraged the generation of new technologies for the production of biopharmaceutical-grade antibody preparations [2]. The use of antibodies, particularly monoclonal antibodies (Mabs), as effective therapeutics in inflammation, cancer, and infectious diseases, is of major importance and represents a multibillion-dollar market opportunity [1]. Target regions of antibodies have been combined into small functional monomeric or multimeric proteins such as Fab and $F(ab')_2$ fragments, single-chain variable fragments (ScFv) which are heterodimers of V_H and V_L stabilized by an hydrophilic linker—and combination of these as diabodies and triabodies.

There are many types of antibodies such as: chimeric, CDR-grafted, transgenic, recombinant fragments, fusion and bispecific. Chimeric monoclonal antibodies are 60-70% human and are obtained by exchanging the variable domain (Fv's) of the human antibody heavy and light chain genes for those derived from the rodent monoclonal. CDR-grafted antibodies, developed in the early 1990's, represented a step further in the humanization of murine Mab's. The epitope is confined to the CDR (complementary-determining regions) and each domain (VH and VL) possesses three of these regions, which are flanked by framework regions. The basic idea of transgenic antibodies appeared in the 1990's and it is related with human antibodies that can be obtained by genetically engineering the immune system of the host organisms [2].

The recombinant fragments are small functional proteins. Antibody fragments containing the CDR regions, such as F(ab)2, Fab, and scFv's (miniantibodies), may have particular advantages over intact antibodies. Fusion and bispecific antibodies were target of several constructs, where the antibody or fragment may be endowed with new properties through fusion with a non-immunoglobulin molecule (ligand). The ligand must not block the regions

of the antibody that are designed to perform their biological action. Antibody-like structures are antibodies that can also be engineered in order to obtain compact and multivalent structures like diabodies, triabodies, etc [2].

Monoclonal antibodies (MAbs) dominate today's biopharmaceutical pipeline products. Commercial manufacturing of a therapeutic antibody requires a process that delivers high yield and process reliability while producing an extremely pure product [3].

Approximately 100 diagnostic and several therapeutic MAbs have been approved worldwide by the regulatory agencies in the last two decades. Downstream processing can contribute up to 80% of the total costs of a biopharmaceutical, which enhances the need for the development of efficient methods for large scale of MAbs purification [4].

3.1.2 Purification of Antibodies

Efficient recovery of native or engineered antibodies from cell culture media is a critical part in minimizing manufacturing costs. Consequently, the downstream processing is highly dependent on the starting material that contains the protein or antibody of interest, together with culture medium components [2].

Rapid developments in biotechnology and the pharmaceutical potential of biomolecules are fueling demand for reliable, as well as efficient methods to purify preparative amounts of proteins, peptides, nucleic acids and antibodies [5].

A typical large-scale monoclonal antibody purification process is often built around the employment of immobilized protein A as the primary capture and purification step in combination with other column operations [3].

There is no standard procedure for the purification of antibodies but in general, the procedure involves typical steps. Initially the volume decreases and most of the water and other main contaminants are eliminated. Next, an intermediary purification is performed (reaching 40-90% of the final degree of purity proposed) and a final purification (~100%) [1]. Usually the initial enrichment use precipitation or filtration techniques where several steps of chromatography are adapted and subsequent purification stages.

The tendency in purification processes is the use of chromatographic matrices. However, non-chromatographic techniques deserve attention for antibodies purification because they skirt some of the problems associated to chromatographic packings.

3.1.2.1 Affinity Separation Techniques

3.1.2.1.1 Affinity Chromatography

Affinity chromatography, developed in 1968, is the most famous technique for the purification of antibodies [6].

Affinity chromatography is a purification method that exploits the biospecific interactions between a protein and a ligand, to economically purify proteins present at very low concentration in complex solutions [7].

The affinity ligands are immobilized on the chromatographic gel through extended hydrocarbon chains which place the ligand at varying distance from the gel matrix backbone; the covalent attachment of ligands to agarose or polyacrylamide gels is made through amino, carboxyl or imidazole groups of the ligand [8].

Biomimetic ligands have been investigated extensively in recent years. These are synthetic chemicals bearing constellations of functional groups which mimic natural ligands but which are easier to produce, less expensive and are more stable [9-12].

The synthesis of these ligands in solution allows validation of each synthetic step, chemical characterization of intermediates, confirmation of the final structure and immobilization onto the solid phase of a defined chemical entity with specified stability, toxicity and efficacy [10].

A great example of biomimetic ligands is the group of protein A mimetics, applied in the purification of antibodies. The general technologies used in the production of biomimetic affinity ligands are rational design (involve modeling protein-ligand interactions and computational tools), synthesis of combinatorial libraries (as a tool to generate large numbers of compounds), and, high-throughput screening strategies (as a tool to generate and select biologically active molecules) [2].

According to the target molecule to separate a new strategy can be designed in order to find something closer of the "ideal molecule" [13].

The biomimetic ligands considered for antibody purification include the synthetic bifunctional ligand (22/8) immobilized in a agarose support, which creates a robust, highly selective affinity adsorbent for human immunoglobulin G (IgG) [10].

In 2006 Feng and co-authors synthesized a novel biomimetic ligand, *N*-benzyloxycarbonyl-$_L$-tyrosine (*N*-cbz-$_L$-Tyr) that was screened by a combination method of molecular docking and immobilized receptor technique. Then, *N*-cbz-$_L$-Tyr was immobilized on Sepharose CL-4B preparing a specific affinity adsorbent for immunoglobulin G (IgG). The experiments proved that *N*cbz- $_L$-Tyr is an effective mimetic ligand for IgG [14].

Figure 3.1 show a schematic representation of the generic steps in an affinity chromatography process.

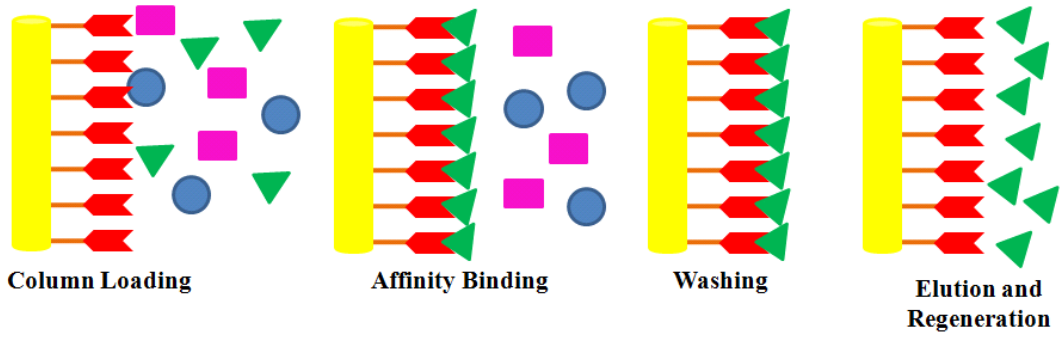

Figure 3.1 - Schematic representation of the main steps in affinity chromatography

Chromatographic processes are traditionally carried out in packed bed columns, which have several limitations. The pressure drop across a packed bed is generally high and tends to increase during a process due to the combined effects of bed consolidation, and bed column blinding caused by accumulated material. Another limitation in conventional chromatography is the dependence on intra-particle diffusion for the transport of solute molecules to their binding sites within the pores. This increases the process time since transport of macromolecules by diffusion is slow, and particularly so when it is hindered [15].

However, there are other alternative techniques that attempt to circumvent such problems including the use of different modes of affinity interactions such as expanded-bed affinity (EBA), affinity extraction, affinity precipitation and membranes [2].

Expanded bed chromatography has been used to recover proteins directly from unclarified feedstocks such as yeast and bacteria homogenates, mammalian and hybridoma cell culture fluid, and transgenic milk [16]. This methodology is just applicable in a narrow range of hydrodynamic parameters as viscosity.

Affinity precipitation is usually introduced in the early stage of downstream processing. This technique permits specific precipitation of oligomeric proteins or proteins containing multiple binding sites using bifunctional ligands. The precipitation can be manipulated by changes of environmental conditions (pH, salt, temperature, etc) [17].

3.1.2.1.2 Affinity Membranes

In recent years alternatives to conventional gel bead chromatography have been proposed and marketed, including perfusion chromatography and membrane chromatography [18].

Adsorptive membranes are available in a range of chemistries and geometries which permit their applications as clarification, concentration, fractionation and purification tools in a biorecovery sequence.

Affinity membranes were designed to bypass the limitations of conventional affinity gel chromatography: slow intraparticle diffusion in large beads, or low flow-rates due to high–pressure drops in small beads [7]. These membranes exhibit high binding capacities, similar in magnitude to packed columns and proteins can rapidly be concentrated 10-fold or more with 85-100 % recovery using stepwise elution. Analytical separations of proteins equivalent to those of column chromatography are reached by using sufficient numbers of membrane stacks and gradient elution methods [18].

Affinity membranes allow high flow rates to be achieved at low pressures, enabling the processing of large volumes within short process times [4].

Generally speaking, three types of membrane configuration are used in protein bioseparation: flat sheet, hollow fibers and radial flow [15].

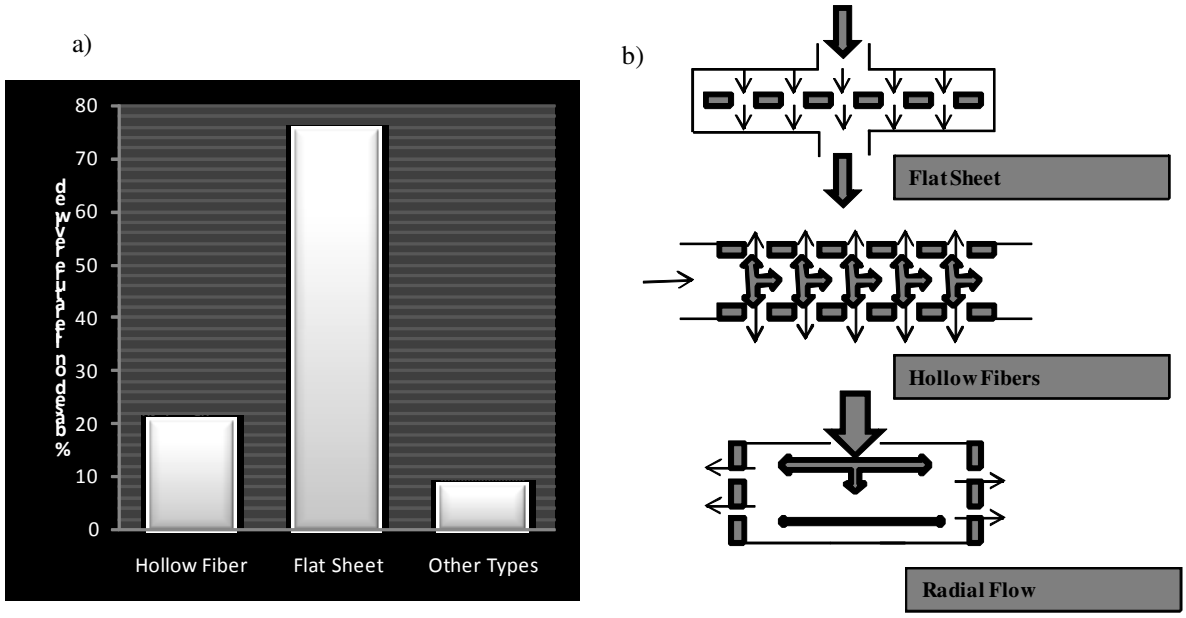

Figure 3.2- a) Membrane adsorber types (geometry) b) Flow in membrane adsorbers (adapted from [15])

In flat sheet membranes, the liquid is usually introduced normal to the membrane surface. In hollow fiber membranes the liquid initially flows parallel to the membrane surface (Figure 3.2) [15]. Flat sheet membranes are by far most widely used. In this work the membranes can be considered flat sheet.

Different types of materials can be used in membrane separation processes as well as specific ligands for targets molecules [15].

The materials used for affinity membranes can be roughly divided into two groups, natural and synthetic polymers [19]. Generally, the synthetic polymers, such as nylon, polysulfone, and polyglycidyl methacrylate are suitable from a mechanical point of view, but are less suitable for the immobilization of the ligand due their low capability. The natural macromolecular materials, such as agarose, dextrin, chitosan and cellulose, are good affinity supports because they are compatible with usual ligands, but are often difficult to process as membranes [19].

In 1995, Roper and Lightfoot reviewed the separation of biomolecules using adsorptive membranes including affinity ion-exchange an hydrophobic membranes [5].

In 1996, Bueno and co-workers studied experimental kinetic aspects of hollow fiber membrane-based pseudobioaffinity filtration [20]. The pseudobiospecific affinity ligand (l-histidine) was immobilized through an ether linkage onto a poly(ethylene vinyl alcohol) hollow fiber cartridge to obtain an affinity support for IgG removal from human plasma. The cartridge was loaded with human serum or human plasma to test its ability to fractionate these protein solutions. The affinity membrane showed high selectivity for IgG. IgM was also adsorbed to a certain extent [20].

Two years later, Charcosset studied the purification of proteins by membrane chromatography discussing in particular the membrane materials, membrane activation and the interaction mode [18]. One interesting aspect described in this work is the importance of spacer arms. The role of the spacer arm is to bind the ligand to the support. Occasionally, a ligand might show poor function due to low steric availability. This rarely happens with high molecular weight ligands, but may occur with low molecular weight ligands. The use of a spacer arm in many cases solves this problem. A longer spacer appeared to offer favourable results at high ligand concentration [18]. An ideal spacer arm should have: (i) proper length (at least three atoms); (ii) no active center which could cause non-specific adsorption between membrane and sample; (iii) bifunctional groups to react with both substrates ligands [21].

E. Klein and co-workers developed affinity adsorption devices prepared from microporous poly(amide) hollow fibers and flat sheet membranes [22]. Microporous poly(caprolactam) hollow fibers and flat sheet membranes have been modified by covalent linkage to produce affinity matrices. This paper report results for immobilized antibodies, r-Pr A (recombinant protein A), and DEAE-functionalized (diethylaminoethyl) copolymers produced on the

membranes. The authors concluded that the performance of affinity membranes is dependent not only on the membrane properties, but also on the configuration in which it is used [22].

In 1999 Dancette et al, studied the purification of immunoglobulins G by protein A/G affinity membrane chromatography [7]. An affinity membrane grafted with protein A/G was characterized for human and mouse IgG purification. Breakthrough curves up to ligand saturation were measured and used to study the effects of flow velocities, feed solution concentrations and protein A/G versus protein A membranes. Increased flow-rate did not decrease the amount of IgG bound to the membranes. Increased feed solution concentration allowed more IgG to bind prior to breakthrough. Kinetic parameters for sorption of immunoglobulins G to immobilized protein A were measured in batch experiments. Finally, this affinity membrane was used to purify IgG from cell culture supernatant. The electrophoresis of the purified IgG fractions did not show any contaminant [7].

In 2001, macroporous cellulose membranes with large pore sizes (1-2 μm) and high porosity (about 60%) were prepared from filter paper by chemical crosslinking. These membranes were activated by introducing epoxy groups with various spacer lengths after which maltose was immobilized as an affinity ligand. The prepared membranes were used for the affinity purification of concavalin A, using a cartridge containing 40 membranes [19].

In the same year, cellulose and derivates of cellulose affinity membranes were developed to separate and purify proteins [21]. Like in the preparation of affinity stationary phases for packed columns, three steps were involved in the preparation of affinity membranes: (1) preparation of the basic membranes, (2) activation of the basic membranes, and (3) coupling of affinity ligands to the activated membranes. It was possible to obtain yields of affinity efficiency between 10-23 % and yields of affinity recovery between 95%-98%.

In 2002, Castilho et al, evaluated the purification of immunoglobulins by comparison of 10 different affinity membranes prepared by coupling various affinity ligands to different microfiltration membranes [4]. Membranes carrying the synthetic peptide TG19318, histidine, a thiophilic ligand and iminodiacetic acid complexed with Zn(II) showed a weak affinity for human IgG, as expressed by apparent association constants (KA) in the order of $10^5 M^{-1}$. They checked that the best materials to immobilize were polysulfone and regenerated cellulose when compared for example with nylon. Besides the high association constants, Protein-A adsorbers based on polysulfone and regenerated cellulose membranes showed several other advantages, such as enhanced charge-to-charge consistency, simpler preparation procedure, membrane sterilisability, good selectivity for IgG purification from cell culture supernatant and good stability throughout repeated adsorption–elution cycles [4].

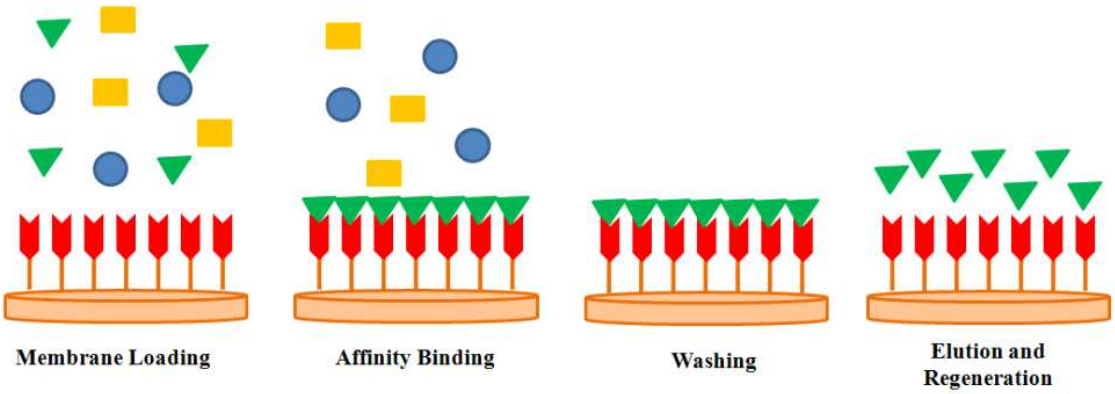

Figure 3.3 - Schematic representation of the main steps in affinity membranes

The developments in the area of membrane to protein separation, transport phenomena on membranes and various separation chemistries were reviewed [15]. An interesting aspect discussed is the problem of pore size distribution as the feed flow will preferentially take place through the larger "flow-pores" and very little material will be carried through the smaller pores. One way to skirt these problems is to use a large number of sheet membranes to even out the pore size distribution related to the dispersion effect.

In 2004, poly(hydroxyethylmethacrylate-co-methacrylolyamido-histidine) membranes were prepared and characterized [23]. L-histidine worked as an amino acid ligand that was used in separation and purification of hIgG. The aim of this method was the elimination of activation and ligand-coupling step during preparation of affinity membrane. In this way, the method offers a simple affinity membrane preparation technique with a desired ligand density. The purity of the eluted hIgG was 95% with 54%-58% of recovery [23].

Recently, in 2007, poly(2-hydroxyethylmethacrylate) (pHEMA) membrane was prepared by photo-polymerization and a dye ligand was immobilized on the membrane surface (pHEMA-RG-5) [24]. pHEMA-RG-5 membranes were prepared using organic solvents and the surface modification was studied by measuring contact angles. The maximum IgG adsorption was observed at pH 6.0. To test the efficiency of IgG isolation from human serum with the pHEMA-RG-5 membrane, the purity (81%) of the eluted IgG was determined by HPLC with a 67% of yield recovery. The IgG capacity adsorption by the dye–ligand immobilized on the membrane was 33.75 mg mL^{-1}. The experimental results indicated that pH, ionic strength and temperature had an important effect on adsorption equilibrium of IgG. Table 3.1 shows a brief summary of polymeric membranes and their geometry as well as their immobilized ligands and specific targets.

Table 3.1 – Resume of common affinity membranes applied to the purification of various proteins

Membrane Material	Ligand	Target	Adsorber Geometry	Ref
Poly(ethylene vinyl alcohol)	l-histidine	IgG and IgM	Hollow fibers	[20]
Synthetic polymers	l-histidine	Protein A and G	Hollow fibers	[18]
Poly(amide)	Recombinant protein A	IgG	Hollow fibers and flat sheet	[22]
Poly(methyl methacrylate) and Polyacrylonitrile	Protein A	mIgG	Hollow fibers	[7]
Cellulose	Maltose	Concaval in A	Flat Sheet	[19]
Cellulose and derivates	Protein A	IgG	Flat Sheet	[21]
Polysulfone Nylon and Cellulose	Protein A, Peptide TG19318, histidine and thiophilic ligand	IgG	Flat Sheet	[4]
Poly(hydroxyethylmethacrylate-co-methacryloylchloride)	l-histidine	hIgG	Flat Sheet	[23]
Poly(2-hydroxyethylmethacrylate)	Dye-ligand	IgG	Flat Sheet	[24]

3.1.3 Ionic liquids and cellulose

Ionic liquids (ILs) are a new class of compounds that emerged in the last ten years. They act much like good organic solvents, dissolving both polar and nonpolar species [25]. They can be defined as a molten salt with a melting point below 100°C. Ionic liquids are organic salts, invariably possessing a high degree of asymmetry that frustrates packing and thus inhibits crystallization. The possible choices of cation and anion that will result in the formation of ILs are numerous [25]. The physical and chemical properties are determined by a combination between anion and cation. In contrast to organic solvents these liquids are assigned as "green solvents", and their use is becoming more frequent.

Cellulose is the most abundant renewable resource in the world [26]. Derivatized products have many important applications in the fiber, paper, membrane, polymer, and paints industries [27].

Cellulose is a very consistent and compact macro-molecule insoluble in water and in most common organic liquids [26], making difficult the modification of its properties.

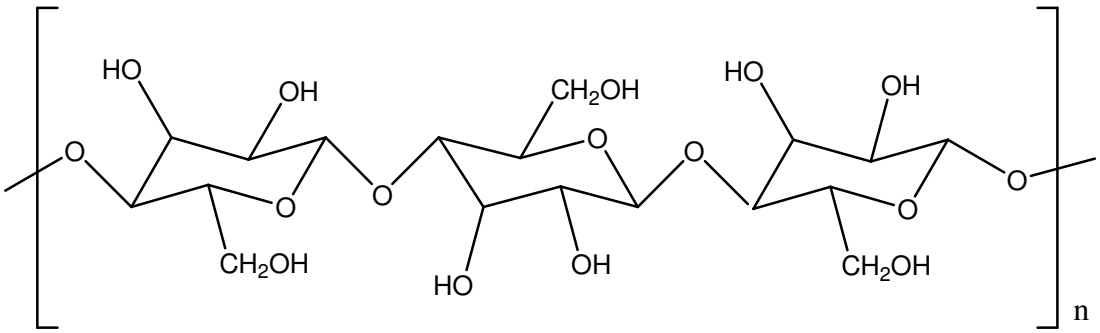

Figure 3.4 - Cellulose Structure

The traditional methods for cellulose dissolution are usually complex and sometimes expensive, making use of aggressive toxic solvents that are not treatable or reused [28]. The same problem appears in extraction processes that involve cellulose. To skirt these obstacles, a new strategy to dissolve this biopolymer was designed [28-30].

Since early 1934, Graenacher discovered that when melting N-ethylpyridinium chloride, in the presence of bases containing nitrogen, it was possible to dissolve cellulose. This was perhaps the first example of cellulose dissolution in ionic liquids, although this concept was not defined at the time [26, 30]. Since then, some studies on cellulose dissolution in ionic liquids have been performed, and in last decades the inquiry and interest in these liquids as alternative to traditional solvents grew exponentially [31].

It was discovered and studied two ionic liquids able to dissolve cellulose, 1-allyl-methylimidazolium chloride [Amim][Cl] and 1-butyl-3-methylimidazolium [Bmim][Cl]. These two ionic liquids contain one atom of chlorine which allows to break definitive hydrogen bonds in cellulose, and thus to promote its dissolution. However, [Bmim][Cl] is the ionic liquid more efficient to dissolve cellulose described in literature [26, 30, 31].

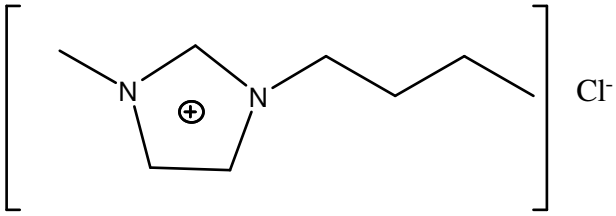

Figure 3.5 - [BMIM][Cl] structure

Rogers et al, studied the solubility of pulp cellulose in ionic liquids, and regenerated it [31]. They studied nine ionic liquids at different temperatures to dissolve cellulose, and concluded that the better ionic liquids to do it were the ionic liquids that contained Cl^- anion. In the same work, they developed a new method for introducing enzymes into cellulose matrices which can be formed into membranes, films or beads in order to understand this biological activity.

There are many reports on the importance of ionic liquids and cellulose with the purpose to understand the existing interactions, the properties of the ionic liquids, the recovery of these liquids and other curiosities [25, 29]. However, in this work the only interest is to show that ionic liquids are a good and "green" alternative solvent in cellulose treatment, allowing membrane preparation without organic solvents.

It is important to remark that it is possible to recover the ionic liquids. It is demonstrated in the literature [32] that ionic liquids can be distillated, without losing their outstanding properties.

In this work these procedures were adopted, becoming a viable and economic strategy.

3.1.4 Aims of the work

Matrices based on cellulose are frequently used as a carrier for protein immobilization because of their biocompatibility and hydrophylicity, being this fact a motivation to this work. The aims of this chapter were to develop affinity cellulose membranes for the purification of antibodies using biomimetic compounds as affinity ligands (e.g. Ligand 22/8-artificial protein A). The research strategy involved: (i) preparation and characterization of cellulose membranes; (ii) synthesis and characterization of ligands; (iii) functionalization of cellulose membranes; (iv) ligand attachment on to the cellulose membranes; (iv) adsorption/desorption tests of human IgG in cellulose membranes.

3.2 Experimental

3.2.1 Materials

3.2.1.1 Chemicals

All the reagents used were at least 98% pure. Citric acid (purity ≥ 99 %), disodium hydrogen phosphate monodibasic (pro analysis), disodium hydrogen phosphate dibasic (pro analysis), disodium tetraborate, ethanol absolute, Folin Ciocalteau and sodium citrate dihydratate were purchased from Merck. Isopropanol and sodium bicarbonate were purchased from Riedel-de-Haën. Acetone and ethyl acetate were supplied by Roth. 6-aminocaproic acid, 3-aminophenol, 4-amino-1-naphthol hydrochloride, cyanuric acid, N,N-dimethylformamide (DMF), dimethylsulfoxide (DMSO), epychlorydrin (ECH), picrysulfonic acid solution or trinitrobenzenesulphonic acid (TNBS) were purchased from Sigma Aldrich. [BMIM][CL] was purchased from Solchemar.

3.2.1.2 Biochemicals

Cellulose (99 % purity) and human IgG (reagent grade > 95% purity) were supplied by Sigma Aldrich.

3.2.2 Methods

3.2.2.1 Preparation of cellulose membranes

Cellulose membranes were prepared by phase inversion method using [BMIM][Cl^-] as the solvent and water as the anti-solvent.

The ionic liquid was melted at 100ºC because at room temperature it is solid. When the [BMIM][Cl^-] was liquid, cellulose was added. This dissolution occurred in 12h and the resulting casting solution was loaded into a teflon cap (with a diameter of 68 mm and 1 mm height). When the solution was homogeneously distributed in the disk, it was immersed in a water bath. After twenty minutes, the cellulose membrane precipitated and the water, that extracts the ionic liquid, was recovered to be later distilled. This last step was repeated 3 times in order to remove all the ionic liquid from the membrane composition.

The casting solutions were prepared by cellulose dissolving in [BMIM][Cl] with the following composition: 5 and 10 % (w/w). All the experiments were realized using the same amount of ionic liquid (4 g) at 100 ºC during 2 h.

3.2.2.2 Characterization of membranes

Membranes morphology studies were based on SEM data. SEM micrographs were obtained on a Hitachi S-2400 equipment. All samples were mounted on aluminum stubs using carbon cement (D-400, Neubaeur Chemikalien) and were gold coated.

The permeability to pure water was determined by measuring the water flux trough the membranes using a 10 mL filtration unit (Amicon Corp., Model 8010) with an effective area of 4.1cm^2. All the experiments were carried out varying the applied hydrostatic pressure from 0-2.4 bar. At least three clean water flux measurements were performed for each membrane.

The permeability of the membranes was obtained by the slope of linear relation between flux and pressure, and it is given by Darcy Law:

$$F = Lp \times \Delta P$$

Figure 3.6 - Darcy's law. F: Flux (L m^{-2}h^{-1}); Lp: Permeability (L m^{-2}h^{-1}bar^{-1}); ΔP: Drop of pressure (bar)

Membrane hidrophobicity was evaluated through the measurement of the contact angles of water droplets in a Goniometer MODEL CAM 100.

Pore sizes distribution was determinate in a Micromeritics Auto Pore IV mercury porosimeter using sample weights between 0.080-0.122g in order to obtain a good distribution. These analyses were performed in two steps, first applying low pressure at 345 KPa and in the second applying high pressure at 223 MPa. The results were treated using the SigmaPlot program.

The tensile properties of the membranes were determined with tensile testing equipment (*MINIMAT firm-ware* v.3.1) at room temperature. The samples were cut into strips with 2x15 mm^2. The length between the clamps was set at 5 mm and the speed of testing set at 0.1 mm min^{-1}. A full scale load of 20 N and maximum extension of 90 mm were used.

The elastic modulus was calculated from the slope of the linear portion of the stress-strain curve. Samples were tested either in dry state at 25 ºC and in wet state.

Load extension graphs were obtained during testing and converted to stress strain curves applying equations:

$$\text{Stress} = \sigma = F/A$$
$$\text{Strain} = \varepsilon = \Delta l/L$$

Figure 3.7 – Equations of stress and strain. F: Applied force; A: Cross sectional area; Δl : Change in length; L: Length between clamps

Elementary analysis was performed in order to confirm the absence of any ionic liquid residues in the matrix of cellulose membranes, using a FlashEA 1112 Series Analyzer. A complete CHNS report was automatically generated by the Eager 300 data handling software package and displayed at the end of the analytical routine.

3.2.2.3 Synthesis of ligand

3.2.2.3.1 Synthesis of 3-(4,6-dichloro-1,3,5-triazin-2-ylamino)phenol (A)

A solution of 3-aminophenol (0.01 mol; 1.095 g) in acetone (15 ml) was added dropwise to a cyanuric chloride suspension made by pouring cyanuric chloride (0.01 mol; 1.849 g) in acetone (15 ml) into cold deionised water (25ml) under stirring in an ice bath. $NaHCO_3$ (0.011 mol; 0.846 g) in distilled water (10 ml) was added to maintain the pH between 6 and 7 during the reaction. After 1.5h the reaction finished and a white powder, 3-(4,6-dichloro-1,3,5-triazin-2ylamino)phenol formed. The aqueous solution was filtered and washed with cold distilled water in order to remove salts to afford a white powder in a yield of 85% (4.01g) and a melting point in the range 197–201°C; ^{1}H-NMR (400 MHz, DMSO) δ_H: 6.58 (1H, d, *o*-H or *p*-H), 7.02 (1H, d, *o*-H or *p*-H), 7.09–7.30 (2H, m, *o*-H and *m*-H); ν_{max}(KBr)/cm^{-1} 3366(OH) cm^{-1} and 3093(NH) cm^{-1} ; *m/z* M^+ found 256, $C_9H_6N_4Cl_2O$ requires M^+: 257; These results are in agreement with the values described in the literature [10]. Estimated purity: ≈ 95%. (See appendix section)

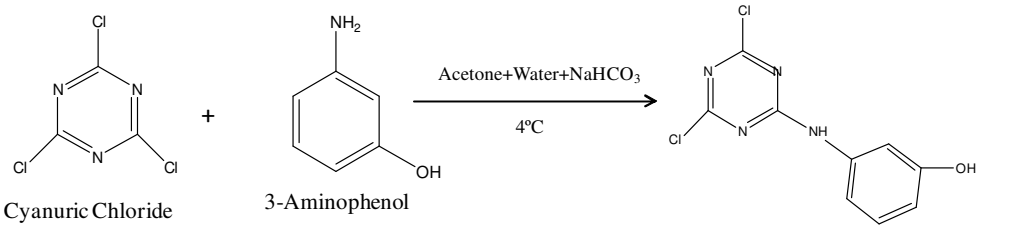

Figure 3.8 - Synthesis of compound A

3.2.2.3.2 Synthesis of 4-(4-(3-hydroxyphenylamino)-6-chloro-1,3,5-triazin-2-ylamino)naphthalen-1-ol (B)

$NaHCO_3$ (0.001 mol; 0.846 g) was used to bring the pH of a 4-amino-1-naphthol hydrochloride (1.819 g) solution to neutral in a mixture of acetone (15 ml) and distilled water (15 ml). This mixture was added to a solution of 3-(4,6-dichloro-1,3,5-triazin-2ylamino)phenol (0.008 mol; 2.1704 g) in acetone (25 ml) and heated to 45 ºC in a sand bath. $NaHCO_3$ (0.001 mol; 0.846 g) in distilled water (10 ml) was added to maintain the pH

between 6 and 7 during the reaction. After 5h, the mixture was dried on a rotary evaporator and added ethylacetate (80 ml) and distilled water (20 ml) to perform the extraction as a purification step of the 4-(4-(3-hydroxyphenylamino)-6-chloro-1,3,5-triazine-2-ylamino)naphthalen-1-ol. The organic phase was recovered and the solvent evaporated.

4-(4-(3-hydroxyphenylamino)-6-chloro-1,3,5-triazine-2-ylamino)naphthalen-1-ol was solubilized in ethanol (50 ml) at 30-40 ºC just in 30 minutes and a activated charcoal was added to remove impurities. The solution was filter by gravity just to remove the activated charcoal, and dried on a rotary evaporator.

The 4-(4-(3-hydroxyphenylamino)-6-chloro-1,3,5-triazine-2-ylamino)naphthalen-1-ol is a brown powder which decomposed at 180 °C in a yield of 79 % (1.89g) and a melting point in the range 120–130 °C; δ_H (400 MHz, DMSO): 6.36–8.1 (1H, overlapping-multiplet , Ha), 9.6 (1H, d, Hb), 10.04 (1H, s, Hc); ν_{max}(KBr)/cm^{-1} 3372 (OH) cm^{-1} and 2958 (NH) cm^{-1} ; M^+ found 379, $C_{19}H_{14}N_5O_2Cl$ requires M^+: 380, *m/z*. These results are closer of the values described in the literature [10]. Estimated purity: ≈ 95%. (See appendix section)

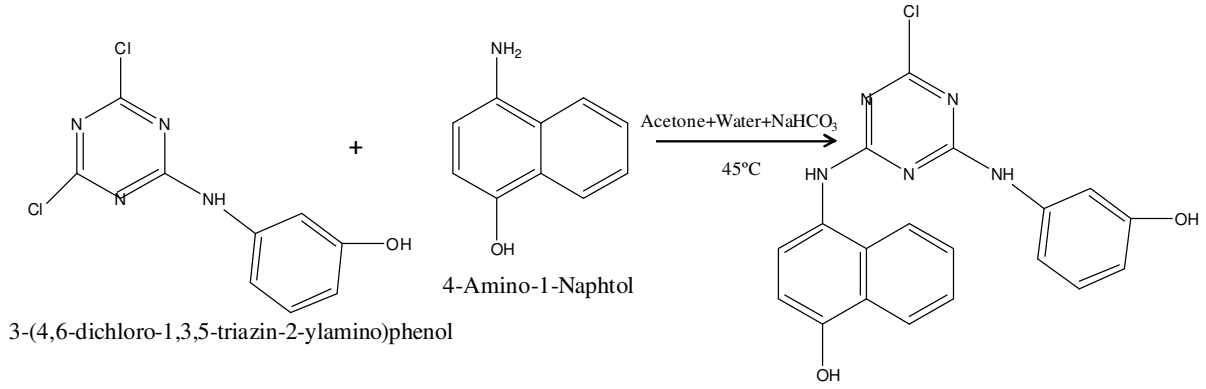

Figure 3.9 - Synthesis of compound B

3.2.2.3.3 Synthesis of 4-(4-(3-hydroxyphenylamino)-6-(6-aminohexylamino)-1,3,5-triazin-2-ylamino)naphthalen-1-ol (C)

Hexane-1,6-diamine (0.824 ml) was added to a solution of 4-(4-(3-hydroxyphenylamino)-6-chloro-1,3,5-triazine-2-ylamino)naphthalen-1-ol (0.006 mol; 2.405 g) in acetone (40 ml) and distilled water (10 ml), and in a sand bath at 80 ºC during 48h. $NaHCO_3$ aqueous solution (0.001 mol in 10 ml) was added to maintain the pH between 6 and 7 during the reaction.

After 48h, the solution was dried on a rotary evaporator and the ligand, 4-(4-(3-hydroxyphenylamino)-6-(6-aminohexylamino)-1,3,5-triazin-2ylamino)naphthalen-1-ol, was solubilized in ethanol (20 ml) and water (80 ml) to do an extraction. This step was performed 2 times. After extraction the organic solution was dried again on rotary evaporator.

The ligand, 4-(4-(3- hydroxyphenylamino)-6-(6-aminohexylamino)-1,3,5-triazin-2ylamino)naphthalen-1-ol is a powder with 40% (1.04g) yield and a melting point in the range of 230°C; δ_H (400 MHz, DMSO): 1.2-1.45 (1H, d, Hd), 6.12-8.7 (1H, overlapping-multiplet, Ha); ν_{max}(KBr)/cm^{-1} 3297 (OH) cm^{-1} and 2936 (NH_2) cm^{-1}; M^+ found 58, 98, 281, $C_9H_6N_4Cl_2O$ requires M^+:459, *m/z*. The pretended molecular weight was not found however the molecular weight of fragments confirmed the presence of the desired compound. Estimated purity: ≈ 85%. (See appendix section)

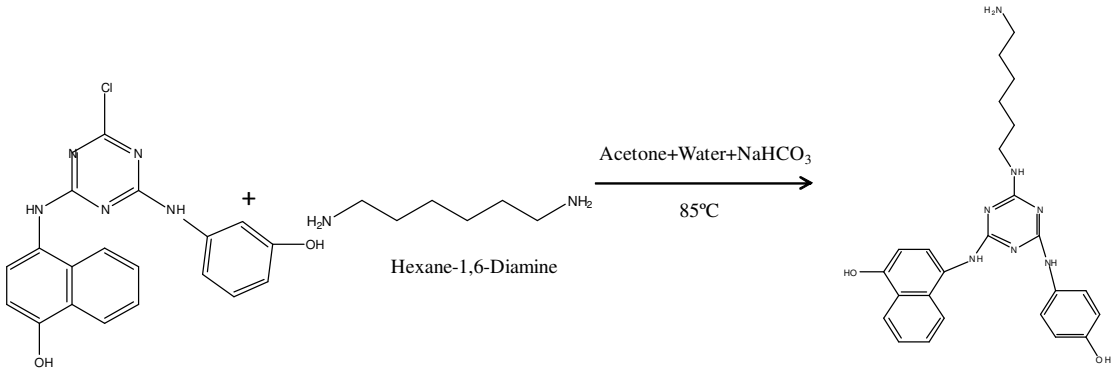

4-(4-(3-hydroxyphenylamino)-6-chloro-1,3,5-triazin-2-ylamino)naphthalen-1-ol

4-(4-(3-hydroxyphenylamino)-6-(6-aminohexylamino)-1,3,5-triazin-2-ylamino)naphthalen-1-ol

Figure 3.10 - Synthesis of compound C

The rotary evaporator used in all evaporations was a Büchi equipment with vacuum pump V-700 and heating bath (20-580 ºC).

3.2.2.4 Ligands Characterization

^{1}H- and ^{13} C- RMN spectra were recorded on a Bruker ARX 400MHz spectrometer. Approximately 10 mg of sample were dissolved in 500 µL of deuterated DMSO.

FT-IR measurements were performed using Winfirst Lite equipment (16 scans and 1cm^{-1} resolution). A small amount of each sample was mixed with dried KBr (1:5 mass ratio) and thin pellets were prepared.

The mass spectra and the melting point were performed in MICROMASS equipment GCT model using filionization mode and in Stuart Scientific SMP1 equipment at 360 ºC, respectively.

3.2.2.5 Activation of cellulose membranes

Cellulose membranes possess free OH groups that must be activated for further activation. Activation procedures were performed in a Selecta shaker equipment and in Boekel Scientific equipment, model 230402. Three different cellulose 10% membranes were activated one of them for control purposes which will not be functionalized.

3.2.2.5.1 Epoxy activation

The cellulose membranes were covered with 9 ml of distilled water, 70.4 µl of NaOH (0.1M) and 0.63 ml of epychlorydrin (ECH). It was incubated for 3h, at 35ºC on a rotary shaker (140 rpm). After that time the epoxy-activated membrane was washed with 40ml of distilled water to remove possible ECH on the membrane.

3.2.2.5.2 Epoxy activation test

The epoxy activation content was determined by adding 3ml of sodium thiosulphate (1.3M) to 1g of epoxy activated membrane and incubated at room temperature for 20 min. This mixture was neutralized with HCl (0.1M) and the amount of HCl used registered. The volume of 0.1M HCl added corresponded to the number of OH- moles released. The HCl was added until pH 7. The protocol resulted in 150 ± 30 µmol of epoxy groups/g membrane.

3.2.2.5.3 Amination of activated cellulose membranes

After the epoxyactivation of the cellulose membrane, the epoxy groups reacted with an excess, [5eq, 8ml], of hexane-1,6-diamine using water as solvent for 12h at 30 ºC . In the end of incubation, the membrane was washed with water, removing possible unreacted hexane-1,6-diamine.

3.2.2.5.4 Amination test

The extent of amination on cellulose membrane was determined by using the 2,4,6-trinitrobenzenesulphonic acid (TNBS) test. Aminated membrane, 0.1 g, was weighted and hydrolyzed with 500 µl of HCl (5M) at 50 ºC for 10 min. Upon cooling, the hydrolyzed sample was neutralized with NaOH (5M) and added to 1ml of sodium tetraborate buffer (0.1M, pH 9.3) and 25 µl of TNBS (0.03M). Samples were incubated at room temperature for 30 min prior to measuring their absorbance at 420nm. The negative control was 1ml of

distilled water to which sodium tetraborate buffer and TNBS solution (amounts cited above) were added. The calibration curves were constructed with 6-aminocaproic acid (0-2 μmol mL^{-1}).

The value obtained was 22 μmol of NH_2 /g cellulose membrane.

3.2.2.6 Functionalization of cellulose membranes

After the activation step, the membrane is ready to be functionalized with the synthesized ligands. Immobilization procedures were performed in a Selecta shaker equipment and in a Boekel Scientific equipment, model 230402.

Table 3.2 - Strategy of ligand immobilization and their abreviations

Membrane	Ligand	Ligand Abbreviation
M1	4-(4-(3-hydroxyphenylamino)-6-chloro-1,3,5-triazine-2-ylamino)naphthalen-1-ol	B
M2	4-(4-(3- hydroxyphenylamino)-6-(6-aminohexylamino)-1,3,5-triazin-2ylamino)naphthalen-1-ol	C

3.2.2.6.1 Immobilization of 4-(4-(3-hydroxyphenylamino)-6-chloro-1,3,5-triazin-2-ylamino)naphthalen-1-ol (B)

According with the epoxy content determined in 3.2.2.5.2, an excess of B, [5 eq, (240 μmol; 91×10^{-3}g)], was added to the membrane using a mixture of solvents (1:1) water-DMF. The amount of solvent used was the necessary to cover the membrane, and the solution was incubated on rotary shaker (140 rpm) for 72h at 85ºC. After 72h the membrane was washed with water-DMF (1:1) to remove B that was physically adsorbed. Figure 3.11 shows the scheme of activation membrane and B immobilization.

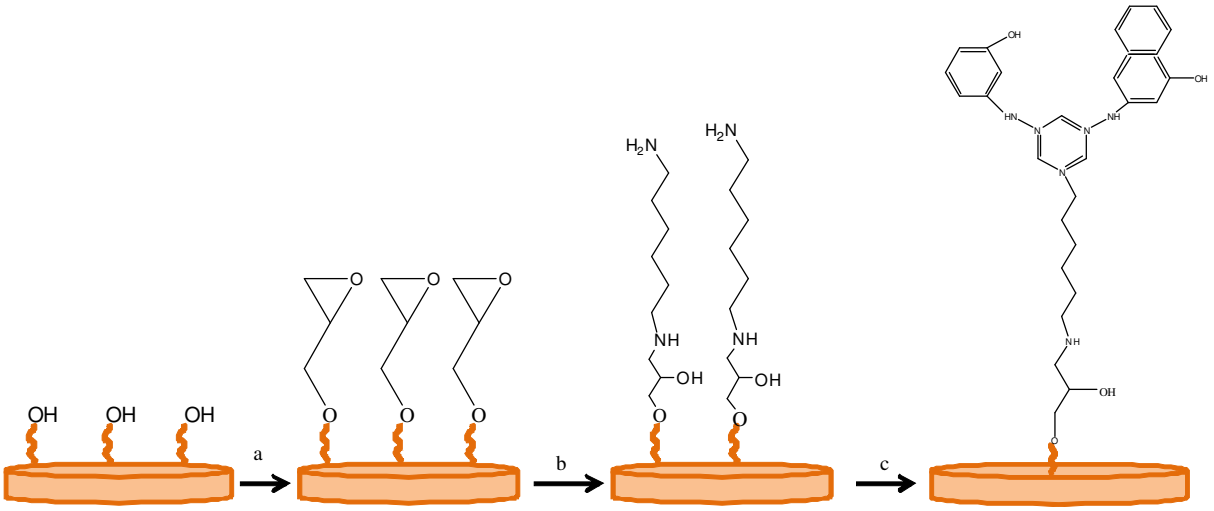

Figure 3.11 - Scheme of M1 activation and B immobilization: a) epoxyactivation, b) amination, c) immobilization of compound B

3.2.2.6.2 Immobilization of 4-(4-(3-hydroxyphenylamino)-6-(6-aminohexylamino)-1,3,5-triazin-2-ylamino)naphthalen-1-ol (C)

According with the epoxy content that was determined in 3.2.2.5.2 an excess of C, [5eq, (435 µmol; 0,2 g)], was added to the membrane using water as solvent. The amount of solvent used was the necessary to cover the membrane, and the solution was incubated on a rotary shaker (140 rpm) for 72h at 85ºC.

After 72h the membrane was washed with water to remove C that was physically adsorbed. Figure 3.12 shows the scheme of activation membrane and C immobilization.

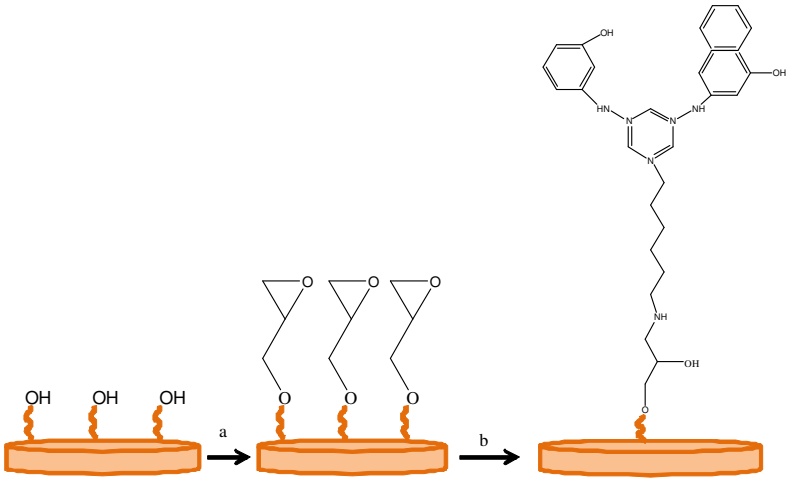

Figure 3.12 - Scheme of M2 activation and C immobilization: a) epoxyactivaction and b) immobilization of compound C

3.2.2.7 Determination of immobilized ligands in cellulose membranes

The amount of B and C immobilized on the cellulose membranes was determined by subtracting the ligand contained in the washing liquors from the initial ligand used in the immobilization step.

The extinction coefficient (Ɛ) of each compound was determined for their λ maximum (λ_B= 270 nm and λ_C=265 nm) in a Helios Alpha Double-Beam UV/VIS spectrophotometer varying absorbance between 220-280 nm.

The collected washing liquors were analyzed in a Helios Alpha Double-Beam UV/VIS spectrophotometer at 270 and 265nm respectively, using a mixture of solvents with water-DMF (1:1) and water-DMSO (1:4) as a solvent, respectively.

3.2.2.7.1 Qualitative test for phenols

An aqueous solution of sodium carbonate (20%, w/v) was sprayed onto a filter paper containing 0.2 g of cellulose membranes (control, M1 and M2). The filter was allowed to dry for a short period before spraying with Folin-Ciocalteau reagent. The presence of phenol was indicated by the formation of a blue spot.

3.2.2.8 Binding hIgG to functionalized membranes

The binding measurements were performed in a vessel filtration unit of 10 ml (Amicon Corp., Model 8010) with an effective area of 4.1cm^2. All the experiments were carried out varying the applied hydrostatic pressure from 0 to 2 bar.

In membrane control the pressure applied was 1 bar, while in M1 was 2 bar and in M2 was 3 bar, using 500 rpm.

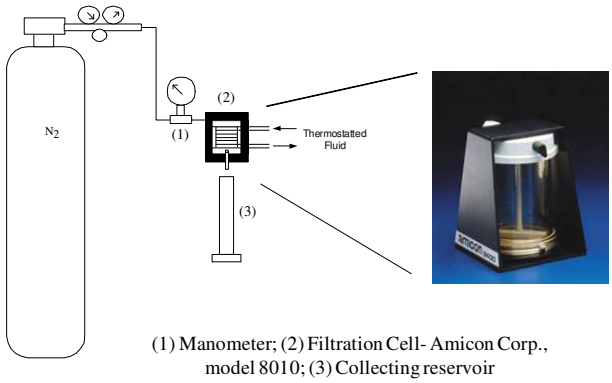

(1) Manometer; (2) Filtration Cell- Amicon Corp., model 8010; (3) Collecting reservoir

Figure 3.13 - Schematic apparatus of hIgG purification

First it was necessary to wash the functionalized membranes and eliminate all possible vestiges of ligand still absorbed after washes.

To remove all the possible ligand vestiges the membrane was washed with regeneration buffer (NaOH 0.1M in 30% of isopropanol) until the absorbance of the recovered samples was zero at ligand specific wavelength (i). This buffer is very strong and to avoid possible destructions or changes in membrane conformation, it was washed with 10 ml of distilled water (ii). Next, the membrane was equilibrated with sodium phosphate buffer (0.05 *M*, pH 8.0), the same that was used to prepare hIgG solution, until the absorbance of recovered samples was zero at ligand absorbance (iii). In these conditions the hIgG solution is ready to be loaded on the membrane. The hIgG solution (6ml) in PBS (0.5mg ml^{-1}) was prepared at room temperature, loaded through the membrane and the absorbance read at 280nm (iv). After sodium phosphate buffer (0.05 *M*, pH 8.0) was passed in order to wash unbound hIgG until the absorbance at 280 nm was zero (vi). To recover bound hIgG the membrane was washed with sodium citrate buffer (0.05 *M*, pH 3.0) until the absorbance at 280 nm was zero (vii). The steps (i) and (ii) were repeated to bring the membrane back to initial conditions.

All samples collected were analyzed in a Helios Alpha Double-Beam UV/VIS spectrophotometer.

3.3 Results and Discussion

3.3.1 Cellulose Membranes

3.3.1.1 Influence of casting solution and porosity

In this study, all the experiments were performed using 4g of [BMIM][Cl] at 40ºC during 2h. Only cellulose concentration was changed in casting solutions.

Table 3.3 presents a summary of the composition of casting solutions prepared as well as the porosity obtained.

By increasing the polymer content in casting solution, a decrease in the membranes porosity is noted. In addition to polymer content in casting solution there are other parameters that have an important role in pore size such as: the membrane preparation method, solvent, temperature and structure thickness how was described in the previously chapter.

Table 3.3 – Effect of cellulose content in casting solution and membrane porosity

Experiment	% (w/w) of cellulose in casting solution	Membrane	Porosity (%)
1	5	Cellulose 5%	84
2	10	Cellulose 10%	71

SEM micrographs show the different membrane morphologies obtained by tuning the polymer content in it. Two drying process were performed. One of them was by evaporation and another by liofilization. Figure 3.14 and Figure 3.15 show the different membranes morphologies for experiments 1 and 2, varying the percentage of cellulose in casting solution.

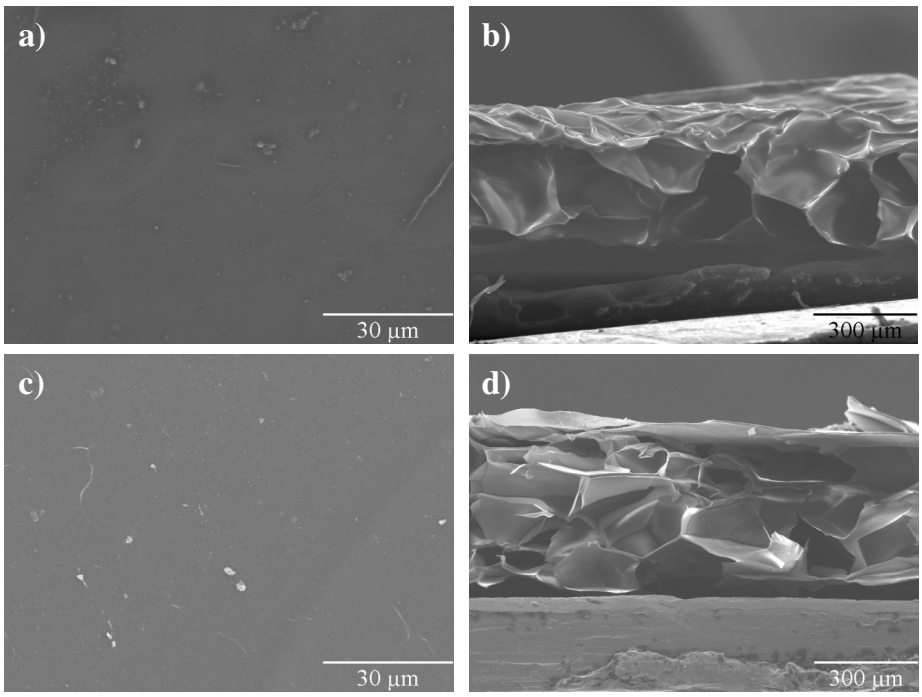

Figure 3.14 - Cellulose membranes 5% (w/w): a) surface (dry method: evaporation) b) cross-section (dry method: evaporation) c) surface (dry method: liofilization) d) cross-section (dry method: liofilization)

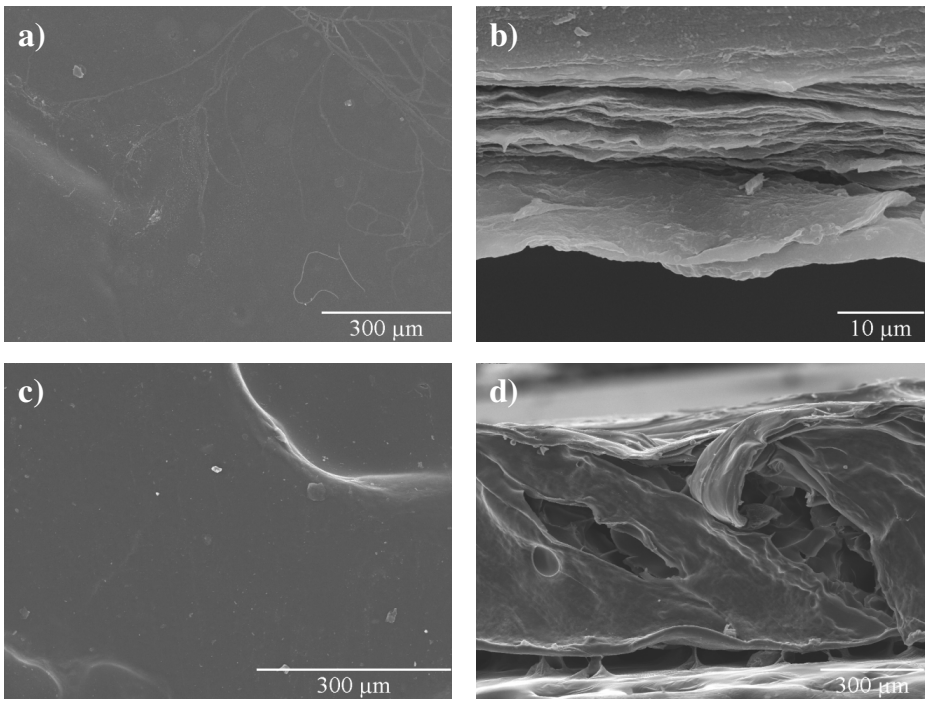

Figure 3.15 - Cellulose Membranes 10% (w/w): a) surface (dry method: evaporation) b) cross section (dry method: evaporation) c) surface (dry method: liofilization) d) cross section (dry method: liofilization)

Observing the SEM micrographs presented in Figure 3.14 and Figure 3.15 it is possible to observe a significant dependence of membranes morphology with the casting solution polymer content and the dryness method used. Membranes prepared from more concentrated polymer solutions have larger pores. This principle is referred in the literature [33].

Membranes prepared from 5% (w/w) cellulose solutions present regular and semi-spherical pores while from 10% of cellulose the pores appear as sheets overlapped resulting in broad pores.

Another parameter responsible for these different membrane morphologies is the drying process used. Liofilization is more efficient in the water elimination than evaporation leaving the membranes completely dry. Without water in their composition, the configuration of the membrane become different and consequently, the pores are more defined and regular than in membranes with low water percentage in their composition. The morphology differences that resulted from using evaporation or liofilization as a drying method were more significant in cellulose 10%.

The hydrophilic character of cellulose can justify the different configurations by the presence of water or on its absence. The ionic liquid did not have any influence as the elementary analysis confirmed the absence of nitrogen atoms, meaning the absence of ionic liquid in cellulose membranes composition. However, in all SEM images it is not possible to observe pores at the membrane surfaces, meaning that probably in this case the transport occurs by diffusion.

Mercury intrusion porosimetry data shows the pore size distribution, in agreement with SEM's data.

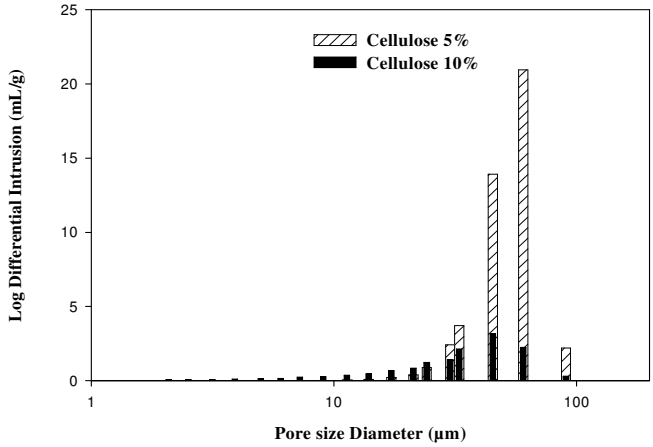

Figure 3.16 - Pores size distribution in cellulose membranes

Cellulose 5% membranes present larger pores (85 µm) than cellulose 10% membranes (70 µm). This is an important aspect because the pore sizes in affinity membranes influences their performance [15]. Therefore, when the amount of cellulose increases in the casting solution the membranes porosity decreases. However the casting solution polymer content is not the only parameter that influences porosity. Other parameters such as: the method used to induce porous structures [34, 35], the selected solvent and anti solvent [35], the temperature, the pressure and the geometry of membrane [15] have a significant influence.

The obtained porosities were different from the usually obtained in affinity membranes [21] but the parameters named above help to understand these differences. The obtained porosities are closer to the values described in the literature (82%-85%) [36] for cellulose devices used in separation processes.

Generally, an ideal affinity membrane should have micro or macroporous structures to allow fast fluid fluxes [37] and these membranes fulfill requirements.

3.3.1.2 Water permeability and contact angles

The pure water flux, which is defined as the volumetric flow rate divided by the membrane area and the pressure difference, was determined for all the membranes varying the applied hydrostatic pressure from 0 to 3 bar.

The permeabilities obtained to cellulose 5% and cellulose 10% was 0.2 and 0.5 L m^{-2} $h^{-1}$$bar^{-1}$, respectively.

The permeability of the membranes rises with the increase of polymer concentration, contrarily to the trend described in the previous chapter.

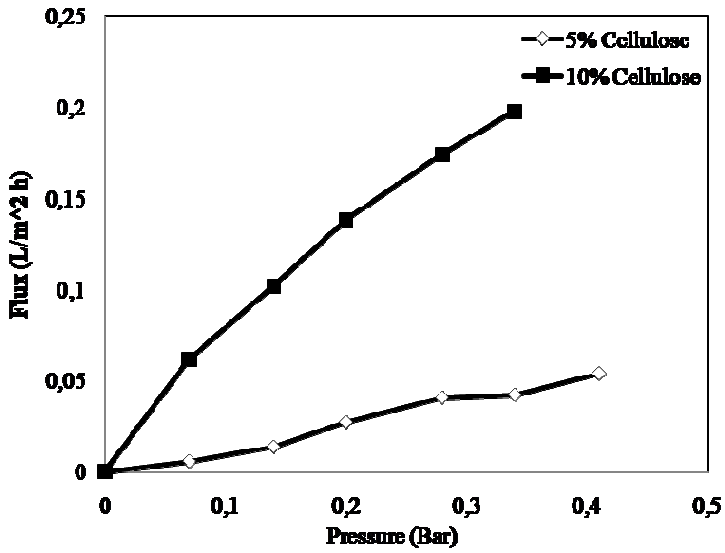

Figure 3.17 - Water flux of cellulose membranes

In Figure 3.17 it is possible to observe that cellulose 10% membrane has a higher permeability compared with cellulose 5% membrane. However, previously it was mentioned that the water flux in these membranes followed a diffusion transport, so increasing the cellulose content in membrane composition, makes OH groups more available, the membrane becomes more hydrophilic, allowing a higher water flux as it is observed for cellulose 10%. The observed fast fluid fluxes suggest that these membranes are promising ones to bioseparation [37].

Sometimes, to improve the desired permeability of cellulose membranes they are chemically modified with functional groups to allow changes in cellulose structure and to adjust the permeability values to the desired values [21, 37, 38].

The contact angle measurements were first attempted with water. However the measurements could not be taken because cellulose membranes are too hydrophilic. Squalene, a strong oil with 30 carbons was used instead, but still it was not possible to perform the measurements. The water and squalene drops were immediately absorbed.

The high amount of OH groups at the surface might be related also with the use of water as anti-solvent during membrane preparation. The solvent used as anti-solvent has a main effect on the chemical groups that appear more on membrane surface as it was demonstrated in the previous chapter. The failure on contact angle measurements confirms the high hydrophilic character of these membranes.

3.3.1.3 Mechanical properties measurements

In order to study mechanical properties of cellulose membranes, tensile tests were performed. Figure 3.18 and Figure 3.19 represent the relation between the force (stress) supported by the membranes and the respective elongation capacity (strain). These figures show different mechanical behaviors depending on the cellulose concentration used in the casting solution and on the dried process used.

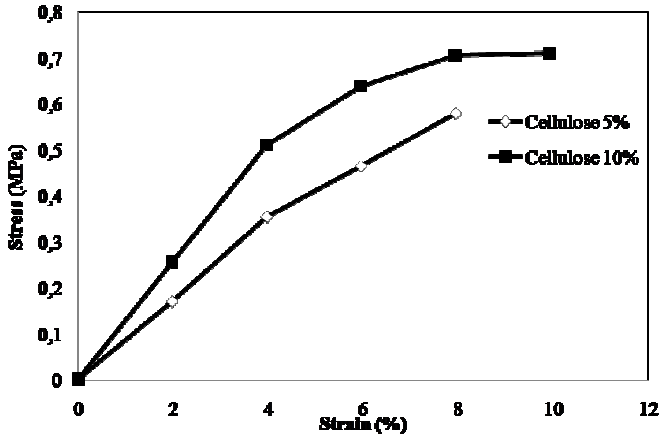

Figure 3.18 - Mechanical properties of cellulose membranes dried by liofilization

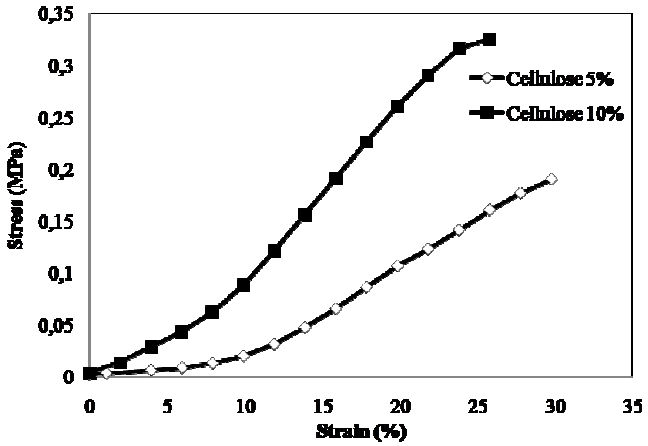

Figure 3.19 - Mechanical properties of cellulose membranes dried by evaporation

Cellulose 10% support more stress (0.7 and 0.35 MPa in Figure 3.18 and Figure 3.19, respectively) than cellulose 5% membranes (0.6 and 0.2 MPa in Figure 3.18 and Figure 3.19, respectively) as expected. Membranes dried by evaporation (Figure 3.19) are more elastic as they exhibit higher stresses at break. It should be also remarked the different behavior in terms of plasticity. Membranes dried by liofilization are less elastic and the cellulose 10%

starts to exhibit a plastic behavior. Membranes dried by evaporation do not show a plastic behavior.

A possible explanation for the different behaviors observed with these different drying methods could be the presence of water at the end of drying process, since some water remain in the membrane after the evaporation method. This can lead to changes in the cellulose structure and consequently the stress they can support.

The mechanical behavior of cellulose membranes prepared in this work is closer to the observed for cellulose nanofibers used as affinity membranes [36].

Another important aspect in tensile tests is Young's modulus (MPa), which is the slope of stress–strain and gives a rigidity measurement of the material.

Table 3.4 - Young module of cellulose membranes

Dried Process	Membrane	Young Module (MPa)
Liofilization	Cellulose 5%	7
	Cellulose 10%	15
Evaporation	Cellulose 5%	0,6
	Cellulose 10%	12

The results of the Young modulus are lower when compared with some values described in the literature [28, 39], however these membranes have a thickness < 1mm and were prepared without organic solvents in opposition to the mentioned in literature, and these parameters influence the material rigidity. Many factors can explain these lower values such as the thickness and the size of the membrane, the porosity, the crystalline parts of cellulose, the cellulose type and geometry, the amount of cellulose and the solvent that was used in membrane preparation [39, 40].

Completely dried cellulose membranes (dried by liofilization) are more rigid than the others. However, independently of the drying process, cellulose 10% membranes have similar Young modulus, meaning that both can be interesting candidate membranes for the development of an affinity membrane.

3.3.2 Synthesis of biomimetic ligands

3.3.2.1 Synthesis of 3-(4,6-dichloro-1,3,5-triazin-2-ylamino)phenol (A)

The basic principle to produce ligands, compound B and compound C, from cyanuric chloride is that the least reactive amine reacts with the first chlorine atom and the most reactive amine with the last chlorine atom. Therefore the chlorine atoms on cyanuric chloride become progressively deactivated as more substitutes are added to the triazine ring.

The synthesis of ligand 22/8 (compound B) has been studied and it was proven that reacting first cyanuric chloride with 3-aminophenol higher yield of reaction was obtained than with 4-amino-1-naphthol [10].

The yield of reaction, mass spectra, ^{1}H- and ^{13}C-NMR, FT-IR and melting point are closer to the values described in the literature for this compound [10].

3.3.2.2 Synthesis of 4-(4-(3-hydroxyphenylamino)-6-chloro-1,3,5-triazin-2-ylamino)naphthalen-1-ol (B)

Following the previous principle, the intermediate compound A reacted with 4-amino-1-naphthol over a period of 5h with 75% of yield and the obtained values for mass spectra, ^{1}H-NMR, FT-IR and melting point are closer to the values described in the literature [10] for this compound. However, from spectra analysis it was possible to confirm that B has purity between 80 - 90% even though its complex synthesis path.

Consequently, in ^{1}H-NMR and ^{13}C-NMR spectra there are overlapped peaks that make difficult the identification of B hydrogens and carbons. For further studies it will be interesting to obtain 2D-NMR to separate the overlapped peaks improving the identification of specific hydrogen or carbons.

3.3.2.3 Synthesis of 4-(4-(3- hydroxyphenylamino)-6-(6- aminohexylamino)-1,3,5-triazin-2-ylamino)naphthalen-1-ol (C)

To synthesize compound C it was necessary to add the spacer arm, hexane-1,6-diamine to compound B and this reaction occurred during 72 h at 85 ºC with 40 % of yield.

The obtained values for mass spectra, ^{1}H-NMR, FT-IR and melting point confirm the presence of compound C. However, the purity of compound remained low (less than 90%) and this is explained by the fact that compound B has some impurities when was used as

reagent to this synthesis. As mentioned before, future studies should be performed by 2D-NMR to separate the overlapped peaks.

Compound C was extracted with a solvents mixture (20%-80%) ethyl acetate-water in order to eliminate the impurities. This compound possesses an amphiphilic character. Other purification techniques, as flash chromatography can be used in future studies to optimize the purification step.

3.3.3 Membranes activation and immobilization of the ligand in cellulose membranes

Two routes for ligand immobilization were followed (Figure 3.11 and Figure 3.12) in order to evaluate the influence of the immobilization method, and consequently the hIgG binding efficiency. Both membranes were activated with epoxy groups in order to form reactive groups to attach the ligands. In the first route, hexane-1,6-diamine was immobilized on the support being necessary to quantify the amine groups to the surface. In the second route, the hexane-1,6-diamine reacted first with compound B forming compound C, that further reacted with epoxy activated membrane.

There are many activation procedures [21], although the adopted procedure to activate and functionalize the membranes was based in the optimized procedure for agarose [10]. The activation results of membranes were different from agarose but different structures and geometries can explain these differences.

Table 3.5 shows the activation results for both membranes.

Table 3.5 – Functionalization results of the cellulose membranes

Functionalization Parameters	Membrane 1	Membrane 2
Epoxyactivation (µmol epoxy/g memb)	120	180
Amination [NH_2]/g memb	22	-
Amount of Ligand Immobilized (µmol/ g memb)	16	93

These two routes were studied because a lot of parameters [21] can influence the activation process such as: ligand type, ligand solubility, chemistry repulsion, binding capacity, spacer arm, etc [21].

According with epoxy activation tests it was possible to activate in average 150 µmol epoxy/g membrane. This value is very superior to the described in the literature for agarose (50 µmol epoxy/g moist weight gel) [10]. The amination of M1 was performed with hexane-1,6-diamine. This compound acts as a spacer arm between the surface of the membrane and the small biomimetic ligand. However, during membrane activation it is conceivable that the two terminal amine groups react simultaneously with neighbor epoxy groups. This could justify the lower value for free amine (22 µmol/g memb) when comparing with free epoxy groups (120 µmol/g memb). On the other hand, the amination test used was developed and optimized for agarose. This test quantifies amines in solution, being necessary to first hydrolyze the agarose support. The conditions optimized for agarose may not be adequate for the cellulose membranes. In this case, the amount of amines quantified might be inferior to the actual value at the membranes surface.

Cellulose membranes and agarose are structures with completely different geometries and this can be a key point to explain the difficulty to adapt the agarose procedure to the membranes.

In both immobilization routes the colorimetric test confirms the presence of phenol groups from compounds B and C on membrane surface.

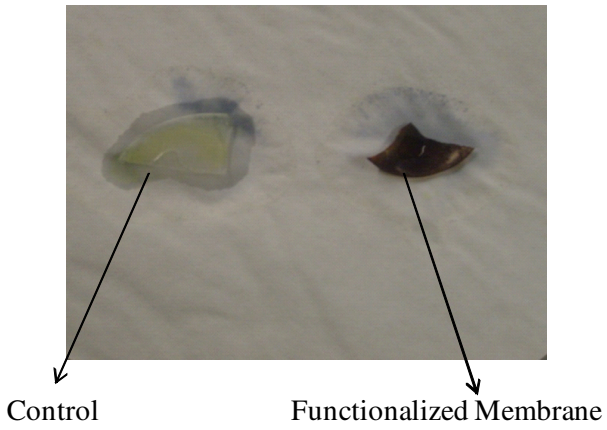

Figure 3.20 - Phenol's test to M1 (Folin Ciocalteau)

For M1 it is not clear the blue coloration in the functionalized membrane. However the color of the membrane before ligand immobilization was orange and when submitted to the Folin Ciocalteau it appeared with a dark color. The difference of color between M1 and the control is evident, justifying the presence of phenols groups in M1.

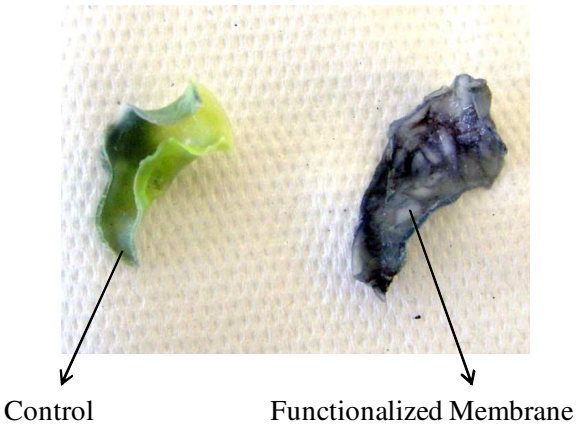

Figure 3.21 - Phenol's test to M2 (Folin Ciocalteau)

In M2 the blue spot is evident because the membrane before ligand immobilization was opaque. In this case the presence of phenols groups is also confirmed by blue coloration.

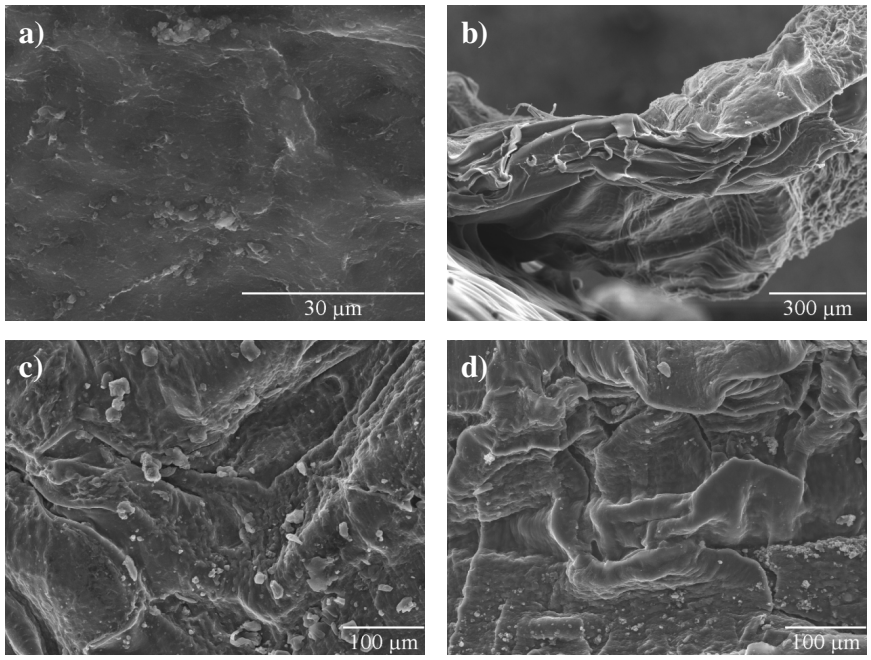

Figure 3.22 – Functionalized cellulose membranes 10% (w/w): a) M1 surface; b) M1 cross-section; c) M2 surface; d) M2 cross-section.

SEM images show that some changes occurred in membrane morphology during the functionalization. The broad pores as sheet overtopped disappeared and the cellulose membrane became irregular without visible and defined pores.

Probably the interaction between solvents used in functionalization process and the polymer as well as the ligands introduction in membrane structure changed the pores and consequently the morphology (Figure 3.15 and Figure 3.22).

The quantification of immobilized ligands was calculated by subtracting from the initial amount that reacted with membrane and the amount that was collected from washing liquors. These values are described in Table 3.5. The amount of immobilized ligand was higher in membrane 2 than in membrane 1 due the different followed routes.

In membrane 1 the procedure was equal to agarose procedure and it was possible to functionalize only 16 µmol/g memb while in agarose it is possible to immobilize 90 µmol of ligand /g moist weight gel. This suggests the functionalization of cellulose membrane following the same procedure, however with less efficiency.

One possible explanation for these results can be the presence of a blocking effect of epoxy groups because the hexane-1,6-diamine is symmetrical, so both sides can react with nearby epoxy groups. Additionally the amine groups rest unavailable to react with compound B as it is represented in Figure 3.23. In case of agarose that is a spherical support, the distance between epoxy groups is not so homogeneous when compared with cellulose membranes, where all epoxy groups are in the same plane being high the blocking effect of epoxy groups. Another reason that can justify this low amount of immobilized ligand can be related with the impurity of the ligands.

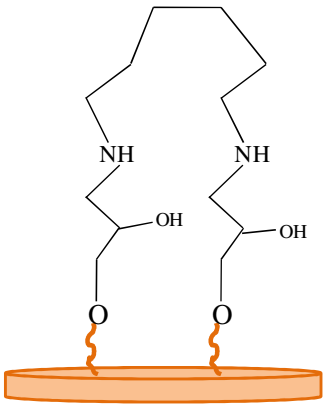

Figure 3.23 – Blocking of epoxy groups

However, in membrane 2 the spacer arm, hexane-1,6-diamine, reacted with B and just when C was formed, the membrane was functionalized. This procedure brought a large difference in the ligand amount immobilized. By this route, the blocking effect of epoxy groups was not so strong, probably because the one side of the spacer arm was occupied with compound B that reacted in solution where the molecules were dispersed, and the dimmers formation isn't so probable, being the other amine group of spacer arm available to bind with epoxy groups in the membrane. Taking this route was possible to functionalize 93 µmol/g memb, a little more

than in agarose [10]. If the compound C purity will be better, probably the yield of immobilization will be still high.

3.3.4 Purification of hIgG

The hIgG binding tests were performed in both membranes. These measurements were done in an Amicon vessel with 10 ml which was submitted at pressures between 0-3 bar. The pressure applied was not the same in all membranes because, as it was previously described, the membrane functionalization changed the structure and morphology of it. First, the idea was to apply the same pressure to M1 and M2 equal to the pressure applied in membrane control, however, the flow rate was very low. For this reason, the pressure was increased to 2 and 3 bar, respectively. In the control membrane the flow rate was 1ml min^{-1}, while in M1 and M2 was 2ml h^{-1}. The flow rate in both membranes was still low with the pressure increase but to avoid the membrane rupture, 3 bar was the maximum pressure applied. This low flow rate is also a result of structure membrane modification during the functionalization.

Membranes were loaded with 6ml of hIgG solution in PBS (0,5 mg/ml), and the recovered samples were analyzed. Two relevant aspects needed to be quantified, the amount of hIgG bound and recovered. With changes in some relevant parameters for the behavior and conformation of antibodies [21] it is possible to purify and recover hIgG. In this work the pH was changed in order to recover the bound hIgG. The hIgG elution from the membrane was performed with a buffer solution of sodium citrate buffer (0.05 *M*, pH 3.0).

The results for cellulose membranes (membrane control, M1 and M2) were different in case of hIgG amount purified and recovered following the same binding procedure.

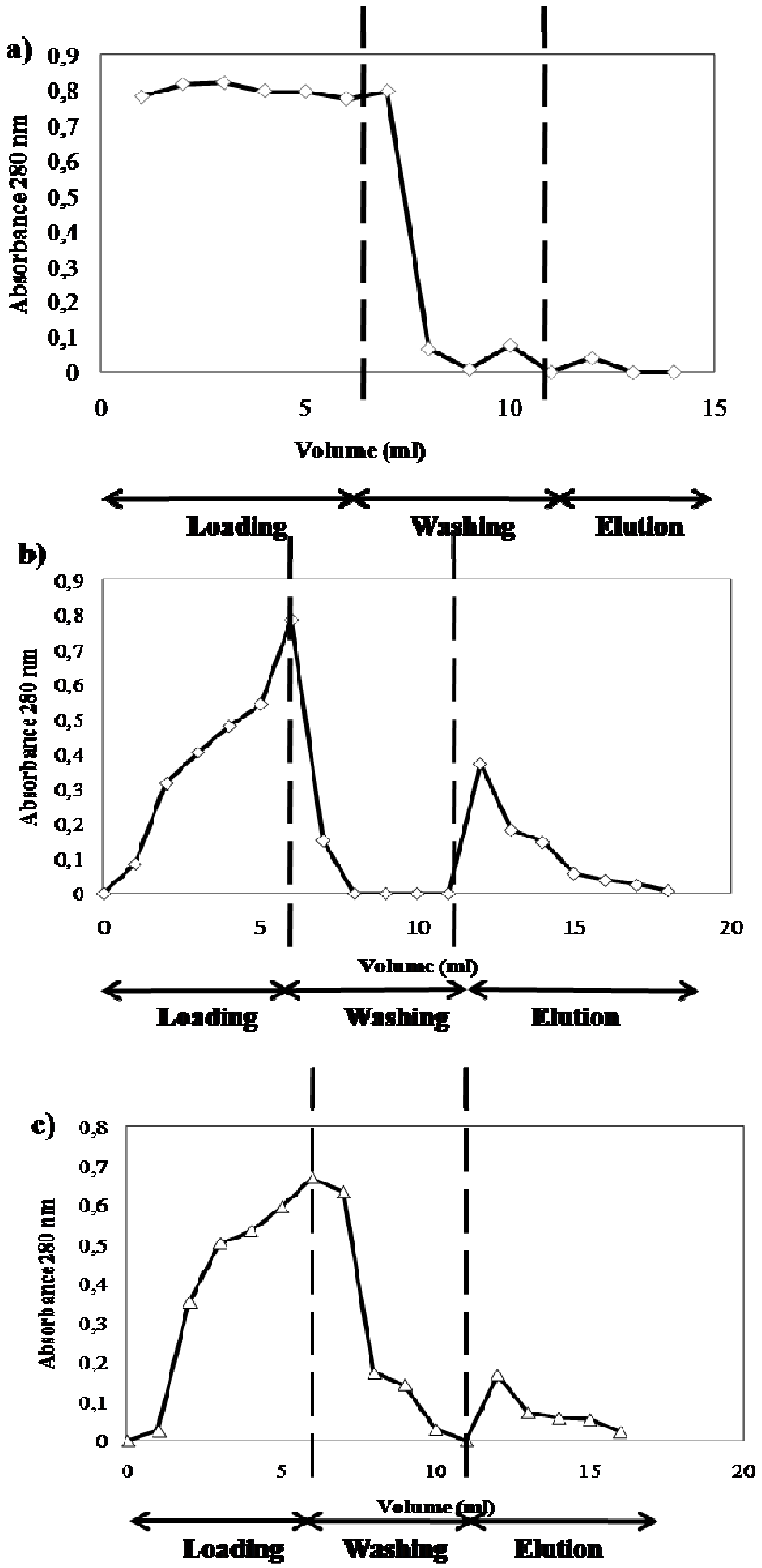

Figure 3.24 - Assay of hIgG adsorption/elution in membrane control (a), M1(b) and M2(c); hIgG (6 ml) solution in PBS (0.5mg ml^{-1}) (loading), PBS (0.5mg ml^{-1}) (washing) and sodium citrate buffer (0.05 *M*, pH 3.0) (elution)

Figure 3.24 shows the performance of cellulose membranes due to the bind/elution tests with hIgG in control, M1 and M2, respectively. The different behavior of M1 and M2 comparing with membrane control justify that all the hIgG restrained is due by ligand action because in membrane control any hIgG is bound.

Table 3.6 shows the values of hIgG bound and recovered using both membranes.

Table 3.6 – Amount of hIgG bound and eluted in control membrane M1 and M2

hIgG Amount	Control	Membrane 1	Membrane 2
Bound (mg/g memb)	0	5	3
Eluted (mg/g memb)	0	3	0.7

Considering the amount of ligand immobilized, it was expected that M2 would bind more hIgG. However, M1 retained hIgG more efficiently and also eluted most of the bound protein (60% as opposed to 23% for M2). Firstly, compound B (M1) was obtained with a higher purity than compound C (M2), which also reflected the purity of the immobilized ligand and an increased specificity of the binding to hIgG. It is conceivable that contaminants present on compound C (e.g. amines) also reacted with the epoxy-activated membrane; and these contaminants can absorb light at the wavelength used for compound C determination. In M1, compound B was immobilized on to aminated membrane being expected that only the last chlorine of the triazine molecule on compound B would react with the surface. Maybe the type of ligand and its immobilization are the key points of these results. Probably, the ligands purification would be more intense in order to define a new strategy of ligand purification as well as the time of immobilization that can be increased to improve coupling yield. However, other parameters should be studied and optimized to better understanding of the interaction between membrane, ligand and hIgG.

Parameters such as pressure, residence times, flow rate, membrane thickness, membrane geometry and porous size have an important role in the design of affinity membranes [5, 15, 21]. Affinity membranes should have micro or macroporous, low residence times and rapid flow rates. It should be necessary to change these parameters in order to identify the optimal operating conditions to high affinity performance.

The amount of hIgG immobilized in both membranes is lower than the amount of hIgG immobilized in agarose (51,9 mg IgG/g moist weight gel) [10]. This is not surprising as in this work no method optimization was performed. The aim was to prove that similar agarose

procedure works with cellulose membranes produced with "green" alternative solvents. Comparing the hIgG bind with others cellulose affinity membranes with other ligands immobilized or with another type of polymeric affinity membranes, the values are different, however the module configuration of these last membranes is different as well as the type of ligand immobilized on them, being these factors very important in membrane affinity performance [18, 21, 36].

In hIgG recovery the results were different for both membranes; membrane 1 obtained the best results. In membrane 1 it was possible to recover 60% of what was possible to purify in membrane 2 by an elution with citrate buffer (0.05 *M*, pH 3.0). These results are closer to results reported in literature to agarose [10]. Membrane 2 had an inferior performance in hIgG recovered than membrane 1 probably caused by the low purity and selectivity of 4-(4-(3-hydroxyphenylamino)-6-(6-aminohexylamino)-1,3,5-triazin-2-ylamino)naphthalen-1-ol (compound C) to hIgG due to immobilization method.

It would be interesting to test different elution strategies to improve the yield of hIgG eluted [10].

3.4 Conclusion

This chapter was divided in two parts, the preparation and characterization of cellulose membranes using ionic liquids as a "friendly" solvent and the functionalization of membranes for hIgG bind/elution. The last phase was also divided in four steps: (i) biomimetic ligands synthesis and characterization, (ii) membranes activation, (iii) biomimetic ligands immobilization on membranes surface and (iv) bind/elution tests with hIgG.

The amount of cellulose present in the casting solution showed to be an important parameter to design different membranes morphologies and porous structures. These morphologies, and consequently the pore size, also depend on the amount of water present in its configuration. In all membrane surfaces the pores were not observed, only in cross section of the membranes.

The mechanical analysis also showed to be different depending on the cellulose amount present in the casting solution and the drying process used. Cellulose membranes completely dried showed to be more fragile as well as the membranes which had less cellulose content in its composition.

The OH groups of cellulose had a strong influence in the water flux, because when the polymer concentration in the casting solution increased, the pore size decreased and consequently the permeability of the membranes increased.

The detailed characterization of cellulose membranes and the analysis of data lead to the selection of membrane prepared from solutions with 10% (w/w) of cellulose which was assumed as the best candidate for further development of affinity membranes.

In terms of ligand synthesis, there were difficulties in attaining the desired purity. On the other hand, the amination of the membrane decreased the amount of free groups for reaction with ligand. Therefore the amount of immobilized ligands was low, especially in M1. Although in the M2 the amount of ligand immobilized was higher than M1, a part of this can be contaminants, which justifies the lower affinity between ligand-hIgG in M2.

The different immobilization routes led to obtain different activation and immobilization results explained by the ligand type and the immobilization method. M2 showed to be the membrane with better results to activation and immobilization efficiency. However, M1 revealed to be better in bind/elution tests with hIgG showing that was immobilized with a ligand more specific to hIgG that in case of M2.

Parameters such as the ligand and its purity, immobilization method, geometry support and affinity interactions between ligand-protein showed to have an important role in a performance of an affinity membrane.

The results obtained to ligand type, activation and immobilization route, hIgG amount bonded and eluted together with the material and its structure characterization, M1 showed to have the best requirements to assume an affinity membrane character.

3.5 References

1. Roque, A.C., Silva, C.O., Taipa, M.A., *Affinity-based methodologies and ligands for antibody purification: Advances and perspectives.* Journal of Chromotography A, 2007. **22**: p. 341-349.
2. Roque, A.C., Lowe, C. R., Taipa, M.A., *Antibodies and Genetically Engineered Related Molecules: Production and Purification.* Biotechnol. Prog. , 2004. **20**: p. 639-654.
3. Zhou, J.X., Tressel, T., *REVIEW: Basic Concepts in Q Membrane Chromatography for Large-Scale Antibody Production.* Biotecnol. Prog., 2006. **22**: p. 341-349.
4. Castilho, L.R., Anspach, F. B., Deckwer, Wolf-Dieter., *Comparison of affinity membranes for the purification of immunoglobulins.* Journal of Membrane Science, 2002. **207**: p. 253-264.
5. Roper, D.K., Lightfoot, E. N., *Separation of biomolecules using adsorptive membranes* Journal of Chromotography A, 1995. **702**: p. 3-26.
6. Wilche, M., Goreck, M., *Affinity Chromatography of Bovine Pancreatic Ribonuclease A.* European J. Biochem., 1969. **11**: p. 491-494.
7. Dancette, O.P., et al., *Purification of immunoglobulins G by protein A/G affinity membrane chromatography.* Journal of Chromotography B, 1999. **723**: p. 61-68.
8. Cuatrecasas P., *Protein Purification by Affinity Chromotography.* The Journal of Biological chemistry, 1970. **245**(1): p. 3059-3065.
9. Filippusson, H., Erlendsson, L. S., Lowe, C. R., *Design, synthesis and evaluation of biomimetic affinity ligands for elastases.* Journal of Molecular Recognition, 2000. **13**: p. 370-381.
10. Teng, S.F., et al., *Affinity chromatography on immobilized "biomimetic" ligands Synthesis, immobilization and chromatographic assessment of an immune globulin G-binding ligand.* journal of Chromotography B, 2000. **740**: p. 1-15.
11. Wang, J., et al., *Synthesis of new 'biomimetic' dye-ligands and their application in the purification of alkaline phosphatase.* Separation and Purification Techonology, 2006. **50**: p. 141-146.
12. Wu, F., Yu, J., *Novel biomimetic affinity ligands for human tissue plasminogen activator.* BBRC, 2007. **355**: p. 673-678.
13. Roque, A.C., Lowe, C.R. , *Advances and applications of de novo designed affinity ligands in proteomics* Biotechnology Advances 2006. **24**(1): p. 17-26.

14. Feng, H., et al., *Screening and chromatographic assessing of a novel IgG biomimetic ligand.* Biomedical Chromatography, 2006. **20**: p. 1109-11015.
15. Ghosh, R., *Protein separation using membrane chromatography: opportunities and challenges.* Journal of Chromotography A, 2002. **952**: p. 13-27.
16. Fahrner, R.L., Blank, G.S., Zapata, G.A., *Expanded bed protein A affinity chromatography of a recombinant humanized monoclonal antibody: process development, operation, and comparison with a packed bed method* Journal of Biotechnology, 1999. **75**(2-3): p. 273-280.
17. Lilius, G., Persson, M., Bulow, L., Mosbach, K., *Metal affinity precipitation of proteins carrying genetically attached polyhistidine affinity tails.* J.Biochem, 1991. **198**: p. 499-504.
18. Charcosset C., *Purification of proteins by membrane chromatography.* J.Chem. Tehnol. Biotecnhol., 1998. **71**: p. 95-110.
19. Guo, W., Ruckenstein, E., *A new matrix for membrane affinity chromatography and its application to the purification of concanavalin A.* Journal of Membrane Science, 2001. **182**: p. 227-234.
20. Bueno, S.M.A., et al., *Experimental kinetic aspects of hollow fiber membrane-based pseudobioaffinity filtration: process for IgG separation from human plasma.* Journal of Membrane Science, 1996. **117**: p. 45-56.
21. Zou, H., Luo, Q., Zhou, D., *Affinity membrane chromatography for the analysis and purification of proteins.* Journal of Biochemical and biophysical methods, 2001. **2001**: p. 199-240.
22. Klein, E., Yeager, D., Seshadri, R., Baurmeister, U., *Affinity adsorption devices prepared from microporous poly(amide) hollow fibers and sheet membranes.* Journal of Membrane Science, 1997. **129**: p. 31-46.
23. Arica, M.Y., Yalcin, E., Bayramoglu, G., *Preparation and characterisation of surfaces properties of poly(hydroxyethylmethacrylate-co-methacrylolyamido-histidine) membranes: application for purification of human immunoglobulin G.* Journal of Chromotography B, 2004. **807**: p. 315-325.
24. Bayramoglu, G., Okten, H. A., Arica, M. Y., *A dye–ligand immobilized poly(2-hydroxyethylmethacrylate) membrane used for adsorption and isolation of immunoglobulin G.* Biochemical Engineering Journal, 2007. **34**: p. 147-155.
25. Brenncke, J.F., Amrginn, E. J., *Ionic Liquids: Innovative Fluids for Chemical Processing.* ALChE Journal, 2001. **47**(11): p. 2384-2389.

26. Zhu, S., et al., *Dissolution of cellulose with ionic liquids and its application: a mini-review.* Green Chemistry, 2006. **8**: p. 325-327.
27. Swatloski, R.P., et al., *Dissolution of Cellose with Ionic Liquids.* JACS, 2002. **124**: p. 4974-4975.
28. Jie, X., et al., *Influence of drying method on morphology and properties of asymmetric cellulose hollow fiber membrane.* Journal of Membrane Science, 2005. **246**(2): p. 157-165.
29. Heinz, T., Schwikal, K., Barthel, S., *Ionic Liquids as Reaction Medium in Cellulose Functionalization.* Macromol. Biosci., 2005. **5**: p. 520-525.
30. Kosan, B., Michels, C., Meister, F., *Dissolution and forming of cellulose with ionic liquids.* Cellulose, 2008. **15**: p. 59-66.
31. Turner, M.B., et al., *Production of Bioactive Cellulose Films Reconstituted from Ionic Liquids.* Biomacromolecules, 2004. **5**: p. 1379-1384.
32. Earle, M.J., et al., *The distillation and volatility of ionic liquids.* Nature, 2006. **439**(16): p. 831-834.
33. Reverchon, E., Cardea, S., *Formation of cellulose acetate membranes using a supercritical fluid assisted process.* Journal of Membrane Science, 2004. **240**: p. 187-195.
34. Temtem, M., Casimiro, T., Aguiar-Ricardo, A., *Solvent power and depressurization rate effects in the formation of polysulfone membranes with CO2-assisted phase inversion method.* Journal of Membrane Science, 2006. **283**: p. 244-252.
35. Liu, H., Hsieh, Y-L., *Ultrafine Fibrous Cellulose Membranes from Electrospinning of Cellulose Acetate.* Journal of Polymer Science, 2002. **40**: p. 2119-2129.
36. Ma, Z., Kotaki, M., Ramakrishna, S., *Electrospun cellulose nanofiber as affinity membrane.* Journal of Membrane Science, 2005. **265**: p. 115-123.
37. Yang, l., Hsiao, W., Chen, P., *Chitosan–cellulose composite membrane for affinity purification of biopolymers and immunoadsorption.* Journal of Membrane Science, 2002. **197**: p. 185-197.
38. Xiao, Y., Chung, T-S., *Functionalization of cellulose dialysis membranes for chiral separation using beta-cyclodextrin immobilization* Journal of Membrane Science, 2007. **290**(1-2): p. 78-85.
39. Eichhorn, S.J., Young, R. J., *The Young's modulus of a microcrystalline cellulose.* Cellulose, 2001. **8**: p. 197-207.

40. Bledzki, A.K., Gassan, J., *Composites reinforced with cellulose based fibres.* Progress in Polymer Science, 1999. **24**: p. 221-274.

4. Final Conclusions

The major breakthrough of this work was the development of polymeric membranes for bioseparation purposes using both $scCO_2$ and ionic liquids as alternative solvents.

New P(MMA-co-MAA) copolymers were successfully synthesized in $scCO_2$, and different P(MMA-co-MAA) membranes with tunable porous structures were also prepared using a $scCO_2$-assisted process.

The use of $scCO_2$ in the reaction step introduced high performance in the resulting copolymers such as interesting molecular average weights and glass transition temperatures, comparing to traditional methods.

The different polymeric membranes produced by phase inversion method from different polymer-solvent solutions presented distinct morphologies and properties. The use of $scCO_2$ as an anti-solvent showed to have a great ability to control the membrane morphology while ionic liquid showed to be a good alternative solvent to dissolve cellulose, comparing with organic solvents (e.g: carbon disulfide and N,N-dimethylacetamide), but with less control on the membrane morphology.

Cellulose membranes were prepared from polymer-ionic liquid solution and water showed to be a good alternative to induce the phase inversion and produce membranes with high mechanical performance and structure.

Cellulose membranes can be modified with a biomimetic ligand with affinity for antibodies, by two different routes revealed different hIgG amounts absorbed and eluted. Parameters such as purity of the ligand, support geometry, ligand immobilization route and pH conditions in absorption/elution tests, showed to have a strong influence in the affinity membrane performance. A good adjustment of these parameters is a key point for the efficiency of these membranes for affinity purification purposes. The preliminary results with hIgG suggest that further work should continue to develop new affinity membranes using alternative solvents and green technologies.

5. Appendix Section

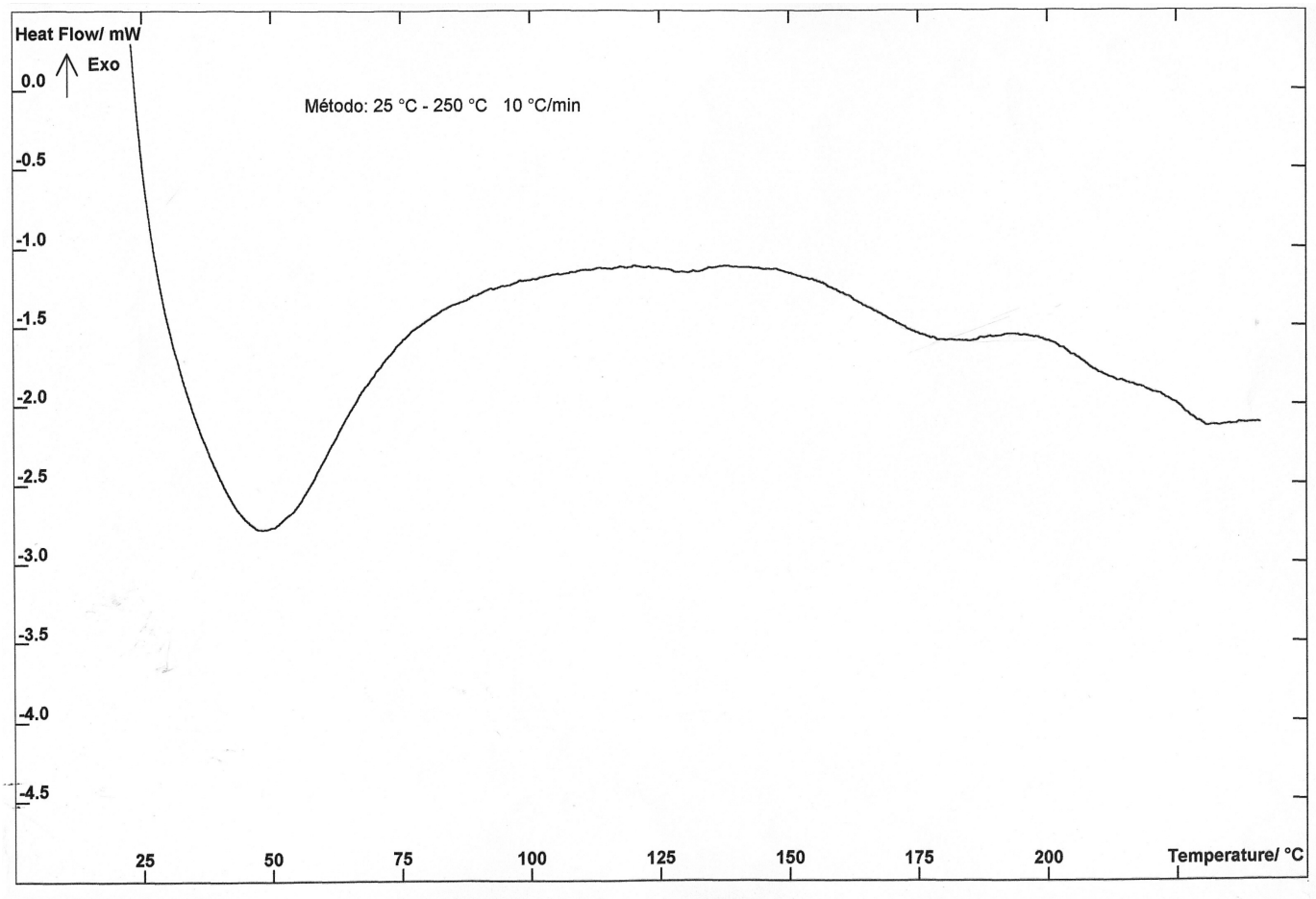

Appendix 1 - DSC of CO75_25

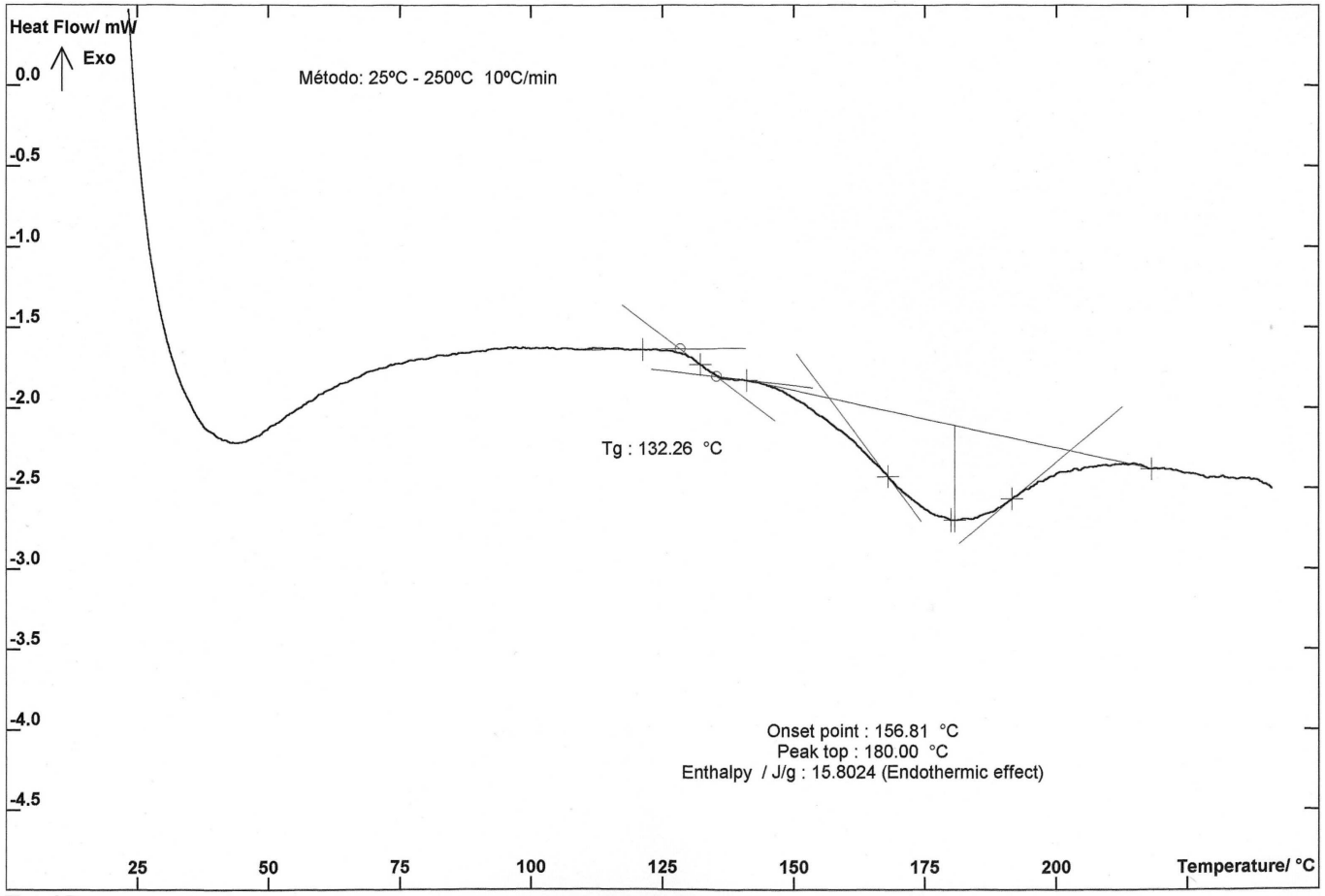

Appendix 2 - DSC of CO90_10

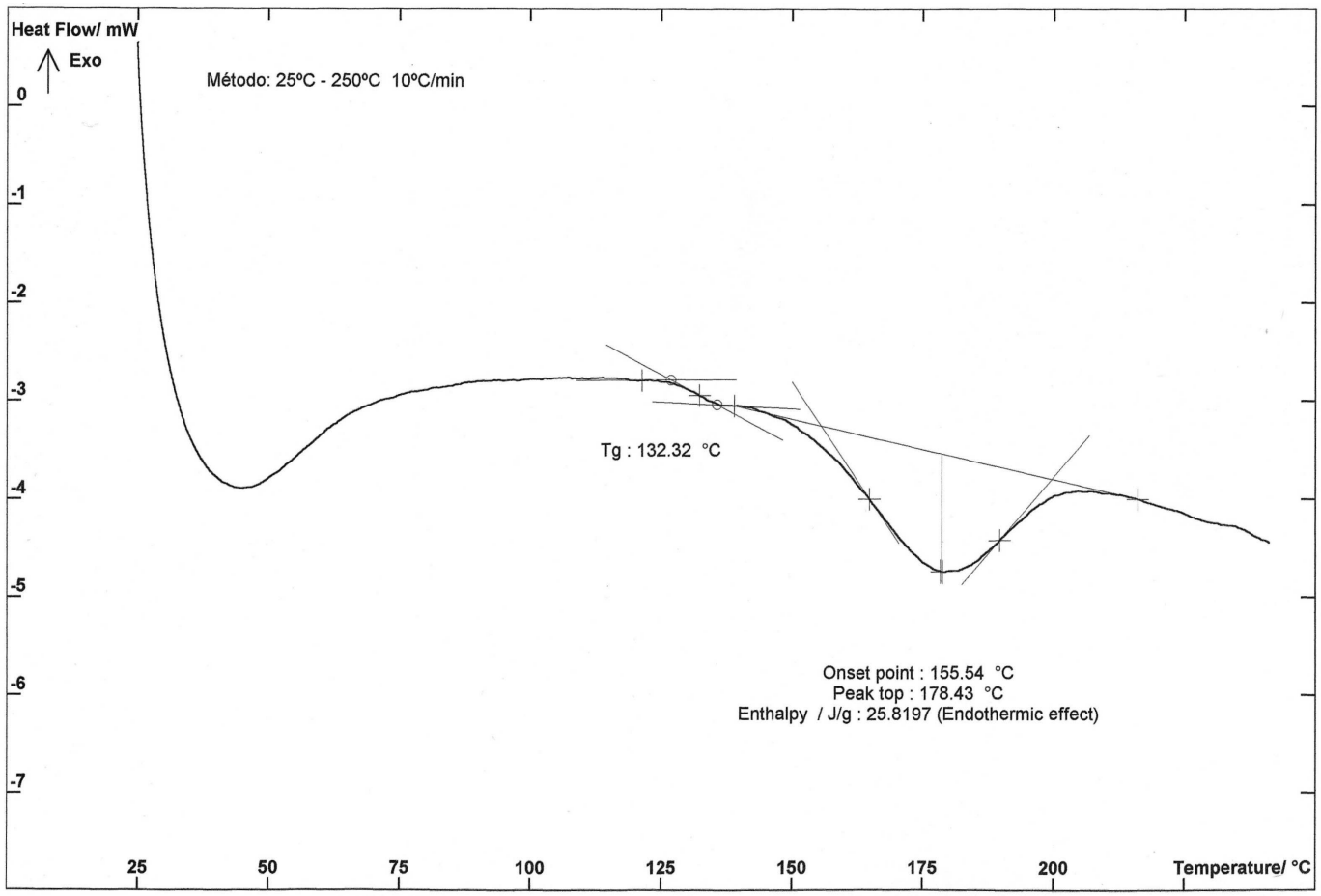

Appendix 3 - DSC of CO95_5

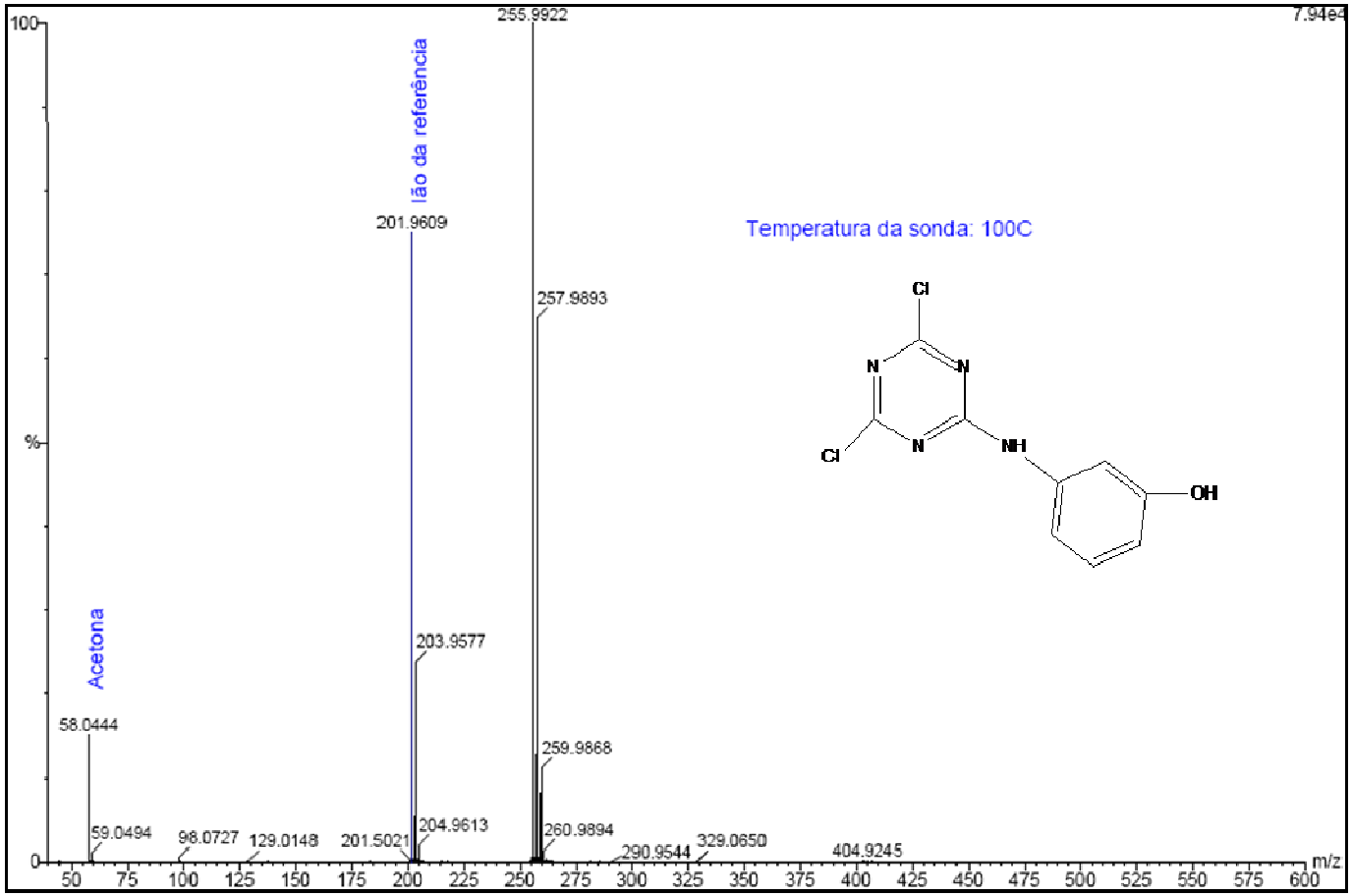

Appendix 4 - M.S of compound A

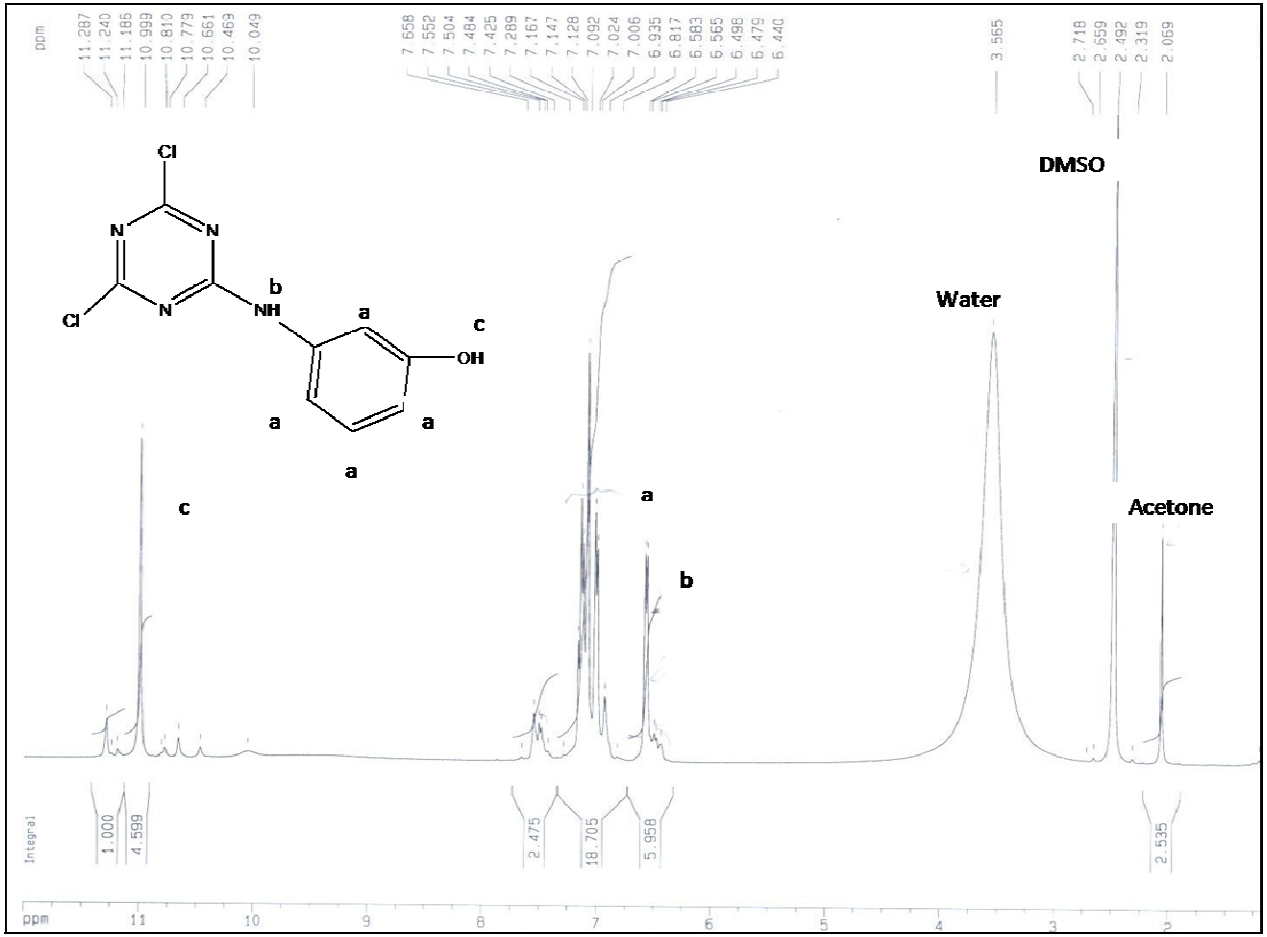

Appendix 5 - ^{1}H-NMR of compound A

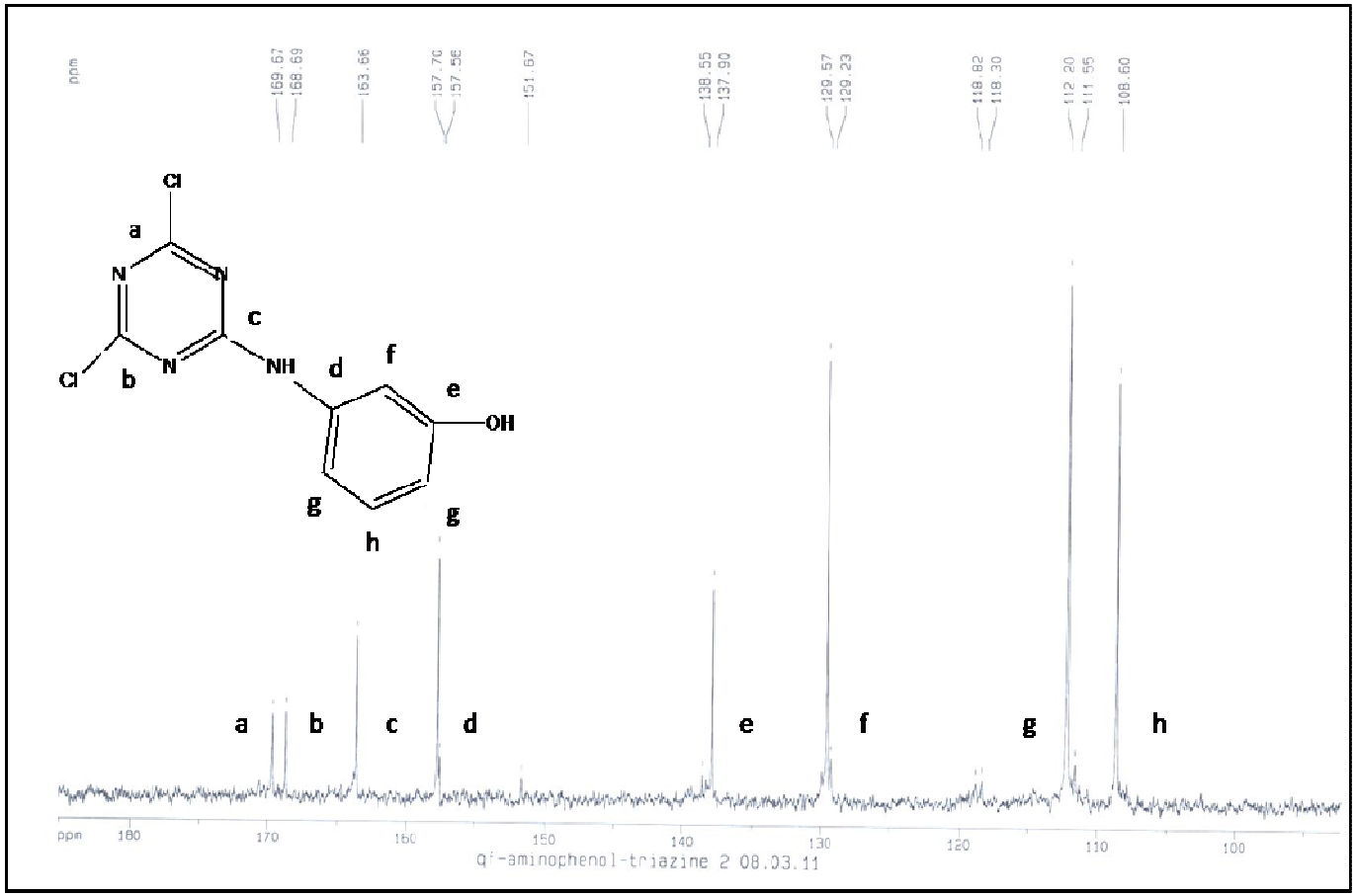

Appendix 6 - ^{13}C-NMR of compound A

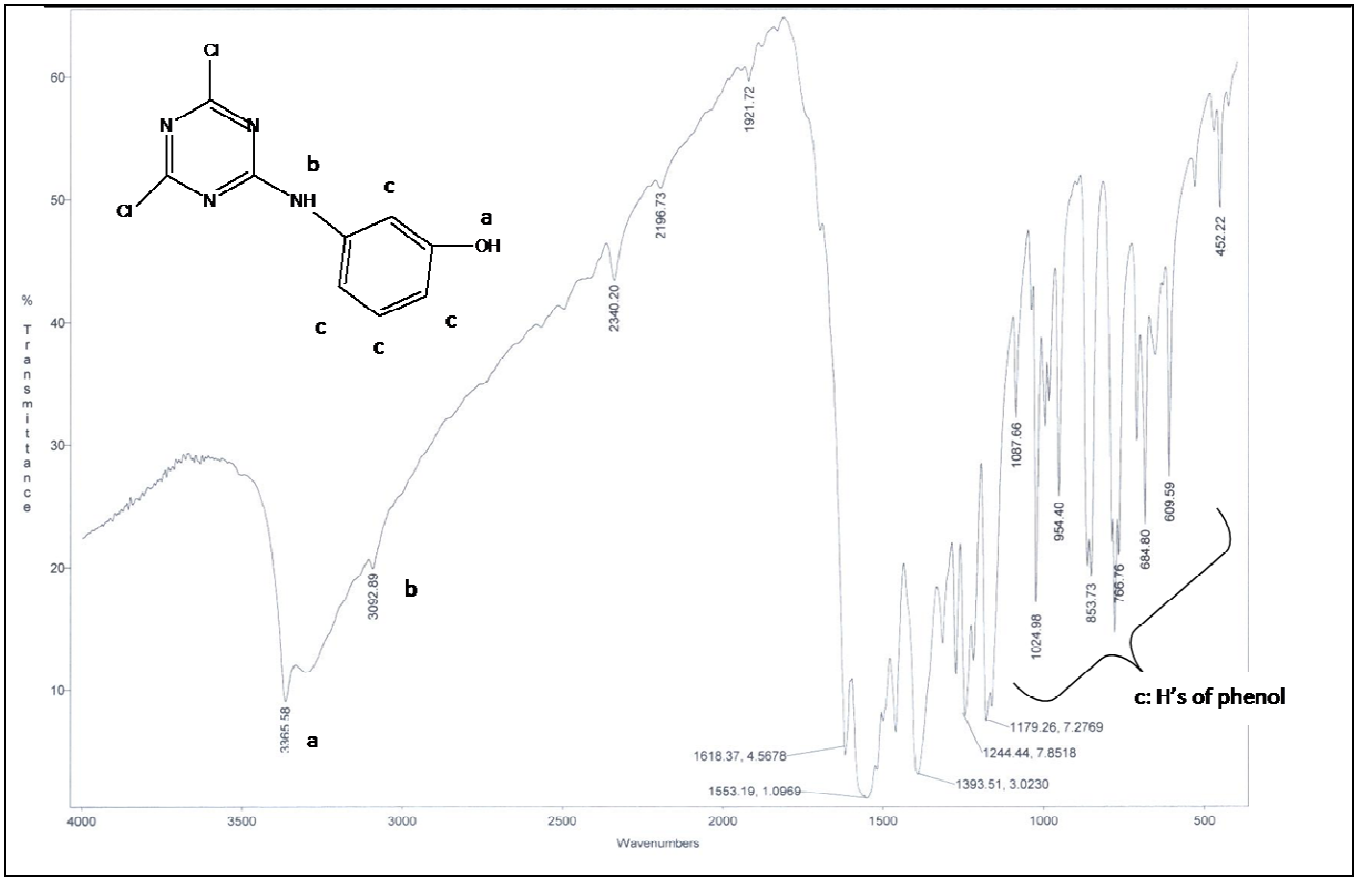

Appendix 7 - FT-IR of compound A

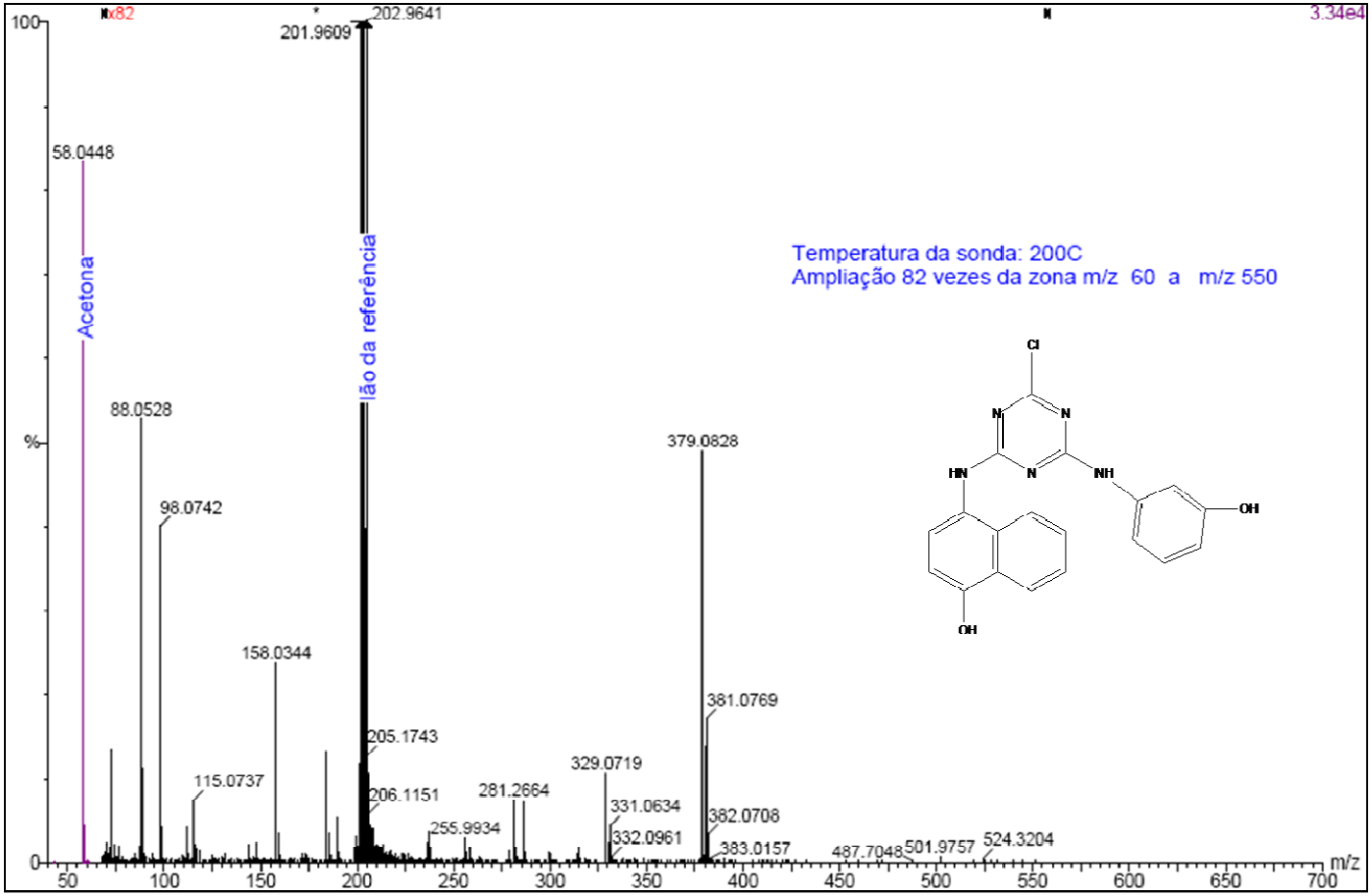

Appendix 8 - M.S of compound B

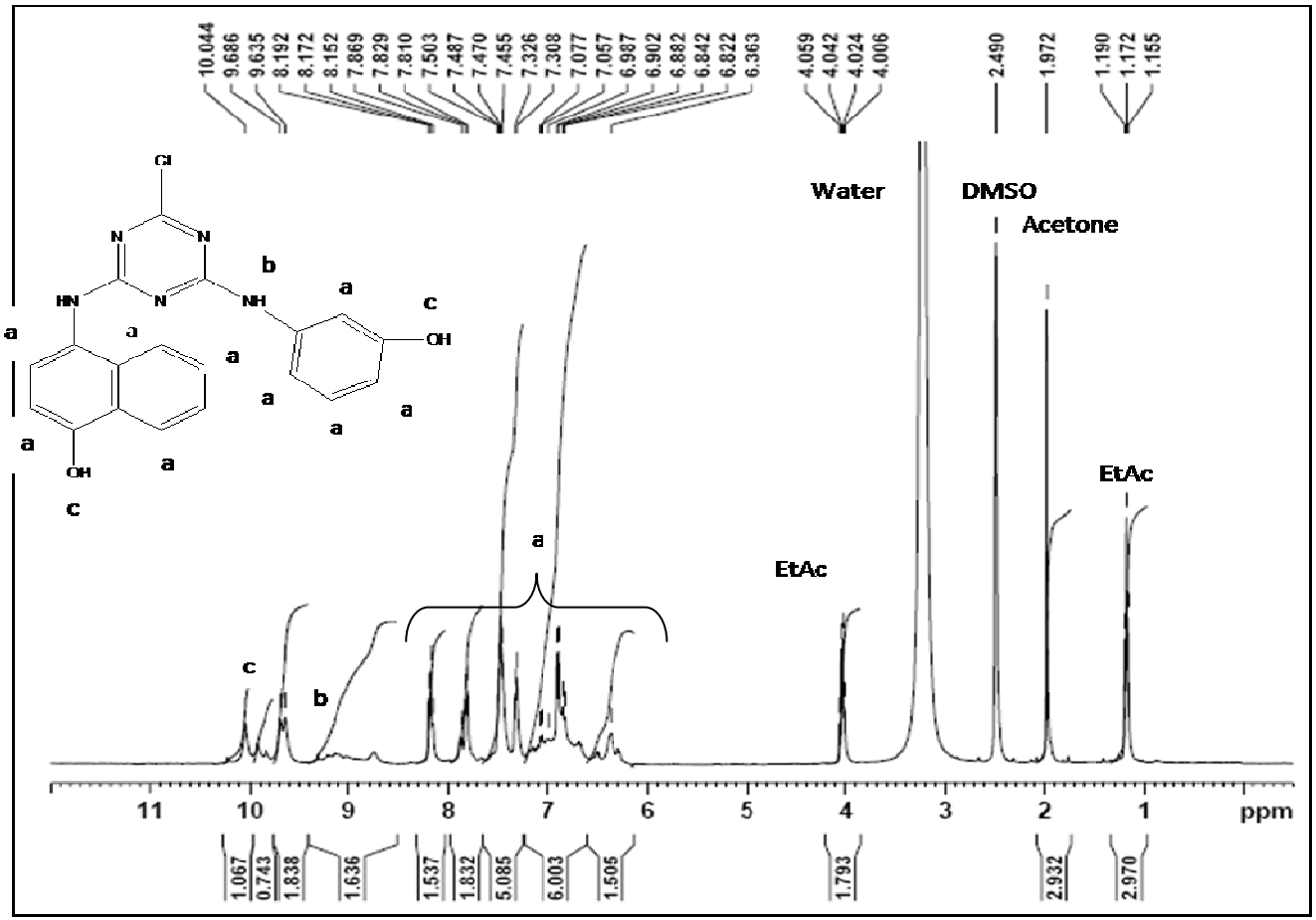

Appendix 9 - ^{1}H-NMR of compound B

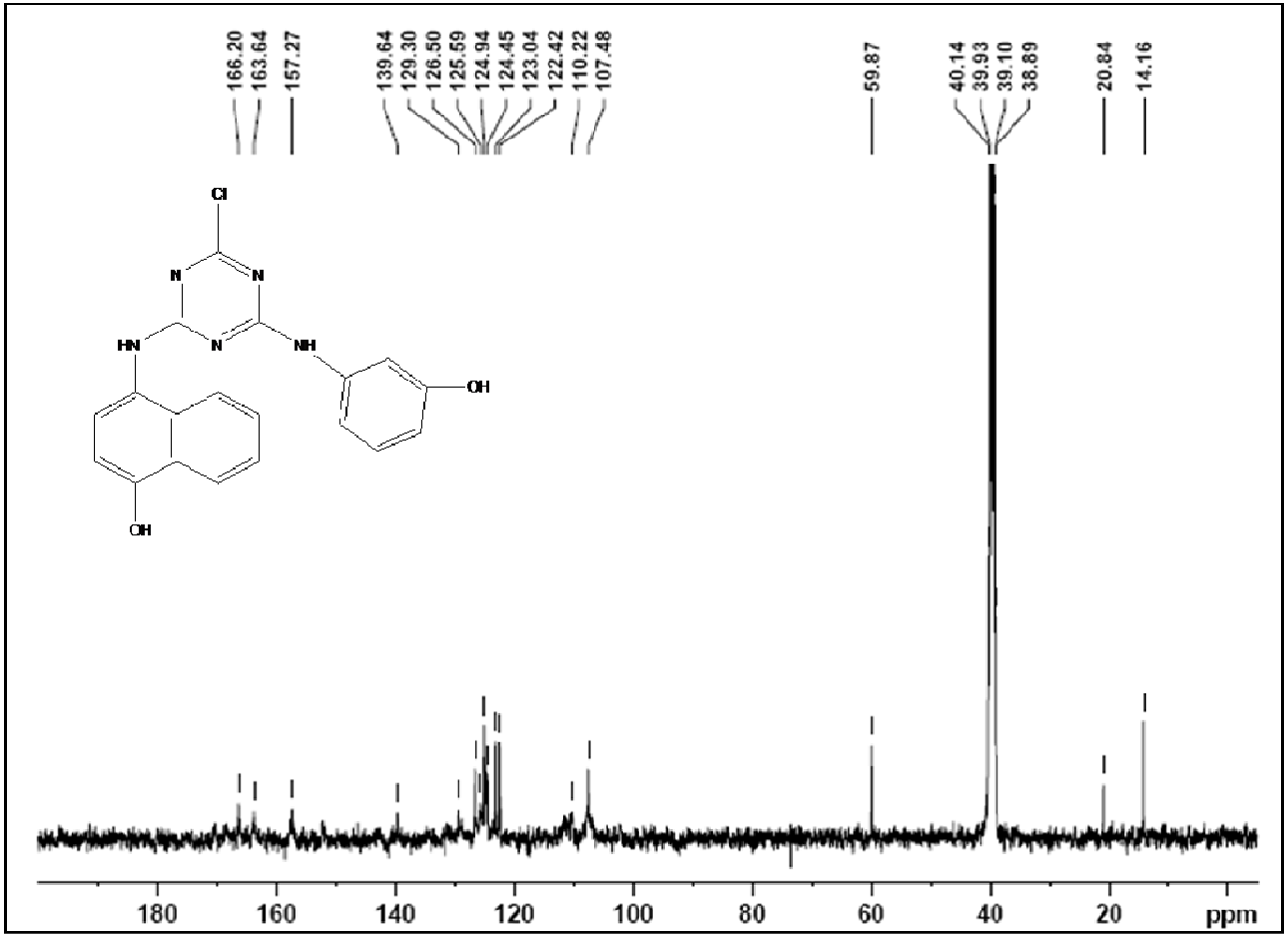

Appendix 10 - ^{13}C-NMR of compound B

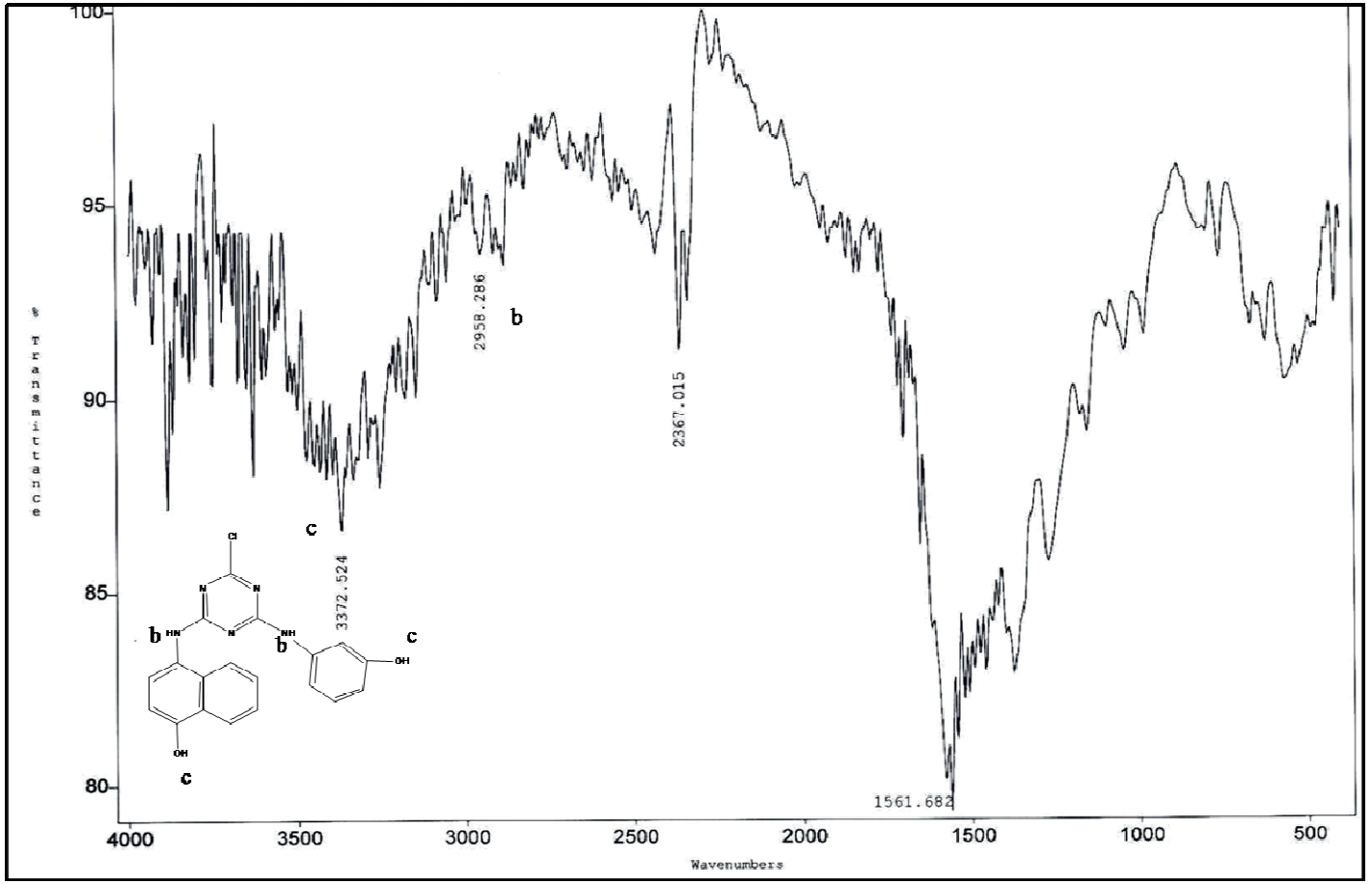

Appendix 11 - FT-IR of compound B

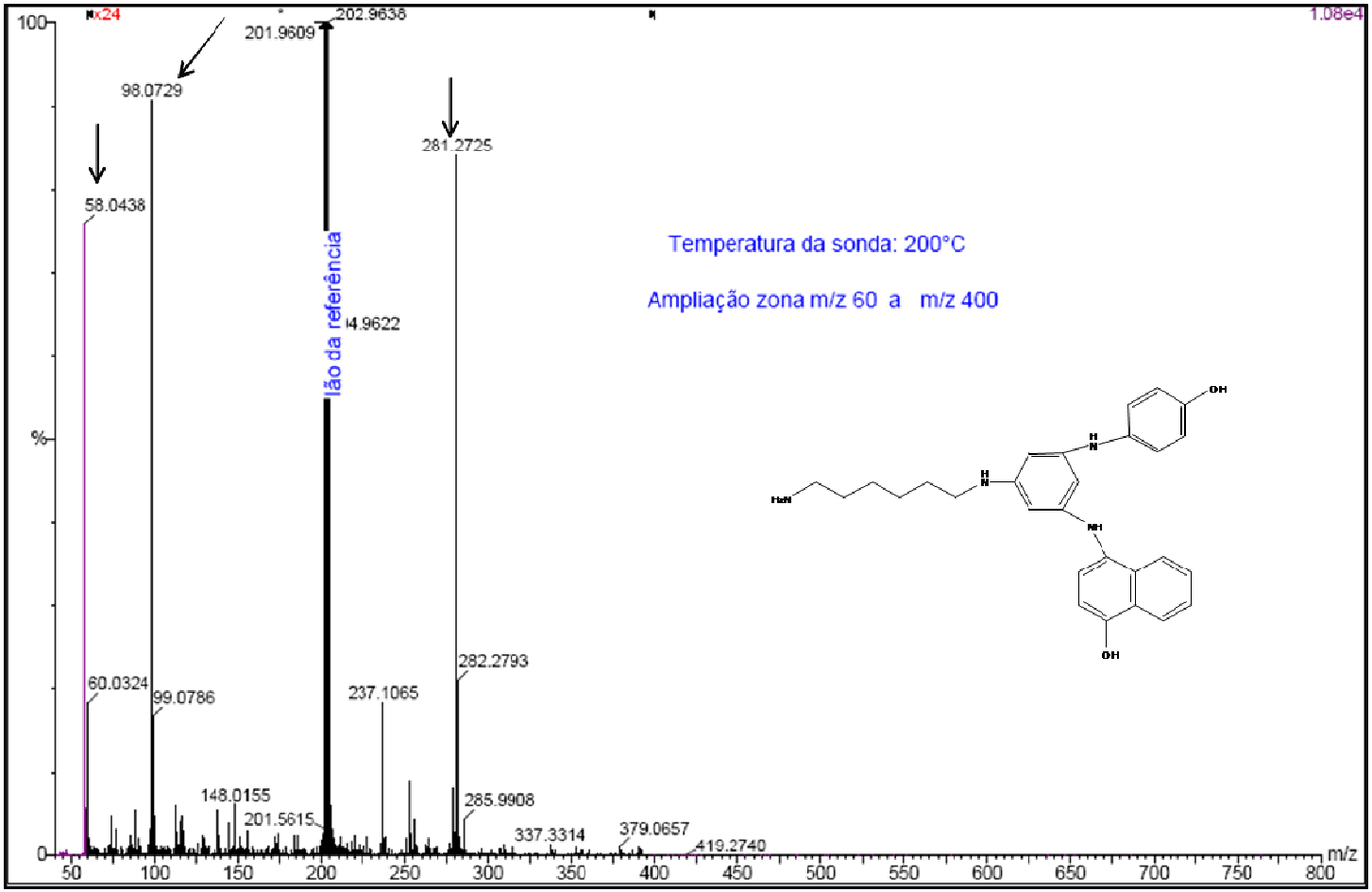

Appendix 12 - M.S of compound C

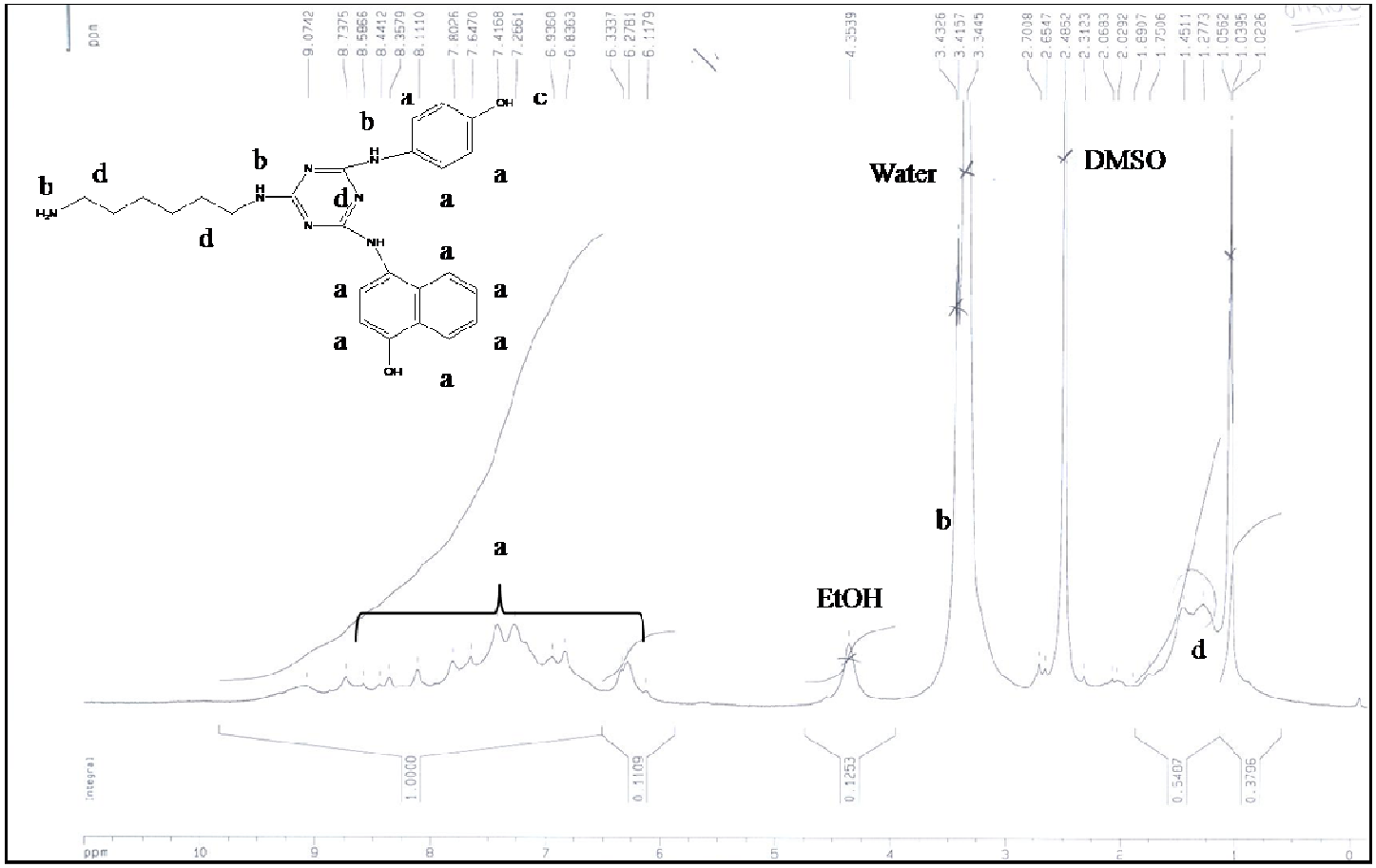

Appendix 13 - ^{1}H-NMR of compound C

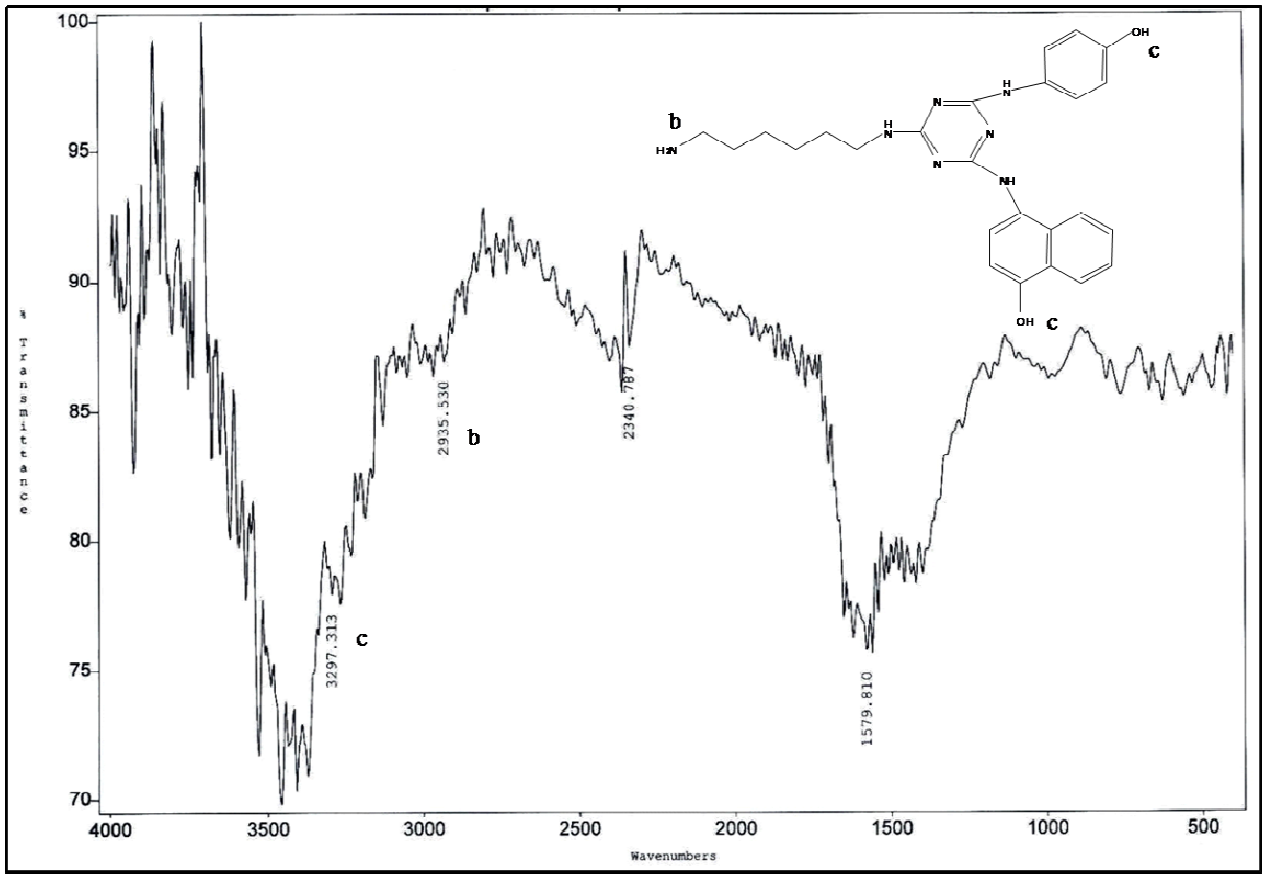

Appendix 14 - FT-IR of compound C